

ALMA MATER STUDIORUM – UNIVERSITY OF BOLOGNA

SCHOOL OF ENGINEERING AND ARCHITECTURE

DICAM

Department of Civil, Chemical, Environmental and Materials Engineering

Master Degree : Environmental Engineering

Curriculum : ERE, Earth Resources Engineering

Master Thesis of

Groundwater Quality, Protection and Modelling

***Preliminary stages and studies for the development of a
3D aquifer physical model***

CANDIDATE

Laura Balzani

PROMOTOR ULG

Prof. Serge Brouyère

CO-PROMOTOR UNIBO

Prof. Lisa Borgatti

Academic Year 2018/19

Session II - 3 OCTOBER 2019



ULiège – UNIVERSITY OF LIEGE
Within a Dual Degree programme with
Alma Mater Studiorum - UNIVERSITY OF BOLOGNA

University of Liège - Faculty of Applied Sciences – Department ARGenCo

Academic Year 2018 - 2019

Master of Environmental Earth and Resource Engineering

« Ingénieur civil des mines et géologue, à finalité spécialisée en géologie de l'ingénieur et de l'environnement »

Master Thesis

***Preliminary stages and studies for the development
of a 3D aquifer physical model***

Student :

Laura BALZANI

Promotor:

Prof. Serge BROUYÈRE (ULG)

Co-Promotor:

Prof. Lisa BORGATTI (UNIBO)

Members of the Jury:

Serge BROUYÈRE

Alain DASSARGUES

Sébastien ERPICUM

Abstract

Groundwater issues are among the most important sustainability studies related to topics considered as critical point for the future of planet Earth (Gleeson et al., 2010) in the perspective of a sustainable world. Analyses are focused on two complementary aspects: quantity and quality. Thus, once physical behaviour is analysed, it is coupled with chemical characterisation studies, in order to obtain a better view of an investigated site. The work of this Master thesis begins with a brief overview of the literature which summarizes the challenges of teaching hydrogeology by theoretical lessons coupled with practical activities. The focus is on laboratory experiments implemented on physical models. In fact, to fully understand the process of groundwater flow and solute transport, and to demonstrate the basics fundamental concepts behind, it is important to visualize them in a lab-scale. This thesis is undertaken in the context of the installation of a 3D physical model at the University of Liège as a support to teaching and research works: dimension, set up, construction and support devices used for system optimal functioning are presented. The global aim of the work is to prepare everything needed to set up the sand tank. This is a fundamental step in order to be able to pre-dimension real experiments, to give ideas about the magnitude order of the expected results and to check the reliability of mathematical results and/or low-dimensionality models. Part of the document is centred on the characterization of porous aquifer materials to implement in the physical model, in particular through sand column one-dimensional lab experiments performed on four distinguished types of quartz sands (differentiated by the particles size): in particular a Constant Head Permeability Test and a Salt Tracer Test (KCl). A numerical model of the 3D tank is also developed by the use of GMS-MODFLOW-MT3DS and few experiments are simulated (gradient variation, pumping test at different pumping rates, and tracer test).

Table of contents

Abstract	3
Table of contents	5
List of Figures	9
List of Tables	11
Nomenclature	13
Introduction	19
Chapter 1	
Use of laboratory scale physical models as a support to teaching and research in hydrogeology	21
1. <i>Hydrogeology and lab-scale physical models</i>	21
2. <i>Why physical models are useful for</i>	23
3. <i>Dimensionality-based classification and examples of application</i>	25
4. <i>Description of flow equations and associated parameters</i>	33
4.1 Bulk and particle densities.....	33
4.2 Porosity: total and effective.....	33
4.3 Hydraulic head.....	35
4.4 Darcy's Law, Hydraulic conductivity and effective velocity.....	35
4.5 Groundwater flow in steady state conditions.....	37
4.6 Groundwater flow in transient conditions: transmissivity and storage.....	38
4.7 Boundary Conditions for flow problem.....	40
5. <i>Description of forward transport equations</i>	40
5.1 Solute transport equations.....	40
5.2 Longitudinal dispersivity.....	41
5.3 Boundary Conditions for a solute transport problem.....	42

Chapter 2

Set up of the physical model to be developed	43
1. <i>Dimensions</i>	43
2. <i>Construction</i>	45
3. <i>Filling material</i>	47
4. <i>Control of the hydraulic gradient</i>	47

Chapter 3

Sand Column Experiments	49
1. <i>Preliminary studies on available sands</i>	49
2. <i>How to characterise the sand(s)</i>	52
3. <i>Columns preparation</i>	56
3.1 <i>Set up of samples</i>	56
3.2 <i>Possible further improvement and extensions</i>	58
3.3 <i>Possible extensions</i>	59
4. <i>Results of experiments performed on sand(s)</i>	60
4.1 <i>Preliminary columns parameters evaluation</i>	60
4.2 <i>Bulk density (ρ_{bulk})</i>	62
4.3 <i>Total porosity (n_{tot})</i>	63
4.4 <i>Hydraulic conductivity (K)</i>	64
4.5 <i>Effective drainage porosity ($n_{\text{eff,flow}}$) and longitudinal dispersivity (α_L)</i>	77

Chapter 4

Modelling of 3D physical sand tank	91
1. <i>Conceptual Model</i>	91
2. <i>Numerical implementation</i>	94
3. <i>Simulations performed</i>	99
3.1 <i>Steady state flow</i>	99
3.2 <i>Pumping Test</i>	101
3.3 <i>Tracer Test</i>	107
4. <i>Sensitivity analysis</i>	111

Chapter 5

Conclusions 115

Annex 0: Physical model additional images 117

Annex I: Basics of solute transport solving methods used 118

Annex II: Column preparation preliminary stages 122

Annex III: Empirical formulas for K estimations: observations 127

Annex IV: Constant Head Permeability Test Results 129

Annex V: Statistical analysis on empirical K 131

Annex VI: TRAC interpretation graphs 138

Annex VII: 7 layers model: Constant pumping test results 142

Bibliography 147

Sitography 155

Acknowledgements 157

List of Figures

FIG 1 Integrated hydrogeology pedagogy associated to an iterative loop over three class components. Within this iterative loop, each component supports the others with chains of mutual feedback. Inspired from Gleeson et al. (2012) and Hakoun et al. (2013).	24
FIG 2 Aquifer model constructed by students for the groundwater remediation lab activity (Hilton, 2008).....	25
FIG 3 Apparatus for hydraulic conductivity determination: Falling head test (Nicholl et al., 2016)	27
FIG 4 Experimental setup of Constant-head test (black) and Tracer test (black and blue) (Cai et al., 2015)	27
FIG 5 Physical 2D model of an aquifer: scheme + real example (sources : Lane, Guide to Sand tank, and https://etc.usf.edu/clippix/picture/front-view-of-the-groundwater-model.html , consulted in July 2019).....	29
FIG 6 Experimental sandbox set up (Jose et al. 2004)	30
FIG 7 Lab-scale flow tank: A-Colloidal borescope (Wu et al. 2008) and B-Monitoring well (Verreydt et al. 2015)	32
FIG 8 Darcy's Law (source: PPT Permeability in soils, Geotechnical Lab, Civil Eng Texas University).....	36
FIG 9 Dimensions and pictures of the sandbox developed at ULiège.....	44
FIG 10 Sand tank holes and connections.....	46
FIG 11 Components view of the sand tank (modified from iFLUX, 2018).....	46
FIG 12 Mariotte Bottle used to keep and provide constant hydraulic head (Nicholl et al.2016)	48
FIG 13 Constant head open overflow devices	48
FIG 14 Available type of sands to characterize through column experiments (A,B) and impurities check by sieving (C).....	50
FIG 15 Granulometric Curve to determine geotechnical parameters of all studied sands.....	51
FIG 16 A) Soil type analysis: graph to estimate a priori total and effective porosities, with retention capacity; and B) Aquifer analysis (Eckis, 1934 modified)	51
FIG 17 Schematic diagram of experimental equipment for tracer test in soil column (Ujfaludi, 2010).....	53
FIG 18 Overview of methods for the hydraulic conductivity determination (Ritzema 2006)	54
FIG 19 Constant head permeameter (Domenico and Schwartz 1990).....	55
FIG 20 Funnel use, compaction, saturation and observation of the final columns preparation	58
FIG 21 Metallic plate to apply to the filter.....	59
FIG 22 Bulk density lab evaluation	62
FIG 23 Schematization of the packing of spherical grains and possible pore size (Říha et al., 2018)	65
FIG 24 Final constant head set up : A schema and B real system used	71
FIG 25 Falling head operational scheme	73
FIG 26 Statistics on N1 empirical K-values (all formulas)	76
FIG 27 Brief injection of tracer: syringe manually pressed.....	78
FIG 28 Probe to monitor the EC-values, and water sampling during tracer test.....	79
FIG 29 Implementation of tracer test: A) the scheme and B) the practical set up	80
FIG 30 Pre-dimensioning of the KCl tracer test for sand-columns: A) Infinite and B) Semi-infinite (selected)	81
FIG 31 Correspondence of EC values (Probe vs Lab analysis): sand 1to2 (A) and N1 first test (B)	82
FIG 32 EC-Curves comparison between lab and probe measurments after injection: test1 N1sand (A) and test5 3to5sand (B).....	83
FIG 33 Ion concentration: comparison Cl- and K+ breakthrough curves (sand N1, second test).....	84
FIG 34 Linear correspondence between EC and concentration[K+]: case of sand 1to2 (A;C-EC,Lab vs mg/L, mmol/L; B;D-EC,Probe vs mg/L, mmol/L).....	85
FIG 35 Linear correspondence between EC and concentration[Cl-]: case of sand 3to5 (A;C-EC,Lab vs mg/L, mmol/L; B;D-EC,Probe vs mg/L, mmol/L).....	86
FIG 36 BTCs normalized comparison between the different sand samples.....	87
FIG 37 Interpretation of breakthrough curve of Cl- ions concentration (mg/L) in 1to2 sand.....	89
FIG 38 Interpretation of breakthrough curve of Cl- ions concentration (mg/L) in N1 sand (second test)	89
FIG 39 BCs of FLOW numerical model of physical 3D sand tank.....	93
FIG 40 Conceptual model implementation through coverages in GMS	95
FIG 41 Tracer injection model coverage visualisation (without grid) in GMS	97
FIG 42 Steady state flow ($\Delta h = 7$ cm): lateral and top view, grid visualization	100
FIG 43 Graph showing the different phases of a constant rate (British Columbia, 2007).....	102
FIG 44 Pumping step test: typical series of pumping rates (Everett, 1995 modified)	102

FIG 45 Step test implemented.....	103
FIG 46 Step pumping test: heads variation	104
FIG 47 Step pumping test: Drawdown variations.....	104
FIG 48 Step pumping test: water table variation passing from Q2 to Q3	105
FIG 49 Examples of results associated to brief and continuous injection breakthrough curves numerically obtained	107
FIG 50 Comparison BTCs continuous tracer inj (A-MOC, B-TVD, C-Comparison) correcting the value of the dispersivity	108
FIG 51 Continuous tracer injection with MOC and TVD advection solution (plume comparison at min 25, red background corresponding to zero concentration).....	109
FIG 52 BTCs continuous injection simulated applying increment in prescribed Δh (MOC solution used)	110
FIG 53 Change in water surface in relation to variations of K (m/s)	111
FIG 54 Head comparison while varying K value (A for K_{N5} , B for K_{3to5}).....	112
FIG 55 BTCs for Continuous tracer injection MOC (changes in n_{eff} and α_L).....	114
FIG 56 BTCs for Brief tracer injection, MOC solution, and changes in n_{eff}).....	114
FIG 57 Different examples of 2D physical aquifer model: landfill presence and different geological structures (https://www.realscienceinnovations.com/groundwater-models.html , consulted in April 2019)	117
FIG 58 Sand aquifer for classroom demonstrations and example of streamflow generation (A-Silliman et Simpson, 1987; and B-C- Rodhe 2012)	117
FIG 59 Cell and its interfaces identification: Standard finite-difference method (MT3DMS Manual, 1999).....	118
FIG 60 TVD schema of operation (Dassargues, 2019).....	119
FIG 61 Illustration of the method of characteristics (MT3DMS Manual, 1999)	120
FIG 62 Filters bottom of the column: porous disks, net (4 layers to have a more consistent strata- grey in the figure), very permeable sponge material (black in the figure).....	122
FIG 63 Top of the column: little stones used to keep the sands unable to go out from the system during the experiments.....	122
FIG 64 On left side it is shown the column preparation: first layer of water and then sand added; On the right picture the final four columns of the first trial is presented.....	123
FIG 65 Preferential paths visualization and similar correlated problems	123
FIG 66 Sand N1 escaping the system while applying water circulation	124
FIG 67 Air bubbles and channels not filled by water in the finer sand samples plus bubbles of air entering the system together with water	124
FIG 68 Improvement of second and third trial in column preparation: changes in upper filters and hammer use to help air to exit.....	124
FIG 69 Problem of the second trial: still air bubbles trapped and sands exiting the system.....	125
FIG 70 Third trial characteristics (filters details)	126
FIG 71 Statistics on N5 empirical K-values (all formulas)	132
FIG 72 Statistics on N5 empirical K-values (selection of representative results)	133
FIG 73 Statistics on 1to2 empirical K-values (all formulas).....	134
FIG 74 Statistics on 1to2 empirical K-values (selection of representative results).....	135
FIG 75 Statistics on 3to5 empirical K-values (all formulas).....	136
FIG 76 Statistics on 3to5 empirical K-values (selection of representative results).....	137
FIG 77 Seven Layers model: central lateral section of water heads, while applying $Q_{pump} = 6.5 \times 10^{-5} \text{ m}^3/\text{s}$	142
FIG 78 Seven Layers model: drawdown while applying $Q_{pump} = 6.5 \times 10^{-5} \text{ m}^3/\text{s}$	143
FIG 79 Seven Layers model: central lateral section of water heads, while applying $Q_{pump} = 1 \times 10^{-4} \text{ m}^3/\text{s}$	143
FIG 80 Seven Layers model: water head and relative drawdown, while applying $Q_{pump} = 1 \times 10^{-4} \text{ m}^3/\text{s}$	144
FIG 81 Seven Layers model: central lateral section, while applying $Q_{pump} = 2.5 \times 10^{-4} \text{ m}^3/\text{s}$	144
FIG 82 BTCs for Continuous tracer injection TVD (changes in n_{eff} and α_L).....	145

List of Tables

TABLE 1 British Soil Standard Classification of Sandy soil	49
TABLE 2 Geotechnical parameters estimated for the four types of sand studied	50
TABLE 3 Expected and estimated ranges for sands parameters to be determined	51
TABLE 4 Summary of columns preliminary measurements.....	61
TABLE 5 Results of bulk dry densities evaluation for all the four types of sands studied with glass experiment.	63
TABLE 6 Results of bulk densities for all sands studied through column samples.....	63
TABLE 7 Total porosity of all types of sand studied	64
TABLE 8 Results of analytical computation (Terzaghi K as the closest to the experimental ones; range of variation).....	68
TABLE 9 K-values calculated experimentally for each sand sample with CH test (range of variability min-max in green).....	72
TABLE 10 Data of injections on different samples	78
TABLE 11 Tracer tests summary of analysis on first tracer arrival and peak time.....	87
TABLE 12 Summary of estimated parameters by the use of TRAC for all sands tested	90
TABLE 13 Packages implemented in MODFLOW for the flow model.....	96
TABLE 14 Flow (MODFLOW) and Transport (MT3DS) simulation solver characteristics.....	98
TABLE 15 Results of steady state flow simulations	99
TABLE 16 Step pumping test: influence radius and drawdown for higher pumping rate	106
TABLE 17 Different pumping rates applied on the 2 Layer Numerical Model.....	106
TABLE 18 Results of main ideal tracer tests with N5 sand.....	109
TABLE 19 Comparison of results of constant pumping rate test due to changes in K value	111
TABLE 20 Constant Inputs of empirical formulas (source: https://www.engineersedge.com consulted in April 2019)	127
TABLE 21 Summary of all empirical computation formulas and results	128
TABLE 22 Average K values from CHPT.....	129
TABLE 23 Resume of the principal and most representative values for each sand type studied	130

Nomenclature

a	Cross sectional area of the water level monitoring device (m^2)
A	Areal section of the column (m^2)
b	Aquifer thickness (m)
B,C,D,E	Linear coefficients/numbers used to make relations between variables (/)
C^v	Volumetric concentration of solute (kg/m^3)
C^{v*}	Volumetric concentration at intermediate time (kg/m^3)
C_u	Uniformity coefficient (/)
Cr	Courant number (/)
\overline{D}_h	Hydrodispersion tensor (m^2/s)
D_L	Longitudinal dispersion coefficient (/)
$D_{10,20,50,60}$	Grains diameter through which n°% of the sample is passing (mm)
D_e	Effective diameter (mm)
EC	Electrical conductivity ($\mu S/cm$)
f', f'', f''' and g', g'', g'''	Functions to represents boundary conditions (/)
g	Gravity acceleration (m/s^2)
h	Hydraulic head (m)
h1	Distance to bottom of the control-hydraulic head device before the test (m)
h2	Distance to bottom of the control-hydraulic head device after a certain time (m)
Δh	Difference of hydraulic heads (m)
∇h	Divergence of hydraulic head
$\overline{grad}(h)$	3D gradient of hydraulic head (m)
i	Hydraulic gradient (/)
$l_{(0)}$	Zero intercept
k	Intrinsic permeability (m^2)
K	Hydraulic conductivity (m/s)
K_d	Distribution coefficient (m^3/kg)

K_x, K_y, K_z	Hydraulic conductivity components (m/s)
\bar{K}	Hydraulic conductivity tensor (m/s)
\bar{k}	Permeability tensor (m ²)
L'	Characteristic linear dimension (m)
L_{column}	Column length (m)
mEq	Milliequivalent (concentration)
\mathbf{n}	Normal vector
$n_{\text{eff,flow}}$	Effective flow/drainage porosity (% or /)
$n_{\text{eff,transport}}$	Effective transport porosity (% or /)
n_{tot}	Total porosity (% or /)
P	Pressure (Pa or N/m ² or kg x m/s ²)
Pe	Pecklet number (/)
q	Specific discharge or Darcy's flux (m/s)
$q_{\text{through hole}}$	Flow linking water tank of sandbox to constant head device, through a hole (m/s)
\bar{q}	3D Darcy's flux (m/s)
q'	Volumetric flux per unit volume representing the source/sink terms (m ³ /s)
Q	Flow rate (m ³ /s)
$\hat{Q}_{\text{in/out}}$	In/out-flow in sand tank system (m ³ /s)
Q_{pump}	Pumping rate to apply during sand tank numerical simulations (m ³ /s)
R	Retardation factor (kg/m ³)
M_v	Reaction rate (kg m ³ /s) source/sink
Re	Reynolds number (/)
S_y	Specific yield (/)
S_r	Specific retention (/)
S_s	Specific storage coefficient (m ⁻¹)
$S_{\text{saturation}}$	Saturation degree of sand(s) (/)
t	Time (s, h, day, etc..)
Δt	Time step (s, h, day, etc..)

T	Transmissivity (m^2/s)
T_{xx}, T_{yy}	Transmissivity in the x and y direction (m^2/s)
TR	Rate of tracer recovered (%)
v	Mean velocity of the fluid (m/s)
\bar{v}_a	Velocity tensor (m/s)
$v_{\text{eff,flow}}$	Effective velocity of flow (m/s)
V_{column}	Volume of column (L or m^3)
$V_{\text{mobile water}}$	Volume of mobile water (L or m^3)
$V_{\text{mobile solute}}$	Volume of mobile solute (L or m^3)
V_{pore}	Volume of pores (L or m^3)
V_{void}	Volume of voids (L or m^3)
V_{solid}	Volume of solid within column-samples (L or m^3)
$V_{\text{total sample}}$	Volume of the sample (L or m^3)
V_{tracer}	Volume of tracer detected (L or m^3)
$W_{\text{all filters}}$	Weight comprehensive of all filters inserted in each column sample (g)
W_{column}	Weight of empty column sample (g)
$W_{\text{sand,dry}}$	Weight of dry sand inserted in each column sample (g)
$W_{\text{sand,sat}}$	Weight of saturated sand inserted in each column sample (g)
$W_{\text{sat,column}}$	Weight of each saturated column sample (g)
x	Distance (m)
Y	Chemical, Geochemical and Biological degradation and sorption reactions
z	Elevation (m)
α	Coefficient volumetric compressibility of medium (Pa^{-1} or m^2/N or $\text{m} \times \text{sec}^2/\text{kg}$)
α_L	Dispersivity (m)
β	Fluid/water compressibility (Pa^{-1})
ϕ_{column}	Column diameter (m)
σ	Upstream coefficient (/)
θ	Water content (/)

λ	Decay constant, or reaction rate (time ⁻¹)
ν	Fluid kinematic viscosity (m ² /s)
μ	Fluid dynamic viscosity (Pa·s or N·s/m ² or kg/m·s)
ρ	Particle density (g/cm ³ or kg/m ³)
ρ_{bulk}	Bulk density (g/cm ³)
ρ_{fluid}	Fluid density (g/cm ³)
$\chi(n)$	Porosity function

*“ The best part of research is the excitement of learning something new,
even if that discovery means that my initial hypothesis was wrong. ”*

(Jean Bahr)

*“Don't mind me, I'm from another planet.
I still see horizons where you are drawing borders.”*

(Frida Kahlo)

*“Having problems is a great opportunity.
It's one of the best way to learn .”*

(Herbie Hancock)

Introduction

Groundwater issues are among the most important sustainability studies related to topics considered as critical point for the future of planet Earth (Gleeson et al., 2010). The focus of hydrogeologists is on groundwater resources, which need special care for a sustainable world. Their analysis is mainly focused on two complementary aspects: quantity and quality. For both, lots of field experiments are needed to characterize the water reserves whether in natural or polluted conditions. It requires a combination of geologic and hydrologic information, that can allow to determine the groundwater hydraulic conductivity values, and investigate groundwater flow (either under natural conditions either in presence of pumping wells). This knowledge is a pre-requirement to be able to properly manage groundwater resources, avoiding adverse effects on ecosystems and simultaneously meeting the increase of human demand. Once physical behaviour is analysed, it can be coupled with chemical characterisation studies, in order to obtain a better view of an investigated site.

Hydrogeology is effectively a multi-faces discipline which allows a collaborative work between environmental experts with a broad variety of backgrounds. And generally involves a combination of preliminary geologic knowledge, lab tests, field measurements and modelling. To do so, it is important to develop and promote an educational framework able to meet the multidisciplinary nature of the current hydrogeological problems, starting from demonstration of the basics fundamental concepts of this subject. To fully understand the process of groundwater flow, it is in fact important to better visualize it and thus to scale it down to lab-scale.

The work of this Master thesis begins with a brief overview of the literature which summarizes the challenges of teaching hydrogeology by theoretical lessons coupled with practical experiences both in lab and then in the field, in order to provide the basis for the development of a pragmatic problem-solving approach. This thesis is undertaken in the context of the installation of a 3D physical model at the University of Liège as a support to teaching and research works. Thus, the global aim of the work is to prepare the sand tank set up and support the required conceptual and technical choices. This is a fundamental step in order to be able to pre-dimension real experiments, to give ideas about the magnitude order of the expected results and to check the reliability of mathematical results and/or low-dimensionality models.

The 1st Chapter is dedicated to hydrogeological physical models. Reasons why they exist and issues concerning their use are presented, together with a list of different type of models. The focus turns to the characterisation of them associated to their dimensionality (1D, 2D and 3D). Examples of lab experiences developed are also described, in relation with the theoretical concepts behind.

The 2nd Chapter introduce the 3D physical model (sand tank) financed by the University of Liège. This section briefly show dimensions, set up, construction and support devices used for system optimal functioning. The box is supposed to be a tool to support hydrogeology teaching lessons. Thus it will be lately tested by difference experiments (such as steady state flow stabilization, pumping and tracer tests).

The 3rd Chapter of the document is centred on the characterization of porous aquifer materials, in particular through sand column one-dimensional lab experiments. The analysis aims to find values of bulk densities, total and effective flow porosities, hydraulic conductivities and longitudinal dispersivities for four distinguished types of quartz sands. The difference between the samples concerns the size of the particles. The variation of the previously cited parameters according to the different grain size is investigated. Performed tests are the Constant Head Permeability Test, the Falling Head Permeability Test, and Salt Tracer Test (KCl). The results of those experiences are compared with the ones obtained by empirical evaluations (15 formulas computed) through statistical analysis.

The 4th Chapter is related to the development of a numerical model of the 3D sandbox defined previously, by the use of GMS-MODFLOW-MT3DS. All the issues associated to the construction of this simple model are presented (BC, grid size, number of layers, dry cells, etc..). Since the physical model has not been built in the time frame of this work, no calibration of the model could be performed using actual lab data. Nevertheless, different simulations were run (gradient variation, pumping test at different pumping rates, and tracer test) in support of dimensioning of real experiments. A basic sensitivity analysis is carried on to see the variations of the system's behaviour once parameters are changed.

Chapter 1

Use of laboratory scale physical models as a support to teaching and research in hydrogeology

1. Hydrogeology and lab-scale physical models

Hydrogeology is the science related to the study of water beneath the land surface, taking into account all the natural water cycle and the interference of the different environmental contexts and ecosystems. In groundwater study and management, a deep understanding of physical, chemical and biological processes and their modelling are great challenges, especially in complex environment. Hydrogeology is mostly a descriptive science that attempts to be as quantitative as possible regarding descriptions, but without the possibility (in many or most cases) of guaranteeing the accuracy of predictions: its models are basically only hypotheses. Indeed, analysis tends always to become more quantitative, rather than qualitative, in order to allow a more precise management of real cases. In particular, concerning application on physical models, three main aspects must be considered: processes simulation, scale and objectives.

The development of hydrologic and hydrogeologic models started in the second half of the 19th century, together with the challenge to obtain tools both helpful for **process understanding** and **scenario (what-if) analysis**. In fact, by definitions, models are able to show results of simulated phenomena and can be used to represent several different natural process. Models are moreover applied at an operational industrial level in order to explore interventions such as pollution remediation, water treatment, water source management (treatment, restriction, desalination), etc .

The foundation of model analysis is the **conceptual model**. A conceptual model in hydrogeology is a representation of the hydrogeological units and the flow system of groundwater. Simplifying assumptions and qualitative interpretation of data and information of a site are included in the conceptual model; its development is actually synonymous with site characterization (Thakur et al., 2017). A conceptual model is always necessary to obtain a physical based model, even if simplifications are necessary because a complete reconstruction of the system is impossible.

Generally speaking, the most intuitive type of hydrogeological models are the so called **physically-based models**. Those are scaled-down forms of real systems (Brooks et al., 1991; Salarpour et al., 2011) based on scientific principles concerning energy and water fluxes. To really understand **water movement and processes**, a large amount of detailed quantitative measurements is required at **different spatial and temporal scales**.

A real **aquifer** is defined as a natural underground area/unit of soil where large quantities of ground water are stored and can interact with the soil matrix, filling the spaces between the particles and creating a kind of underwater “pool” of water which can move, even further to

long distances. This water is also frequently exploited as a source of drinking water or as supply for other activities, through pumping wells or draining galleries. The water table is considered as the upper surface of groundwater below which the soil is permanently saturated with water and where the pressure of the atmosphere is equal to the one of the water. This water table normally is fluctuating with seasons and year by year, depending on how much rain has fallen, how much water has been pumped out for human purposes and how much is also used by plants and animals (Tiab et al., 2007). Groundwater flows preferentially through interconnected pore spaces within aquifers. And it may flow at different rates in different types of aquifers. In fact aquifers are not always uniform either horizontally or vertically because differences in composition and in properties are shown. For those reasons several physical representations of them are possible.

Nowadays, physically based models can be coupled with **mathematical models** which can allow pre-dimensioning of experiments as well as **numerical representation** of simulated processes, even associated to larger chronological datasets. Mathematical models are tools able to provide a quantitative framework both for analysing data from monitoring and assess quantitatively responses of the groundwater systems subjected to external stresses (Islam, 2011). Water movements and processes are modelled either by the finite difference approximation of the partial differential equation representing the mass, momentum and energy balance or by empirical equations (Abbott et al., 1986). It is important to note that a hydrogeological model contains many qualitative and subjective interpretations. Proof of its validity can only be achieved by implementing specific research techniques and then constructing a numerical model and comparing the results from the simulation with the effective observations. It is necessary to have a good understanding of the physical system and all the assumptions incorporated in the mathematical equations. Those assumptions typically involve the direction of flow, the geometry of the aquifer, the heterogeneity or anisotropy of sediments/soil/bedrock, the influence of an unsaturated zone, the contaminant transport mechanisms and all the possible chemical reactions (including biodegradation, etc.). The aim is always to reproduce as closer as possible the description given by a conceptual model in a numerical way.

Mathematical models are in fact used in simulating the components of the conceptual model and comprise a set of governing equations representing the processes that occur. Mathematical models of groundwater flow and solute transport can be solved generally with two broad approaches:

- a) **Analytical solution** which gives the exact solution to the problem: for example, the unknown variable is solved continuously for every point in space (steady-state flow) and time (transient flow). Because of the complexity of the 3D groundwater flow and transport equations, the simplicity inherent in analytical model requires non-realistic assumptions.
- b) **Numerical solution** which gives approximate solution to the problem: the unknown variable is here solved at discrete points in space and time. Numerical models are able to solve the more complex equations of multidimensional groundwater flow and solute transport.

Earlier models concentrated mainly on the flow behaviour whereas more recent models allow to deal with water quality issues, through simulation of contaminant transport.

Despite the significant and continuous improvements of tools and techniques, scientific challenges exist as the credibility of field level application of models. This is linked to the uncertainty associated to the conceptualization of the system in terms of boundary conditions, aquifer heterogeneity, external natural event variations, etc.

The strength of hydrogeological physical + associated numerical models is that they can provide output at high temporal and spatial resolutions, and they can be applied to large scale hydrological processes that are normally difficult to observe.

Generally the quality of hydrogeologic models depends on the quality of the information that can be gathered for its construction, which also depends on the availability of both technological and financial resources.

2. Why physical models are useful for

Physical models are developed and applied to simulate situation and therefore studying the fate and movement of groundwater in natural as well as hypothetical scenarios (Currell et al., 2017).

Generally modelling is a very wide term as used and applied in earth sciences. Regarding groundwater flow processes, the theoretical aspects taught in theory can effectively be illustrated in practical lab sessions, as well as in the field. Therefore, students can characterize phenomena at various scales in terms of time and space, and also with different approaches (comparison of several methods and formulas, empirical versus practical).

An integrated pedagogical approach is defined by Gleeson et al. (2012), and then also by Hakoun et al. (2013), as the combination of three class components into one single teaching course. The loop presented in *FIG 1* is the symbol of the cohesive and mutual relation between lectures, practical classes and field works. The continuity of that loop is the triggering point to stimulate the students' interest and curiosity. The three components considered are:

- 1) Lectures and simple exercises, which have the purpose to set the course background and review all main basic notions, enhancing the students' knowledge with new/advanced concepts, and introducing the technical field methodology;
- 2) Practical active lab experiments which aim to develop specific technical skills, introducing the learner to critical thinking, applying the theoretical concepts learned and using the problem-solving logistics related to the unpredictability of each experience (practice and theory are two different domains);
- 3) Field works in order to develop more specific abilities, re-calling all what was learned during the classes.

Hydrogeology benefits from the fact that many important processes can be illustrated and explained with simple physical models. And in fact the use of physical models to perform real-world activities is becoming a central point especially for civil and environmental engineers because it enhances the hands-on learning of groundwater topics (like basic

groundwater definitions, groundwater flow together with the explanation of the Darcy's law, well hydraulics, contaminant transport, and risk analysis).

As a consequence of the possible broader range of students' background (wide range of earth sciences) who may attend a standard hydrogeology course, it is necessary to start to demonstrate the groundwater basic concepts early in the teaching. In fact, a survey conducted amongst academic hydrogeologists indicates that the greater part of the crucial topics in a hydrogeology course are associated to groundwater flow processes such as hydraulic conductivity determination, Darcy's law, gradient of heads, and transmissivity (Gleeson et al., 2012).

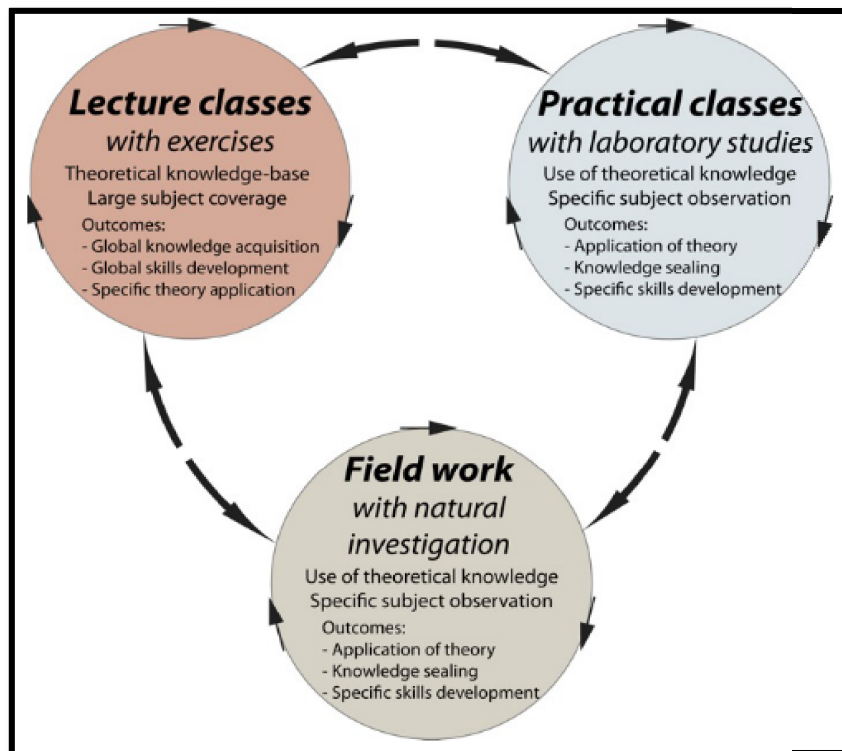


FIG 1 Integrated hydrogeology pedagogy associated to an iterative loop over three class components. Within this iterative loop, each component supports the others with chains of mutual feedback. Inspired from Gleeson et al. (2012) and Hakoun et al. (2013).

Computer simulation depends after all on the programmer and on a list of assumptions made in selecting or deriving appropriate parameters for equations. Whereas with a physical model seeing nature at work is believing. However, the physical model is only an approximation of the reality, it could provide deep understanding of concepts and behaviours that could lately be extended to many other situations.

Finally, physical models like groundwater tank, column of soil etc. are useful not only as demonstrator but also as an instrument around which projects and dissertation work can be arranged (Parkinson, 1987).

3. Dimensionality-based classification and examples of application

The numerous physical models are usually classified based on dimensionality: 0D, 1D, 2D, 3D. Lab experiences linked to them are going further and further increasing the model dimension, in the understanding of phenomena, gradually extending the validity of concepts and knowledge behind.

The easiest one that can be studied are the **0D batch models**, where there is just a mix of water, sediments and chemicals. Through them are basically analysed only the reactions and not the flow. It can be investigated the different behaviour of several contaminant types: a dissolved contaminant (represented by liquid dye), a dense non-aqueous phase liquid (DNAPL) (represented by molasses), and a light non-aqueous phase liquid (LNAPL) (represented by olive oil). For example, a simple test aquifer model can be implemented in a beaker (*FIG 2*): in this way it is possible to compare at least two different models, in terms of movement and remediation of the three aqueous contaminant types cited before, by applying simple pump-and-treat to each contaminant spill.



FIG 2 Aquifer model constructed by students for the groundwater remediation lab activity (Hilton, 2008)

1D models are then still very simple to be described, in terms of experimental set up and lab experiences implemented. They are basically and primarily used to prove Darcy's Law which is one of the most essential concepts in hydrogeology, thus a prerequisite before moving towards more complex issues. Demonstrations were always given firstly through one-dimensional fluid flow models applied to saturated columns of porous media. The experimental apparatus is called **permeameter**, but other similar devices can be used, such as simple, inexpensive, high resistant plastic transparent **columns**. Those can have various dimensions (in length and diameter). Through them many relations and parameters can be studied: hydraulic gradient, porosity, fluid viscosity, particle size influence, volumetric flow rates, etc. (Werner et Roof, 1994; Nicholl et al., 2016).

In column experiments water is free to flow through the pores between soil particles in accordance with Darcy's empirical law (more theoretical notions behind are presented in the *paragraph 4 and 5 of Chapter 1*, concerning flow and transport equations).

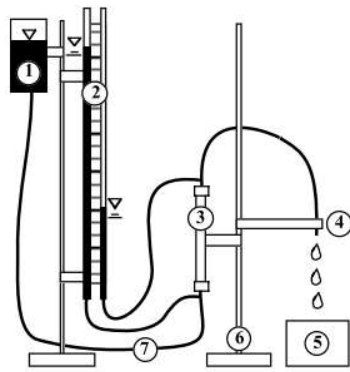
The hydraulic conductivity (K) is a specific parameter used to quantify how well the water flows through a soil medium. It basically depends on the average size of the pores through the soil matrix, on how well the particles fit together, and on the temperature of the surrounding environment which is directly linked to the viscosity of the water (Akbulut, 2016). Those influences can be analysed through soil-column experiences, performing the same kind of test in different soil samples at different conditions.

Research and studies focused on 1D column experiments are the most ancient ones, and they are still widely used to compare and determine values of K and porosity (total, effective and of transport). Basically the flow is driven only by the hydraulic gradient, therefore, orientation of the sample in terms of gravity and references have no effect on the flow rate. Of course where the flow must pass across several different layers of materials, the one with the larger K is dominating the system (Nicholl et al., 2016). Once the Darcy's law is proved, it is possible to move towards more complex problems related for example to transport phenomena. Also tracer test, both with ideal conservative tracer and with contaminants, can be implemented in order to obtain flow and transport parameters estimation (such as the dispersivity coefficient).

For K values estimation two main types of tests can be developed: the Constant Head Permeability Test in *FIG 4*, mainly for medium-coarse soils (Domenico et Schwartz, 1990; Ritzema, 2006; Cai et al., 2015; Hussain et Nabi, 2016; Nicholl et al., 2016); and the Falling Head one in *FIG 3*, which is more specific for finer type of medium (Stibinger, 2014; Johnson et al., 2005).

Other laboratory tests on soil-columns have been performed also to study the dispersion properties of uniform porous media, both in steady and transient flow conditions. The majority of experiences were tested in uniform matrix like glass beads (Rumer, 1962; Harleman, 1963; Lepage, 2013), sands (Blackwell, 1962; Harleman, 1963; Wierenga et Van Genuchten, 1989; Khan et Jury, 1990; Costa et Prunty, 2006; Kasteel et al., 2009; Mastrocicco et al., 2011; Steyl et Marais, 2014; Cai et al., 2015; Kanzari et al., 2015) and gravels (Rumer, 1962). Also analysis on non-uniform soils are available (Raimondi et al., 1959; Legatsky et Katz, 1966; Ujfaludi, 2010; Steyl et Marais, 2014; Mastrocicco et al., 2011).

The majority of all those studies are developed in saturated soil columns, but there are also researches on unsaturated samples (Childs et Collis-George, 1950; Vachaud, 1968; Philip, 1969; Swartzendruber, 1969; Parlange, 1971; Sakellariou-Makrantonaki, 2016). At the same time only a few attempts have been made to study the effect of non-uniform soil structures on the dispersion characteristics (Raimondi et al., 1959; Legatsky et Katz, 1966) even though natural soils, in most cases, consist of non-uniform particles (Ujfaludi, 2010). More details about procedures, equipment, and theory behind those applications will be presented in *Chapter 3* while describing the work performed on four different types of sand.



Apparatus for measuring hydraulic conductivity

Fluid levels are in black, Numbered components and details are as follows:
 (1) Fluid source (constant head reservoir, pump).
 (2) Manometers - open ended tubes, clear plastic, attached to a vertical meter stick (note: capillary effects in small diameter tubes complicate reading the fluid levels).
 (3) Permeameter
 (4) Exit point - contact with atm.
 (5) Outflow container to measure the flow rate (Q).
 (6) Support.
 (7) Clear flexible tubing is used for all lines to facilitate locating and purging air bubbles.

FIG 3 Apparatus for hydraulic conductivity determination: Falling head test (Nicholl et al., 2016)

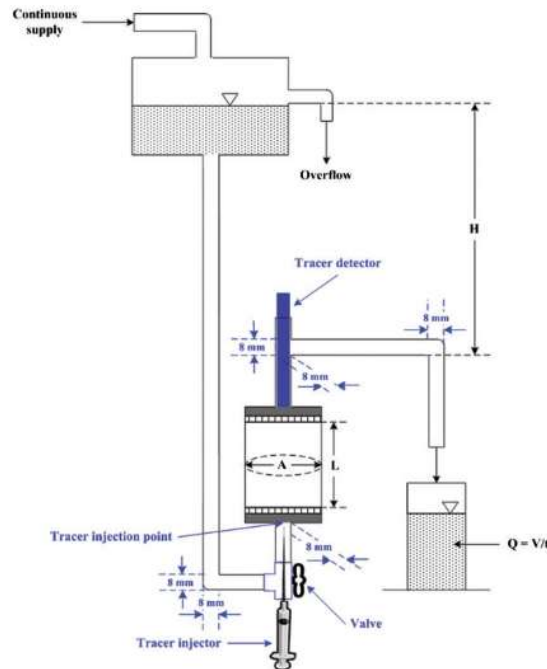


FIG 4 Experimental setup of Constant-head test (black) and Tracer test (black and blue) (Cai et al., 2015)

Concerning representations of physical aquifer, there are both 2D and 3D physical models, differentiated by an increase of complexity (substantial increment in the thickness).

To study and understand some of those basics cited concepts among aquifers, a broad range of experiments can be performed primary in physical **2D models**: influence on the water content in the unsaturated zone, quantitative determination of hydraulic properties as the storage coefficient and the saturated hydraulic conductivity, runoff process, significance of recharge and discharge areas for groundwater, drought period simulation, rain infiltration (through the use of an hand shower device), piezometric head variations, saturation of the system, pumping test (with the simple use of a syringe or a peristaltic pump), and injection

of tracer for transport parameter estimation (conservative tracer and probe recordings) (Hilton, 2008).

Typical dimensions of those considered 2D models are going from 40 cm up to 2 meters in length, from 20 cm up to 1 meter in height, and around few centimetres of thickness. As a consequence, the thickness is generally negligible compared to length and height and parameter associated to phenomena and behaviours in this direction are not investigated.

As usual, in physical 2D model different soil layers are included: some are made by fine sand and some are coarse generally sand or gravel. In other cases, also karst, clay and silt can be present. The majority of those 2D physical models have two aquifers (as it can be seen in the schematic representations in *FIG 5*): an unconfined one, and a confined artesian one along the bottom. In fact, by inter-layering materials with different hydraulic properties multi layer aquifers can be created, confined and unconfined or artesian, porous or fractured (Farrell, 1997).

Many example of concepts and related demonstration experiences are reported in documents as “*Curriculum Guide to the Sand Tank Groundwater Model*” provided by Lane (n.d.), in “*Groundwater flow demonstration model*” written by Farrell (1997), in “*Physical models for classroom teaching in hydrology*” by Rodhe (2012). Furthermore Parkinson (1987) described an experimental sand tank developed for demonstrating the groundwater flow to drains under simulated rainfall.

Many variation of those open-sand plexiglass containers really exist (pictures inserted in **Annex 0**): they allow to study the influence of different geological structure or human build structure, etc.

The flow system for the kind of physical sand tank described is basically driven by two constant head reservoirs, one at each end side of the sandbox. Those types of systems are generally capable of maintaining constant head boundaries simultaneously by ponding water at the top in addition to fixing the hydraulic heads in the two constant head reservoirs (Illman et al., 2010).

Groundwater solute transport studies can also be carried on, with advection and dispersion being the first two mechanisms to be analysed, once groundwater flow is characterized. Then contaminant plume movement can be investigated through multiple sampling or directly visualized (Hilton, 2008).

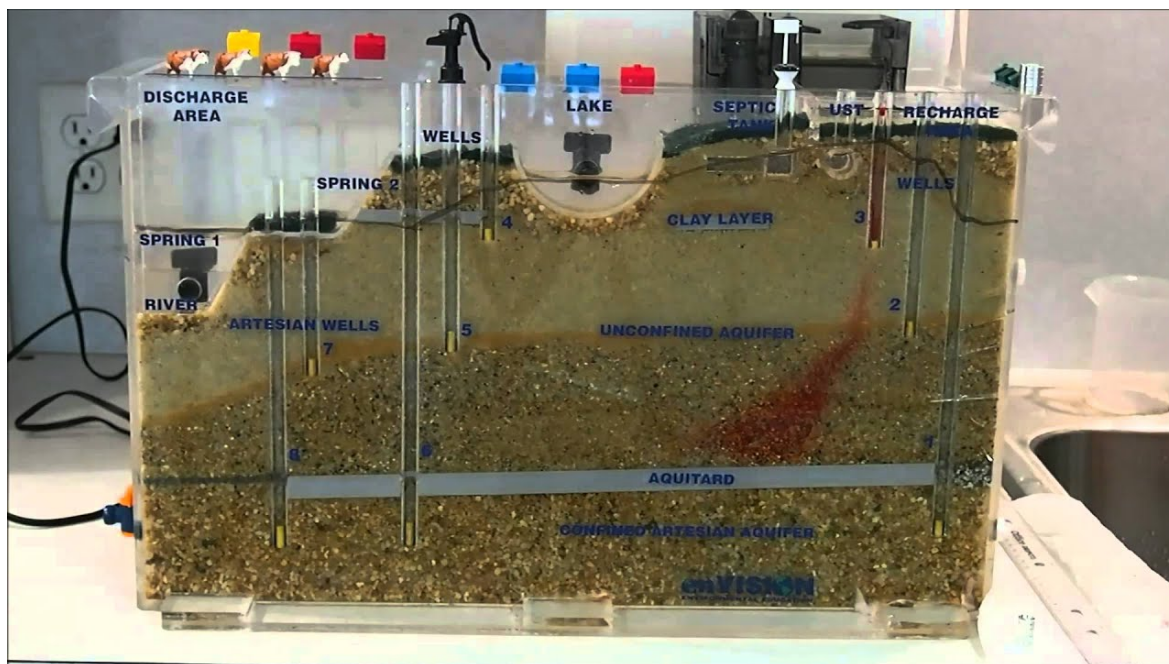
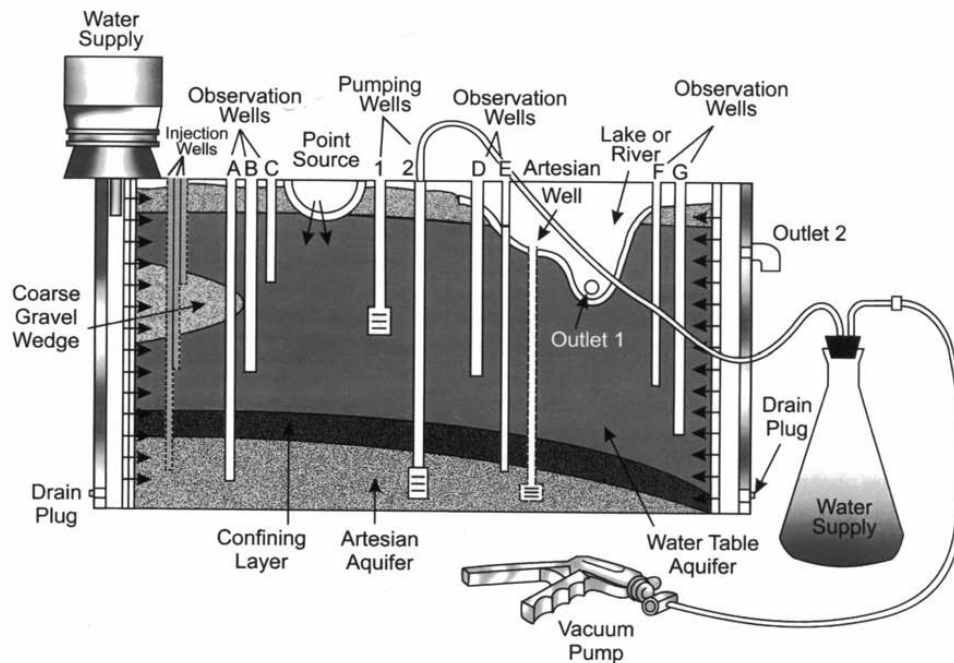


FIG 5 Physical 2D model of an aquifer: scheme + real example (sources : Lane, Guide to Sand tank, and <https://etc.usf.edu/clippix/picture/front-view-of-the-groundwater-model.html>, consulted in July 2019)

3D sandboxes can also be used to observe various fluid flows and thus to validate some solute transport algorithms. Again several different experiences can be simulated, such as a simple steady state stable flow, transient flow, solute transport, pumping tests, flux measurements, etc. Early studies utilize uniform packing of sands to create a homogeneous medium and uniformly heterogeneous packing (Silliman et Simpson, 1987; Schincariol et Schwartz, 1990; Illangasekare et al., 1995, Illman et al., 2010).

More recently, also complex heterogeneity patterns have been packed by various researchers (Welty et al., 1997; Silliman et al., 1998; Chao et al., 2000; Barth et al., 2001; Danquigny et al., 2004; Fernández-García et al., 2005). In heterogeneous sandbox aquifer, simulation of the variability of hydraulic conductivity as a function of space, for understanding and predicting solute transport can be implemented.

Many different implementations are possible: uniform sand, layered sand, and two or plus media containing intermixed regions of coarse and fine sands. Different source zone release conditions can be arranged by modifying the hydraulic conductivity of the injection near field, while the surrounding hydraulic conductivity field remained unchanged. Then the injection of tracer into the source zone should be followed by measuring concentrations as a function of time at the location where tracer was injected and in a detection zone located farther downstream (FIG 6). The resulting breakthrough curves can be characterized in terms of transport parameters (equations in *paragraph 5*) (Gueting et Englert, 2011).

Many experiments to investigate saltwater intrusion and mixing of different densities fluid were also studies on 3D box filled by sand or glass beads (Luckner et Schestakow, 1991; Brakefield, 2008; Goswami et al., 2011).

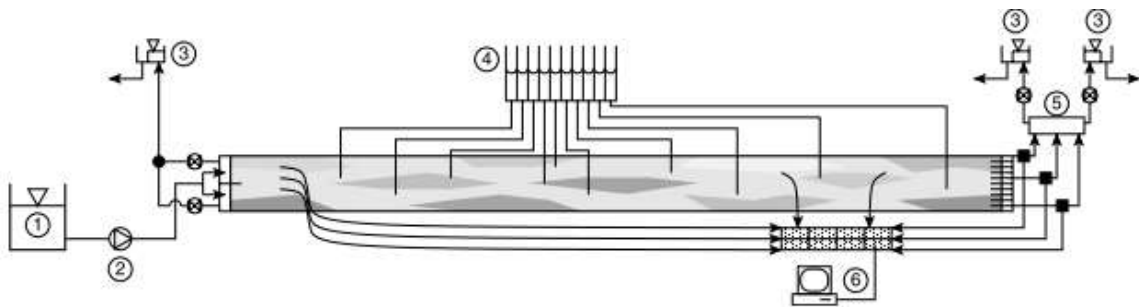


Figure ⇨ Sketch of the experimental setup: 1, storage container with tracer solution; 2, dosing pump; 3, constant-head tanks; 4, piezometer board; 5, hydraulic switchboard; and 6, fluorimeters and data acquisition system.

FIG 6 Experimental sandbox set up (Jose et al. 2004)

3D sand tanks are also exploited to measure groundwater fluxes in a well bore of reference (FIG 7). Based on theoretical predictions and experimental evidence, researchers have been using 3D physical models to validate many groundwater flow velocity and fluxes measurement techniques such as:

- 1) For **FLUX** (passive techniques)
 - i. *Passive flux meters PFM* (Kearl, 1997; Graw et al., 2000; Hatfield et al., 2004; De Jonge et Rothenberg, 2005; Basu et al., 2006; Borke, 2007; Wu et al., 2008)
 - ii. *iFLUX cartridges* (Verreydt et al., 2017)

- 2) For **FLOW RATE** and then **FLUX** (dividing the flow measured by the superficial surface of flow)
 - i. *Borehole dilution methods* (Drost et al., 1968; Grisak, 1977; Giercsak et al., 2006 ; Pitrak et al., 2007)
 - ii. *Point dilution method PDM and Finite volume FVPDM* (Batlle-aguilar et al., 2007; Piccinini et al., 2016; Jamin et Brouyère, 2016-2018)
 - iii. *Direct velocity tool DVT* (Essouayed, 2019)

- 3) For **FLOW VELOCITY**
 - i. *Colloidal borescope CB* (Kearl, 1997)
 - ii. *Point velocity probe PVP* (Labaky et al., 2007; Devlin et al. 2010-2012) and *In-well PVP* (Devlin et al., 2018)
 - iii. *Acoustic doppler velocimeter ADV* (Kraus et al.,1994; Wilson et al., 2001)
 - iv. *Laser doppler velocimeter LDV* (Momii et al., 1993)
 - v. *Heat-pulse flow meter* (Hess, 1986; Kerfoot, 1988)

The added value of lab-scale physical models compared to field-scale experiments is the feasibility: physical models in fact need less time to completely show results of an experience. Thus they allow easier and faster demonstration of concepts and allow direct observations of phenomena. Through them an immediate understanding of water-soil behaviour and interactions is possible. A preliminary approach to get closer to problem-solving and practical issues, starts also to be developed through those experiences in lab. On the other hand, field experiments are closer to reality and allow to develop strategy to deal with practical projects (real site dimension and heterogeneity, real equipment and set up of investigations, etc...).

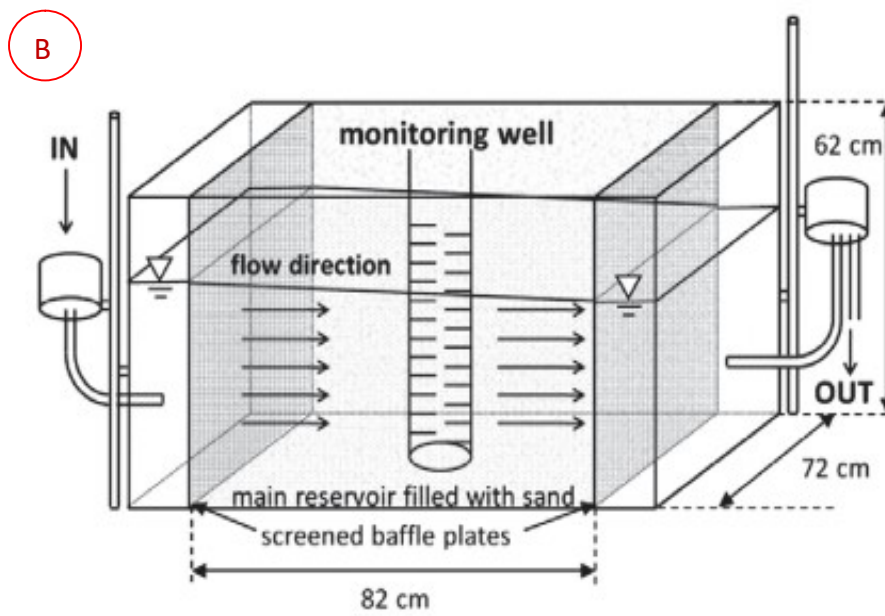
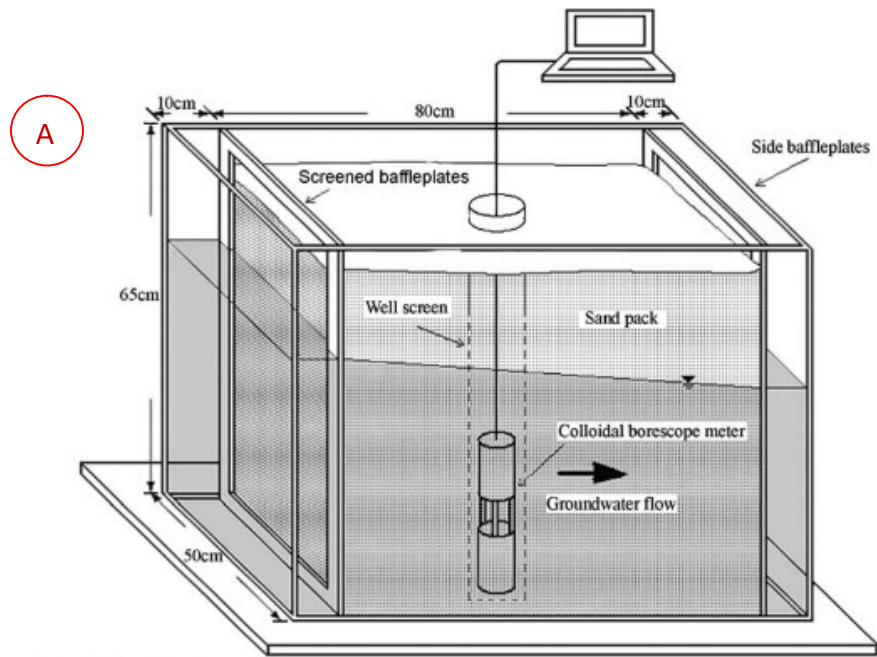


FIG 7 Lab-scale flow tank: A-Colloidal borescope (Wu et al. 2008) and B-Monitoring well (Verreydt et al. 2015)

4. Description of flow equations and associated parameters

While building a numerical model as a reference of a physical system, there are some characteristics to assure. Firstly the model has to be both physically and numerically consistent, meaning that it has to be based on conceptual choices able to simplify the reality in an efficient way and the errors tend to zero for decreasing mesh increments and time steps. It has to be accurate (lower modelling errors), and with quite high resolution. Groundwater flow equations behinds models, are then generally associated to representative elementary volume (REV), which is a finite volume of geological medium used to quantify different properties associated to it. To define a REV, generally the medium should be both continuous and porous, because equations are developed in a continuous dimension. In MODFLOW, the software used in this work, this REV is generally associated to each cell of the model implemented. Additionally, the presented case is related to lab tests, so the used scale is a *macro scale*, generally ranging between centimetres to few meters, and able to be representative for medium properties. A list of the most relevant ones and their description is reported. All mentioned variables and parameters are defined here, therefore once they will be mentioned afterwards in the documents no further explanations will be given.

4.1 Bulk and particle densities

The *bulk density* (ρ_{bulk}) is defined as the dry soil weight divided by the volume of solid soil together with the pores. For mineral soils it commonly ranges from 1.1 to 1.5 g/cm³, and it increases with depth. It tends also to be high in sands and low in soils containing a relevant amount of organic matter. Furthermore, it is conditioned by the process of compaction: higher degree of it tends to raise the value of ρ_{bulk} . It is also known that the high bulk densities generally correspond to low porosity.

The bulk density differs from the so called *particle density* (ρ), which is the volumetric mass of the solid soil that does not take in account the pore spaces and represents the average density of all the minerals composing the soil. For most soils, this value is around 2.65 g/cm³, mainly because quartz has a density of 2.65 g/cm³ and it is usually the dominant mineral. Particle density varies little between minerals and generally it does not have a big practical significance, except in the calculation of pore space.

4.2 Porosity: total and effective

Total porosity (n_{tot}) is the portion of the soil volume occupied by pore spaces. It is generally quantified as a percentage. This property does not have to be measured directly since it can be calculated using values determined for bulk density and particle density with the formula:

$$n_{tot} (\%) = 100 - (\rho_{bulk} / \rho) \times 100 = 100 - (\% \text{ solid space}) \quad (I)$$

Total porosity can be classified as primary or secondary. The primary one is associated to the deposition of the sediments and includes interconnected pores together with the isolated ones, whereas secondary porosity is formed after and includes cavities produced by several phenomena as the dissolution of carbonates, fracturing, etc. Secondary porosity is not considered in the presented case (especially during column experiments described in Chapter 3) because of the homogeneity of the soil used for each sample (sorted sand) and the configuration of the system (as a 1D column experiments).

Effective flow/drainage porosity ($n_{\text{eff,flow}}$) is the portion of the total void space of a porous material in which is really passing the fluid. Effective flow porosity exists mainly to explain the fact that a fluid in a saturated porous media will not flow through all voids, but only through the interconnected ones. It is expressed as a percentage and it is basically calculated as:

$$n_{\text{eff,flow}} (\%) = \frac{V_{\text{mobile water}}}{V_{\text{total sample}}} \times 100 \quad (\text{II})$$

The un-connected spaces are known as dead-end pores and their presence and quantity depend on particle size, shape, and packing arrangement. There is also a portion of fluid contained in interconnected pores which is held in place by molecular and surface-tension forces. This portion is generally known as "immobile" fluid volume and it is not part of the real fluid flow. In many practical cases such as the calculation of travel time of difference substances through porous materials, requires knowledge of this effective flow porosity (Stephens et al., 1998). Effective or either kinematic flow porosity usually cannot be measured in absolute terms so normally it refers to the volume of fluid released by drainage of a saturated medium after a finite interval of time. The formula to analyse is:

$$n_{\text{eff,flow}} (\%) = \frac{q}{v} \times 100 \quad (\text{III})$$

where small v is the mean velocity of the fluid (m/s) and q is the specific discharge or Darcy's flux (m/s), calculated as $q = Q/A$ in which Q is the flow rate (m^3/s) and A , the area section (m^2).

Total porosity generally increases with decreasing grain size, and the portion of interconnected pore space with respect to the total pore space, following the definition :

$$n_{\text{tot}} (/) = S_y + S_r = n_{\text{eff,flow}} + S_r \quad (\text{IV})$$

where the specific yield S_y (which is $< n_{\text{tot}}$) which is either dimensionless either a percentage, and represents the volume of water released from storage by an unconfined aquifer per unit surface area of aquifer per unit decline of the water table (Bear, 1979). This equals the effective flow porosity in case of unconfined aquifer ($S_y = n_{\text{eff,flow}}$). Then, S_r is the specific retention or either retention capacity (dimensionless or a percentage), calculated as the ratio between the volume of immobile water divided by the total volume of the sample.

Normally another parameter can be defined: the effective transport porosity ($n_{eff,transport}$), which is lower than the effective flow porosity, which is lower than the total porosity. This parameter is expressed as a percentage and it is calculated as:

$$n_{eff,transport} (\%) = \frac{V_{mobile\ solute}}{V_{total\ sample}} \times 100 \quad (V)$$

where the volume of mobile solute is generally lower than the volume of mobile water.

4.3 Hydraulic head

The hydraulic head (h), also called water head or either piezometric head, under the hypothesis of an homogeneous incompressible fluid, describes the potential energy of the system at any point. It is calculated as :

$$h = z + \left(\frac{P}{\rho_{fluid} \times g} \right) \quad [\text{in m}] \quad (VI)$$

where z is the elevation (m) above the reference chosen, g is the value of the acceleration of gravity (equals to 9.81 m/s^2), P is the pressure ($\text{Pa} = \text{N/m}^2 = \text{kg} \times \text{m/s}^2$) and ρ_{fluid} is the density of the fluid (taken as 1000 Kg/m^3 in case of water). Practically speaking, the hydraulic head can be defined as the height above the reference level to which the fluid will rise in a manometer, and it is given by the sum of the altitude or elevation plus the pressure head.

4.4 Darcy's Law, Hydraulic conductivity and effective velocity

The Darcy's Law, which firstly describes 1D laminar flow through any kind of saturated porous medium (such as rocks, soil, ...) is one of the most essential concept in the study of hydrogeology. Henry Darcy in 1856 performed his original experiments in the context of municipal water filtration for the city of Dijon, France. Unable to find an existing relation between flow rate and filter size, he performed a series of experiments to have several data available for calculations. Briefly the experiences consisted in pressurized water entering the top of a sealed vertical column filled with sand and exited through a tap at the bottom. Using manometers, Darcy measured the hydraulic heads (h) at the inlet and outlet section of the column. Through those experiments, for a chosen type of sand, he observed that the flow rate (Q) is proportional to the cross-sectional area of the column (A), to the difference between measured water levels inlet and outlet (Δh), and to the inverse of column height ($1/L_{column}$). He discovered that the coefficient of proportionality is varying depending on the type of sand used. In particular he pointed out that generally a coarser sand have a larger coefficient of proportionality than a finer one. This Darcy's coefficient of proportionality is the so called hydraulic conductivity (K).

Hydraulic conductivity (K) is one of the principal and most important soil hydrological parameter. It is a relevant factor for the evaluation of the water flow, infiltration processes and transport within a medium. Hydraulic conductivity is generally expressed by units of velocity (m/s or cm/s or m/h, etc.).

Fluids tend to flow towards the decreasing hydraulic head, therefore the need to put a negative sign in Darcy's equation (in order to make volumetric flow rate Q a positive quantity) while describing the hydraulic conductivity:

$$K = \frac{-Q \times L_{\text{column}}}{A \times \Delta h} = \frac{-Q}{A \times i} \quad [\text{in m/s}] \quad (\text{VII})$$

Where i is the hydraulic gradient (obtained as $\Delta h/L_{\text{column}}$), and L_{column} is the column length (m).

Subsequent to Darcy's original experiments, in case of porous media it was discovered that measures of K increase with ρ_{fluid} and are inversely proportional to fluid dynamic viscosity (μ in Pa·s or N·s/m² or kg/m·s). So in 1940 the scientist Hubbert suggested the existence of an innate material property called intrinsic permeability (k) that is linked to the hydraulic conductivity through the ρ_{fluid} , μ and g :

$$k = \frac{K \times \mu}{\rho_{\text{fluid}} \times g} \quad [\text{in m}^2] \quad (\text{VIII})$$

Darcy's flux (q) in 1D system (such as columns) can be expressed as:

$$q = K \times i = K \times \frac{\partial h}{\partial x} \quad [\text{in } \frac{\text{m}}{\text{s}}] \quad (\text{IX})$$

Where x is the distance taken in the direction of the groundwater flow. Equation IX assumes that flow occurs through the entire cross section of the material without regard to solids and pores. However, Darcy flux is not the actual fluid velocity in the porous media, but it is just discharge rate (Q) per unit cross-sectional area.

A scheme of the Darcy's Law is reported in the FIG 8.

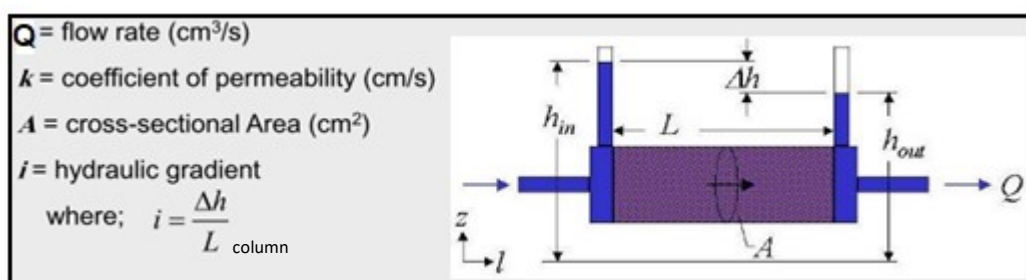


FIG 8 Darcy's Law (source: PPT Permeability in soils, Geotechnical Lab, Civil Eng Texas University)

The extension to 3D case is associated to eq. (XII) where the 3D Darcy's flux \bar{q} (m/s) equals:

$$\bar{q} = -\bar{K} \times \overline{grad(h)} = -\bar{k} \frac{\rho_{fluid} \times g}{\mu} \times \left[\overline{grad\left(\frac{P}{\rho_{fluid} \times g}\right)} + \overline{grad(z)} \right] \quad (X)$$

and \bar{K} is the so called hydraulic conductivity tensor (as well as \bar{k} is the permeability tensor) associated to the directional components of the parameter, therefore used to express anisotropy (heterogeneity) or isotropy of the investigated porous medium. Moreover, the 3D gradient of hydraulic head $\overline{grad(h)}$ is composed by $(\frac{dh}{dx}; \frac{dh}{dy}; \frac{dh}{dz})$.

The actual seepage velocity of groundwater, also named effective velocity of flow $v_{eff,flow}$ (m/s) depends on the real portion of mobile fluid and on the available cross-sectional area through which the flow is occurring. Its value is estimated as:

$$v_{eff,flow} = \frac{K}{n_{eff,flow}} \times \frac{\Delta h}{L_{column}} = \frac{q}{n_{eff,flow}} \quad \text{in [m/s]} \quad (XI)$$

Usually the K-values are strictly dependent both on fluid properties and on material(s) properties. Moreover, in case of soil layers, vertical degree of permeability is very often different from the horizontal one because of the presence of vertical differences in terms of structure, texture, porosity of the soils. Only in some structure-less soils, as the case of sands, the K is considered to be the same in all directions.

Another important observation is that Darcy's law is not valid when the flow is not laminar, for example when $Re > 1$. Reynolds number Re is a dimensionless quantity used in fluid mechanics to help to predict flow patterns in different fluid flow situations. It is :

$$Re = \frac{\rho_{fluid} v L'}{\mu} = \frac{v L'}{\nu} \quad (XII)$$

Where L' is the characteristic linear dimension (m) and ν is the kinematic viscosity of the fluid (m^2/s).

4.5 Groundwater flow in steady state conditions

Under steady state conditions, meaning where no variations of the system over the time are considered, the groundwater flow equation is a composition of the Darcy's law and the conservation of water (in terms of mass or volume, equals in- and out- flows). Those conditions represent the equilibrium and stabilization of a system, thus there are no changes in storage. While implementing steady state conditions, initial conditions will not really affect the final results. However, a good initial condition will lead to a fast and stable convergence of the numerical solver.

There is no time dimension because there are no variations in time, so results are easier to be visualized. And certainly errors in the model set up could be more evident in the final results.

$$\nabla(\rho_{fluid} \times K \times \overline{grad(h)}) + \rho_{fluid} \times q' = 0 \quad (XIII a)$$

$$\frac{\partial}{\partial x_i} \left(\rho_{fluid} \times K_{ij} \times \frac{\partial h}{\partial x_j} \right) + (\rho_{fluid} \times q'_i) = 0 \quad (XIII b)$$

Where q' represents a flux which can be imposed by external conditions (recharge, pumping, etc..). Both sum terms are in $kg/(m^3 \times s)$. Eq (XIII b) is just the indicial notation of eq. (XIII a), with $i, j = x, y, z$. To solve this equation normally the fluid density is taken as a constant, and the main variable is the hydraulic head, so the formula can be rewritten (in a reference system x, y, z) as eq. (XIV), where all terms of the sum are in s^{-1} .

$$\frac{\partial}{\partial x} \left(K_{xx} \frac{\partial h}{\partial x} \right) + \frac{\partial}{\partial y} \left(K_{yy} \frac{\partial h}{\partial y} \right) + \frac{\partial}{\partial z} \left(K_{zz} \frac{\partial h}{\partial z} \right) + q' = 0 \quad (XIV)$$

Where K_x, K_y, K_z are the hydraulic conductivity components along x, y, z axes which are assumed to be parallel to the major axes of K .

4.6 Groundwater flow in transient conditions: transmissivity and storage

While dealing with transient state, thus with system variations over time, it is important to introduce the concept of transmissivity (T) measured in m^2/s . It is roughly defined as the rate at which groundwater flows horizontally or vertically through a medium. It is function of K (respectively horizontal or vertical) and the thickness of the layer (b in meters). Generally speaking it is defined as:

$$T(x, y) = \int_0^{b(x,y)} K(x, y, z) dz \quad (XV)$$

So, in case of confined aquifer with a known thickness it equals the product of $K(x, y)$ and $b(x, y)$. But in case of unconfined aquifer the variable b is substituted with h and an iterative process should be started in order to find the solution (convergence).

The other fundamental parameter to take into account is the specific storage coefficient (S_s) in m^{-1} . It represents the volume of water removed from a unit volume of an aquifer for a unit drop in hydraulic head and it is calculated as:

$$S_s = \rho_{fluid} \times g \times [\alpha + (\beta \times n_{tot})] \cong \rho_{fluid} \times g \times \alpha \quad (XVI)$$

Where α is the coefficient of volumetric compressibility of the medium (reference values for sand are taken from Freeze and Cherry (1979) ranging between 10^{-9} and $10^{-7} Pa^{-1}$ or m^2/N or $m \times sec^2/kg$), β is the water compressibility (equals to $4.4 \times 10^{-10} Pa^{-1}$). Given the fact that the contribute of $\beta \times n_{tot}$ is negligible, only the formula with α can be used.

The global equation of 2D horizontal groundwater flow under transient conditions (variation of storage), is eq. (XVII) in case of confined aquifer:

$$\nabla(T(h) \times \nabla h) + q'' = S_s \frac{\partial h}{\partial t} \quad (\text{XVII})$$

That, in indicial notation (i,j = x,y,z as before) is equal to:

$$\frac{\partial}{\partial x_i} \left(T_{ij} \frac{\partial h}{\partial x_j} \right) - q_i'' = S_s \frac{dh}{dt} \quad (\text{XVIII a})$$

$$\frac{\partial}{\partial x} \left(T_{xx} \frac{\partial h}{\partial x} \right) + \frac{\partial}{\partial y} \left(T_{yy} \frac{\partial h}{\partial y} \right) - q_i'' = S_s \frac{dh}{dt} \quad (\text{XVIII b})$$

And eq. (XIX) in case of unconfined aquifer, $S_s \approx S_y \approx n_{eff,flow}$ as the case simulated in this study:

$$\nabla(T(h) \times \nabla h) + q'' = n_{eff,flow} \frac{dh}{dt} = S_y \frac{\partial h}{\partial t} \quad (\text{XIX})$$

That, in indicial notation, again considering a 2D horizontal transient flow, becomes:

$$\frac{\partial}{\partial x_i} \left(T_{ij} \frac{\partial h}{\partial x_j} \right) - q_i'' = n_{eff,flow} \frac{dh}{dt} = S_y \frac{dh}{dt} \quad (\text{XX a})$$

$$\frac{\partial}{\partial x} \left(T_{xx} \frac{\partial h}{\partial x} \right) + \frac{\partial}{\partial y} \left(T_{yy} \frac{\partial h}{\partial y} \right) - q_i'' = S_y \frac{dh}{dt} \quad (\text{XX b})$$

Where q'' the volumetric flux per unit volume is always representing the source (recharge) and sink (leakage) terms (s^{-1}), and T_{xx} and T_{yy} is transmissivity in the x and y direction. And S_y specific yield is the volume of water released from storage by an unconfined aquifer per unit surface area of aquifer per unit decline of the water table (Bear, 1979), and it is generally equals to effective flow porosity $n_{eff,flow}$ in case of unconfined aquifers. It represents the measure of the “free water” drained by gravity. Both S_s and S_y are applied at all the tank/physical model modelled, no difference are made between void, borders and sand. Furthermore they are coincident in case of unconfined aquifers.

Groundwater flow in aquifers is often modelled as 2D in the horizontal plane, due to the fact that most aquifers have horizontal dimensions hundreds of times greater than the vertical thickness. In such a case, the z component of the velocity associated to the groundwater flow, is comparatively small. Therefore the flow equations (XVIII a) and (XX a) can be rewritten respectively as eq. (XVIII b) for confined aquifer, and (XX b) for unconfined one.

4.7 Boundary Conditions for flow problem

Three main types of boundary conditions BC's can be defined in case of flow problems:

1. Dirichlet conditions: prescribed piezometric head, that can vary with space and time. In the presented case only conditions of this type are implemented.

$$h(x, y, z, t) = f'(x, y, z, t) \quad (\text{XXI})$$

2. Neumann conditions: prescribed flux (first derivative of h) or piezometric gradient normal to the concerned boundary, its value can vary in space and time. It can be equal to zero in case of impervious boundary (as it is in some cases of this study).

$$\nabla h \cdot \mathbf{n} = \frac{\partial h}{\partial n}(x, y, z, t) = f''(x, y, z, t) \quad (\text{XXII})$$

3. Cauchy or mixed conditions: flux depending on piezometric head. It is a linear combination (through two coefficient B and C) of the previous two equations concerning h and its first derivative. It is never used in this study.

$$B \times \frac{\partial h}{\partial n}(x, y, z, t) + C \times h(x, y, z, t) = f'''(x, y, z, t) \quad (\text{XXIII})$$

5. **Description of forward transport equations**

5.1 Solute transport equations

Solute transport is usually a very complex process to study, especially at the field scale because of the presence of several physical-chemical and biological processes that may happen in the soil-water system and their possible variation over space and time (Stanko et al., 2013). In case of water flow presence, the two main mechanism of transport that have to be studied are advection and dispersion. In presence of only advection, the solute is moving with the same velocity of the fluid (water) following the flow stream. While dispersion represent the spreading of the solute around the source and the extension of the path/plume of its propagation. Few basic concepts and knowledge on the equations behind those cited transport mechanisms are reported hereafter (Zheng, 1990; Burnell, 2002; Igboekwe et Amos-Uhegbu, 2012; Dassargues, 2018 and 2019). The global equation is:

$$R \frac{\partial C^v}{\partial t} = -\nabla(C^v \overline{v_a}) + \nabla[\overline{D_h} \times \nabla C^v] + \frac{M_v}{n_{eff,transport}} - R\lambda C^v \quad (\text{XXIV})$$

Where, R is the retardation factor (/), C^v is the volumetric concentration of solute (kg/m^3), $\overline{D_h}$ is the hydrodispersion tensor (m^2/s), M_v is the source/sink of solute mass linked to

groundwater flow rate exchanged with the external world or resulting from chemical reactions and immobile water effects/matrix diffusion ($\text{kg}/\text{m}^3\text{s}$), \overline{v}_a is the advection velocity tensor (m/s) and λ is the decay constant, or reaction rate (s^{-1}). Generally, the 1st term on the right hand side represents **advection** transport, thus it describes the movement of solutes at the average seepage advection velocity of the groundwater flow. The 2nd term indicates the change in concentration due to **hydrodynamic dispersion**, defined as the sum of mechanical dispersion and molecular diffusion. The 3rd term is the effects of mixing with a source fluid of different concentrations at a precise recharge or injection point. And finally the 4th term indicates all degradation reactions effects.

Relationship between the adsorbed and dissolved concentrations can be incorporated into the transport model by the introduction of a retardation factor, R (dimensionless):

$$R = 1 + \frac{\rho_{bulk}}{n_{eff,transport}} K_d \quad (XXV)$$

In which K_d is called distribution coefficient (m^3/kg).

Eq. (XXIV) represents the solute transport governing equation based on assumption that the possible reactions can be limited to equilibrium-controlled sorption. Solution is identical without sorption effects. For a given general equation, there is an infinite number of possible solutions. For steady state flow, the unique and appropriate solution is one that matches the particular boundary conditions of the conceptual model. For transient flow system and for solute transport, also initial conditions are required to obtain the unique solutions of heads and concentrations.

5.2 Longitudinal dispersivity

Dispersion can be defined as a mechanical mixing process caused by the fluid portion that is following the tortuous path (geometrical complex interconnections of flow channels causing variations in terms of velocity). In an isotropic medium, dispersion takes place both parallel and transverse to the direction of the mean flow. So generally two physical parameters are used to express this effect: the longitudinal (D_L) and transverse (D_T) dispersion coefficients. However the dispersion process has a complex influence especially in non-uniform media and mainly within samples with a discontinuous grain-size distribution. Literature tests (Seuntjens et al., 2001; Stumpp et al., 2009; Severino et al., 2010) always present a linear relationship between D_L and the seepage/filtration velocity (u), both for uniform and non-uniform soil samples.

Dispersivity is important because pressure propagation affects directly the driving force for flow. It can be estimated through the interpretation of ideal tracer tests performed in 1D soil-columns. This parameter is generally scale dependent, so in case of lab column experiment will be related mainly to the length and areal variations. A research from Vanderborght and Vereecken (2007) demonstrated that for the short travel distances (from 0 to 30 cm), the dispersivity clearly increases. However, this increase was not occurring for long travel distance. It is also observed that dispersivity increases with an increase in flow rate in fine-textured soils and decreased in coarser ones (Fashi, 2015).

Empirical relationships between the dispersion coefficients and characteristics of the media can be established (Fried et Combarous, 1971). In particular, in case of uniform and homogeneously distributed soil the relationship between the values of D_L (in units of m^2/s) and groundwater flow velocity v (m/s) is a direct proportion expressed generally by the formula:

$$D_L = \alpha_L v^m \quad (XXVI)$$

where α_L is the dispersivity (measured in length units such as m and the value of the exponent m equals values closed to one. Harleman (1963) noted that the exponent m tends to unity with increasing value of uniformity coefficient associated to the granulometric distribution of the particles in the soil sample (presented in the section associated to the empirical formulae used to determine K-hydraulic conductivity values).

5.3 Boundary Conditions for a solute transport problem

Given the complete analogy with flow problems, there are 3 main types of BC's:

- Prescribed concentration (Dirichlet), that can vary in space and time. It is the most used in this study case. A value of concentration can be prescribed, at the place of a mass flux $M_{solute} = q_{solute} C^v_{solute}$.

$$C(x, y, z, t) = g'(x, y, z, t) \quad (XXVII)$$

- Prescribed 1st derivative of the concentration (Neumann), which represents a way to prescribe hydrodynamic diffusion-dispersion mass flux through the boundary. The concentration gradient normal to the boundary can vary in space and in time. In many case this set equal to 0, thus the advection flux at boundaries is computed by the code.

$$\nabla C^v \cdot \mathbf{n} = \frac{\partial C^v}{\partial n}(x, y, z, t) = g''(x, y, z, t) \quad (XXVIII)$$

- Prescribed relation between concentration and its 1st derivative (Cauchy or Mixed), a combination of the previous two. It is never used in the simulations presented after.

$$D \times \frac{\partial C^v}{\partial n}(x, y, z, t) + E \times C^v(x, y, z, t) = g'''(x, y, z, t) \quad (XXIX)$$

Explanation on applied solute transport solving methods are reported in **Annex I**.

Chapter 2

Set up of the physical model to be developed

This section is entirely devoted to the presentation of the physical 3D model that has to be developed at the University of Liège. The aim is to have a tool that can be used in two main fields of application:

- Teaching: to implement hand-on lab experiments to enhance student learning and concepts understanding
- Validation of groundwater investigation techniques

Dimensions, construction, material to insert and functioning are explained hereafter. Then in *Chapter 3*, the focus is on the characterisation of four different types of sands through 1D column experiences. Due to that, a more reasonable choice of the sand to implement in the sandbox can be done, according to the purpose of the experiences (test to perform, technique calibration, etc...). Finally in *Chapter 4* the numerical model developed for this sandbox is presented, and discussion on few lab-experiments are shown.

1. Dimensions

Within the presented work, it is aimed to build a PMMA tank to represent an unconfined sand aquifer. Precise quotation of this 3D model, together with pictures of the empty box, are reported in *FIG 9*.

- Total dimensions of the box are 1470 mm length x 830 mm width x 815 mm height
- Total space that can be filled by sand 1200 mm x 800 mm x 800 mm
- Water reservoirs at two opposite sides 100 mm x 800 mm x 800 mm

As it is possible to see from the plan, several holes should be designed to allow different connections:

- Inlet pipe,
- Outlet pipe,
- Excess flow pipes,
- 24 Control points (mesh of 6 x 4, 200 mm x 200 mm)

More details and specification on components and set up are reported in *FIG 10* and *FIG 11*.

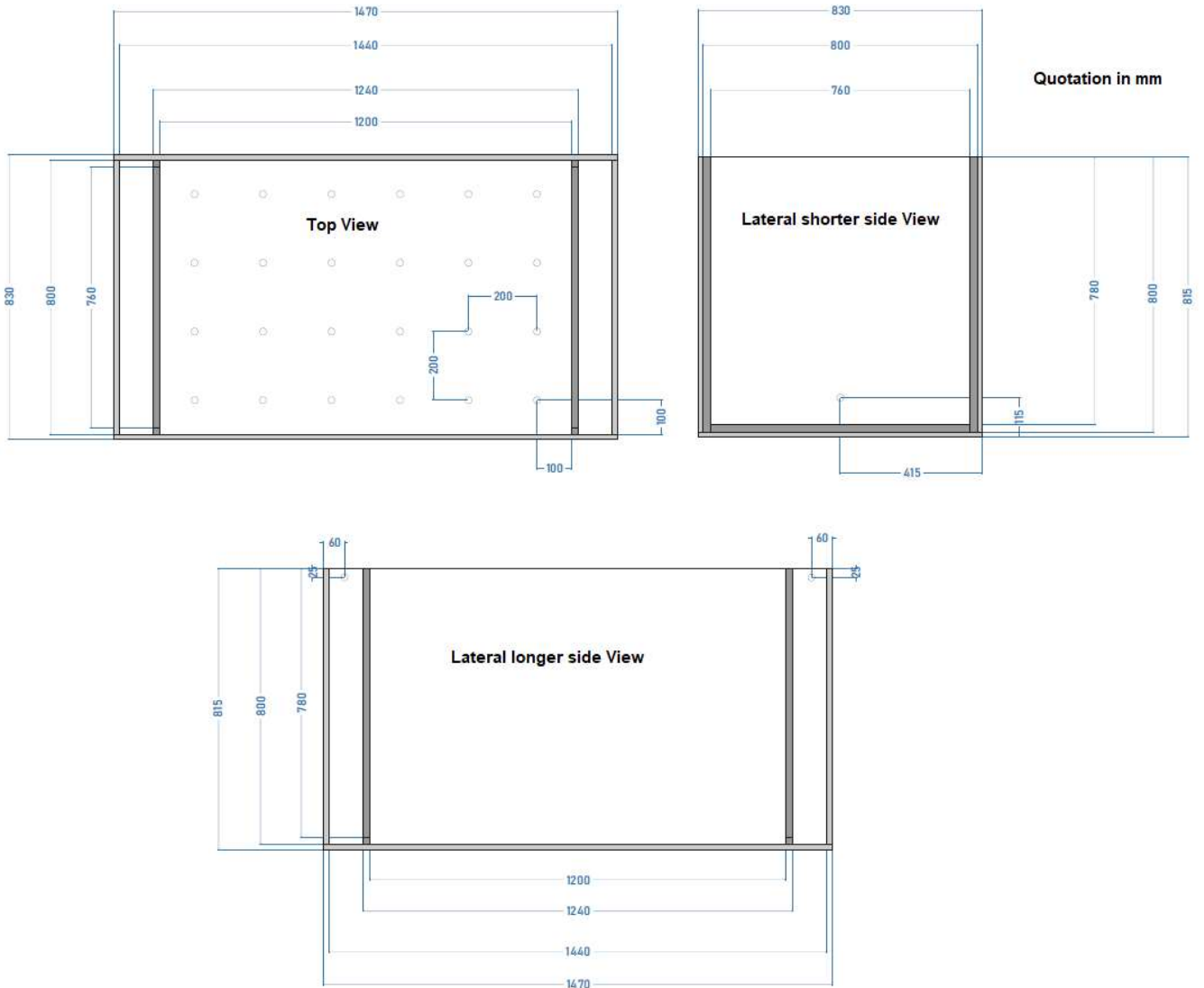


FIG 9 Dimensions and pictures of the sandbox developed at ULiège

2. Construction

The flow-through tank in *FIG 10* (analogous to Kearn 1997; Graw et al. 2000; Labaky et al. 2007; Wu et al. 2008; Verreydt et al, 2015) is made by Poly Methyl Methacrylate (**PMMA**), also known as Acrylic, or Acrylic glass, or **Plexiglass**. It is a transparent thermoplastic often applied in sheet-form, used as a lightweight and shatter-impact-resistant alternative to glass. But it can be also used as in casting resin, inks and coatings. It is generally considered as one of the clearest plastics on the market and technically speaking is classified as a non-crystalline vitreous substance. Sheets are easily heat formed without loss of optical clarity. Implementation of additional longitudinal or either transversal supports (such as strings) might be useful in order to avoid larger deformations of the tank due to sand and water pressures.

The tank is equipped with screened baffle plates, coated with very permeable and not degrading mesh material, separating the sand from the water reservoirs at both ends of the tank. This perforated mesh has to be installed at the wall of communication between sand and water reservoir. And it serves as a porous media/water interface to provide hydraulic control.

The box is supposed to be filled with sand until the height of 70 cm, through which water is circulated in a closed system (saturated system). The flow-through tank should be filled under saturated conditions, to avoid air entrapment and layering.

Inlet and outlet heads are regulated by adjustable height containers. These head regulators are supplied with water pumped from a reservoir. The water levels in the regulators are kept constant by overflow pipes, with excess water spilling back to the reservoir (located close to the aquifer). Then some additional reservoirs can be added to efficiently supply water throughout the length and thickness of the sandbox (as well as a constant or variable recharge could be added).

The water supply should be adjusted to enable a minor water volume discharge and to avoid large water level variations. Inflow and outflow holes to realize water supply connections are supposed to be large enough to allow the passage of the desired inflow/outflow. A maximum exit flow should be dimensioned in order to evacuate which kind of circulation pump is needed.

Nylon soft pipes of different diameters and length are used as connections.

Several control piezometers can be installed inside the box. There are already 24 holes in the bottom of the tank are connected to transparent plastic pipes, which provide the opportunity of visual observations and monitoring of the water levels during tests (*FIG 10*). Monitoring wells can also be added in strategic position (in *FIG 11* one central well is draw). In case of simple pumping test and tracer test, one injection well and one observation point are enough to determine K and dispersivity, even if certainly, having more observations allow a better and more precise interpretation. Central line position should be taken firstly, and then further implementation could be done in other more "random" positions, depending on the expected results and aims.

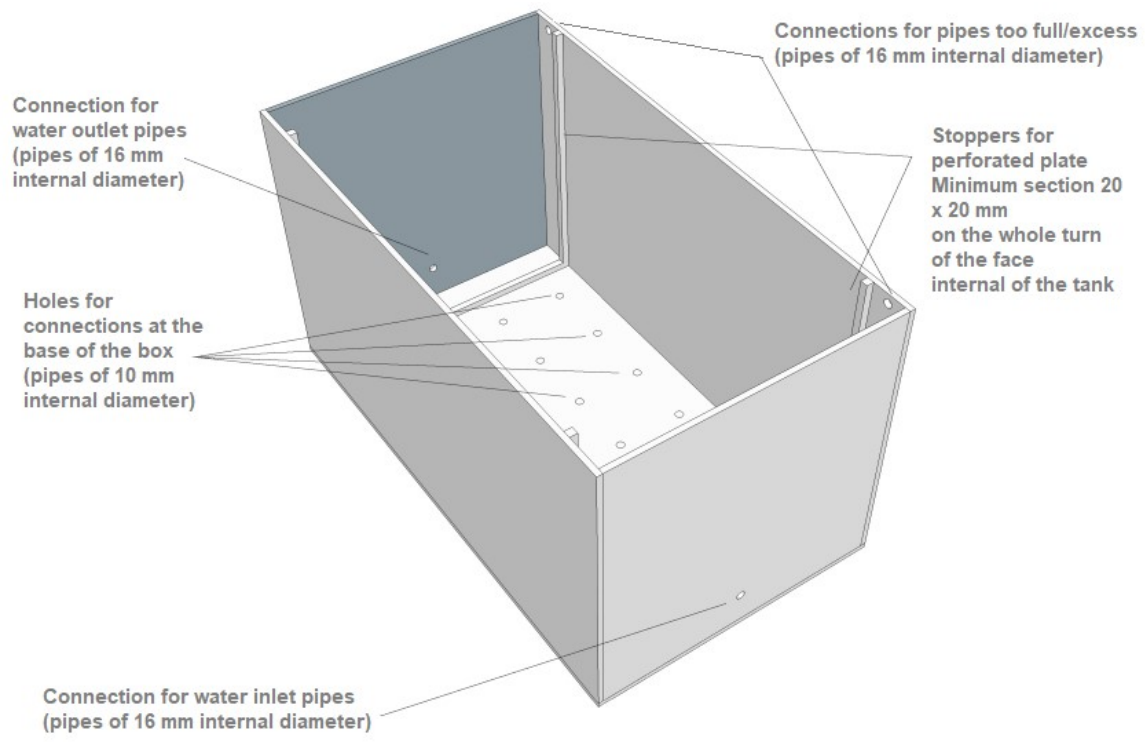


FIG 10 Sand tank holes and connections

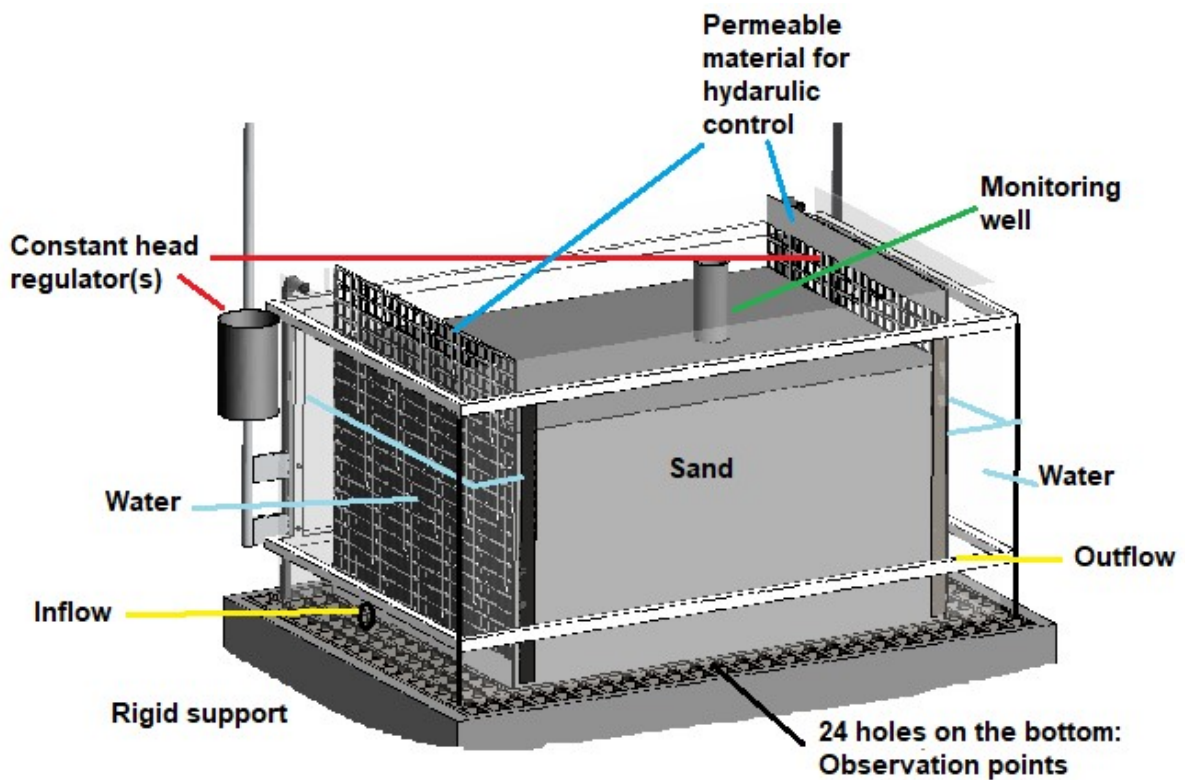


FIG 11 Components view of the sand tank (modified from iFLUX, 2018)

3. Filling material

In order to provide a good functioning of the model, it is important that the hydraulic conductivity of the medium is high enough to give a quick response in the groundwater level and groundwater flow due to changes in the boundary conditions (heads, rate of simulated rainfall). Furthermore, the flow through the aquifer should be possible to be accurately and rapidly measured in terms of volume. And finally also the solute effective transport velocity should be high enough to allow tracer experiments to be performed in a reasonable time.

Sand is taken as the porous media to be implemented in the 3D physical model. In general, sand is a very convenient material to study the properties of flow in porous media: it is easy to work with, and the relatively large K values allows visible amounts of flow to occur even in a short interval of time. Thus the evidence of the relationship between Δh and Q can be really shown at lab scale experiences. Moreover, high flow rates can be applied and that condition allow to perform a large number of experiments and so to have a larger range of data to be compared.

The sand is made by quartz and bought from EUROQUARTZ (<http://www.euroquartz.be>): four different types of sands are previously characterized, due to a lack of technical datasheet, through 1D column experiences (described in *Chapter 3*). The chosen granulometry is ranging between 0.5 - 1 mm.

4. Control of the hydraulic gradient

The water flux through the sand tank has to be realized by creating an hydraulic head difference Δh between inflow and outflow reservoir. The hydraulic gradient must be controlled by constant-head devices connected to the two (both inlet and outlet) small water reservoirs through the drainage holes. Open overflow apparatus (*FIG 13*) or more common Mariotte bottles (*FIG 12*) can be adopted.

The Mariotte bottle consists in a sealed reservoir with an outlet siphon and air inlet, both submerged in the fluid. When flow is initiated, air enters through the inlet tube to replace the fluid leaving the reservoir. Therefore the fluid level in the reservoir does not drop below the bottom of the inlet connection, and also the fluid pressure at the bottom of the air inlet remains equals to the atmospheric one. This effect produces flow at constant head, even though the fluid level within the reservoir is decreasing.

The difference is that using a Mariotte bottle, there is no direct contact between water and air before the fluid is entering the system. With an overflow open device, the water is in contact with the atmosphere, which can a bit influence the experiment (for example: there is an higher possibility that air bubbles could enter the system and influence the parameters determination). Generally, various methods such as pump + water tank or either a direct connection to the sink can be used to supply the fluid to those systems.

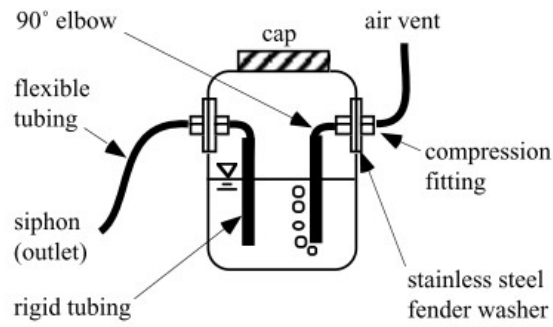


FIG 12 Mariotte Bottle used to keep and provide constant hydraulic head (Nicholl et al.2016)

Finally it was decided to built and assembled open overflow devices to provide the constant head (FIG 13). Water is provided continuously until a constant water level is reached, and the overflow of the water in excess is minimal, constant, and allow a laminar flow to be established.



FIG 13 Constant head open overflow devices

Chapter 3

Sand Column Experiments

In this chapter is reported a practical overview of the lab experiments performed on columns of sand including Constant Head and Falling Head Permeability Tests, and Tracer Tests. The followed procedure is described step by step, starting from the type of sands tested and their preliminary granulometric and empirical analysis. Discussion and observations, together with statistical analyses are included.

It is chosen to separate the study of the sands according to the particle grain size. The difference between the four sand tested is visible, and that helps to better understand the influence of pore size especially on hydraulic conductivity (Nicholl et al., 2016). Preparation of the columns is described (trials, problems encountered and improvements applied). Any numerical model of those 1D column systems is developed because results obtained from physical models are commonly considered reliable.

1. Preliminary studies on available sands

The investigated sands are all quartz sands from EUROQUARTZ (<http://www.euroquartz.be>). The only difference affects the grain size: the maximum particle size is supposed to be 5.6 mm and the minimum 0.1 mm. Therefore, according to the standard British Soil Classification System based on particle size, it can be said that the sands analysed are mainly classified as medium and coarse one. Only one type is having a small fine fraction.

Basic Soil Type	Sub-Type	Range of Diameter (mm)
Sandy	Fine sand	0.06 to 0.2
	Medium Sand	0.2 to 0.5
	Coarse Sand	0.5 to 2.0

TABLE 1 British Soil Standard Classification of Sandy soil

Given that, it makes sense to expect that in term of total porosity and hydraulic conductivity not a big difference will be seen between the four samples. The lower hydraulic conductivity and the lower both total and effective porosities are supposed to result for the finest granulometry, and then a gradual scale is expected going to the coarser type of sand. The quartz sands selected (in FIG 14) will be followed indicated with the name reported below :

- N1 → particles ranging between 0.1 and 0.5 mm
- N5 → particles ranging between 0.5 and 1 mm
- 1/2 → particles ranging between 1 and 2 mm
- 3/5 → particles ranging between 3 and 5.6 mm



FIG 14 Available type of sands to characterize through column experiments (A,B) and impurities check by sieving (C)

Given the fact that no technical datasheets were provided with the sands, the samples were sieved. Dry sieving was applied, using few specific diameters. Then, an empirical interpretation of the main geotechnical parameters was done. The estimated values were then applied in following empirical formulae implemented to estimate a possible range of variation for K values. The evaluated parameters and main results of sieving procedure are schematized in TABLE 2.

	D ₁₀ (mm)	D ₂₀ (mm)	D ₅₀ (mm)	D ₆₀ (mm)	C _u (-)	I ₍₀₎ (mm)
N1 (0.1-0.5 mm)	0.13	0.15	0.24	0.28	2.15	0.1
N5 (0.5-1 mm)	0.53	0.59	0.7	0.76	1.43	0.5
1/2 (1-2 mm)	1.1	1.2	1.5	1.6	1.45	1
3/5 (3-5.6 mm)	3.2	3.6	4.5	5	1.56	3

TABLE 2 Geotechnical parameters estimated for the four types of sand studied

Values of grading characteristics **D₁₀**, **D₂₀**, **D₅₀** and **D₆₀** are related to the sieving procedure and represent the grains diameter correspondents to the specified quantity of particles/fraction of the sample passing through (10%, 20%, 50% and 60%).

C_u is the so called uniformity coefficient which gives the range of grain sizes in a given sample. Higher values of C_u mean well graded samples with a larger range of particle sizes. The C_u for sands is generally calculated as a ratio and between the size opening that will just pass 60% of the sand, the D60 value, divided by the size opening that will just pass 10% of the sand sample, the D10 value (Been et al., 2009).

I₍₀₎ is the so called zero intercept, which represent the value of the interception between the granulometric curve and the x-axis (Alyamani et al., 1993).

To obtain those parameters values, a graph with the granulometric curves of all sand types was manually and roughly draw in order to have an general idea and estimation. Generally the shape of those curves are not such straight lines, but for the general scope of this work no detailed curves were needed. The choice of making those graphs as straight inclined lines (FIG 15) is done according to the results shown by a study on quartz sands published by Senetakis and others in 2013.

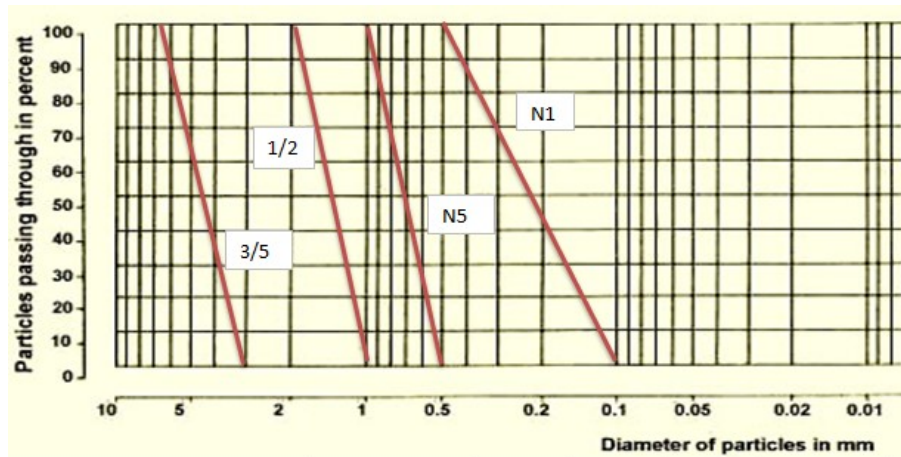


FIG 15 Granulometric Curve to determine geotechnical parameters of all studied sands

The presence of possible impurities was checked in order to avoid additional problems for the set up of the column lab experiments. To do so, a sieve with spaces of the same dimension as the finest granulometry associated to each sand type, was used. Those impurities were only founded in the N1 sands. They were mainly just resembling powder and they were a very small portion in comparison to the quantity of sand sample tested (FIG 14C), so they were considered negligible. A table resuming the expected values and range associated to the parameters to determine (K , n_{tot} and $n_{eff,flow}$) is reported, based both on graphical estimations, literature researches and preliminary calculations. Graphs that were used to make those preliminary estimation are shown in FIG 16.

RANGES EXPECTED	
n total	n eff,flow
22 - 45 %	18 - 33 %
K (m/s) : 10^{-6} and 10^{-2}	

TABLE 3 Expected and estimated ranges for sands parameters to be determined

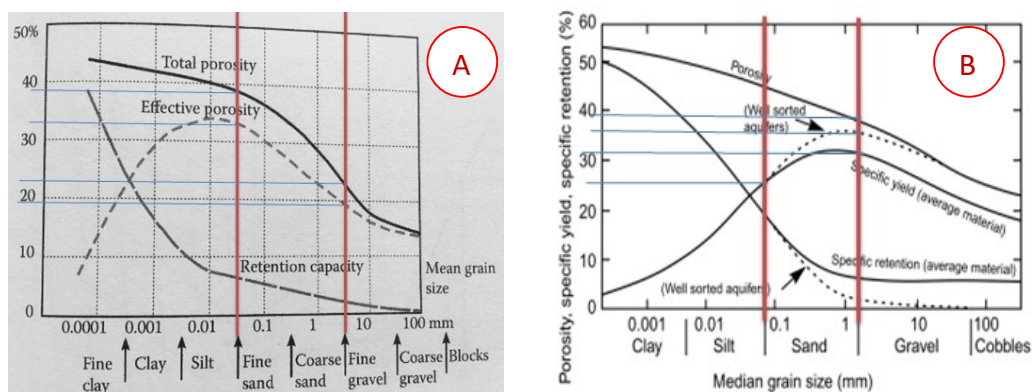


FIG 16 A) Soil type analysis: graph to estimate a priori total and effective porosities, with retention capacity; and B) Aquifer analysis (Eckis, 1934 modified)

2. How to characterise the sand(s)

A list of the main types of test/experiment is reported. They are classified according to the parameter(s) they allow to measure. Parameters definitions are already introduced in *Chapter 1*, therefore here are not present.

A) Bulk density (ρ_{bulk})

To evaluate the bulk density of a medium, many experiments only based on volume and mass computation can be carried on. Bulk density is always dry and it consist of knowing the mass of a certain volume of porous material.

B) Total porosity (n_{tot}) and effective drainage porosity ($n_{\text{eff,flow}}$)

Total porosity n_{tot} can be estimated by simple application of the *equation (1)* reported in *paragraph 4.2 of Chapter 1*. It can be also roughly estimated with column experiments, once the dry column is filled with water and saturated. Knowing the flow entering the system and the height of the samples, the speed at which the column is saturated is directly linked to the total porosity of the medium inside the column. Porosity ratio is multiplied by 100 and therefore expressed as a percent (Gibb et al., 1984). More simply, n_{tot} can be obtained also weighting the saturated volume of porous media and comparing it with the bulk density measurement, using a pycnometer.

Then, the parameter $n_{\text{eff,flow}}$ can be evaluated in laboratory with tracer tests on soil-columns packed with the media to be tested. Samples of outflow water should be periodically collected and undergo for chemical analyses. The Darcy flux can be calculated directly from the steady flow rate and column diameter. Even though the extrapolation of column-test results to field scales is still viewed with some scepticism, those lab experiences can have a didactic purpose. The selected tracer should be conservative and non-sorptive, in order to be influenced only by the flow of water in the porous. Basically speaking, an ideal tracer should be totally un-reactive toward the medium within the column. So no exchange or adsorption reactions should occur and concentrations of a magnitude that cause precipitation must be avoided. Various tracers can be used in laboratory core column studies (fluorescine, uranine, salts as KCl or NaCl, etc..). And, using a common tracer not behaving as water but with specific and known physic-chemical interactions with the medium, either the $n_{\text{eff,transport}}$ can be evaluated through tracer tests on soil columns.

The evaluation of both of those transport and flow effective porosities from tracer tests in small laboratory scale samples is not a common practice. First of all because both parameters show small range of variability in comparison with others, such as K and α_L . And then because the core samples studied are typically very small in comparison with the dimensions of a real aquifer, and so they can be considered non-representative. Furthermore, laboratory cores are almost always analysed in vertical and perpendicular position to the bedding, whereas it is known that aquifer flow and transport are predominantly horizontal in real aquifer. In general, transport and flow parameters (such as flow velocity and porosity, transport velocity and porosity, longitudinal dispersivity) are

really scale dependent. Therefore, column tracer tests may poorly reproduce the site/field conditions. Nevertheless, such lab experiments allow to perfectly apprehend porous flow concept for teaching purposes. In FIG 17 is reported an example of an experimental set up of a tracer test performed on soil columns.

Inverse optimization techniques and implementation of numerical models can be used to interpret tracer tests results and better estimate solute transport parameters. The most used numerical models for inverse modelling are STANMOD (Simunek et al., 1999b) HYDRUS-1D (Simunek et al., 2008), the CXTFIT code (Toride et al., 1995) and TRAC (by BGRM, 2011).

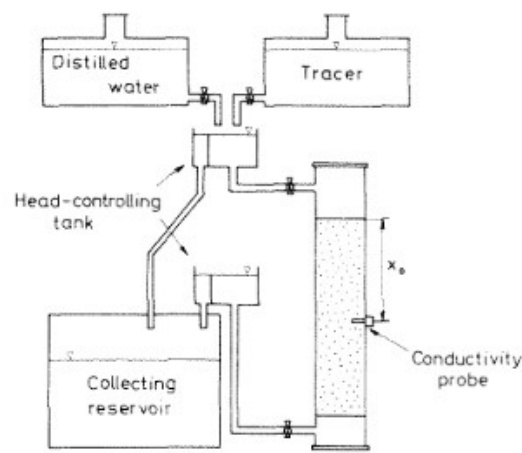


FIG 17 Schematic diagram of experimental equipment for tracer test in soil column (Ujfaludi, 2010)

C) Hydraulic conductivity (K)

Hydraulic conductivity determination of soils can be realized with correlations methods generally called pedotransfer functions, or hydraulics methods applied both in lab and field. The advantage of the correlation-empirical methods is a fast estimation than the direct measurement done through hydraulic methods.

On the other hand, laboratory methods are still fast and cheap, and are used to core soil samples. Then, fields methods, based also on description of the water flow processes, and able to determine K-values around holes made in the investigated soils. The problem with those ones is that the external boundaries and the conditions referred are often not exactly known (Stibinger, 2014).

So field methods are limited for accurate estimation of hydraulic conductivity due to lack of precise knowledge on geometry and hydraulic boundaries of the aquifer. Lab tests are a good alternative, even if they provide lot of problems in the sense of true representative samples (very small volumes in comparison to a real aquifer). Also empirical formulae based on grain-size distribution characteristics are commonly used, because they do not depend on the geometry and hydraulic boundaries of the aquifer (Hussain et Nabi, 2016).

A resuming scheme of available methods to determine K is shown in FIG 18.

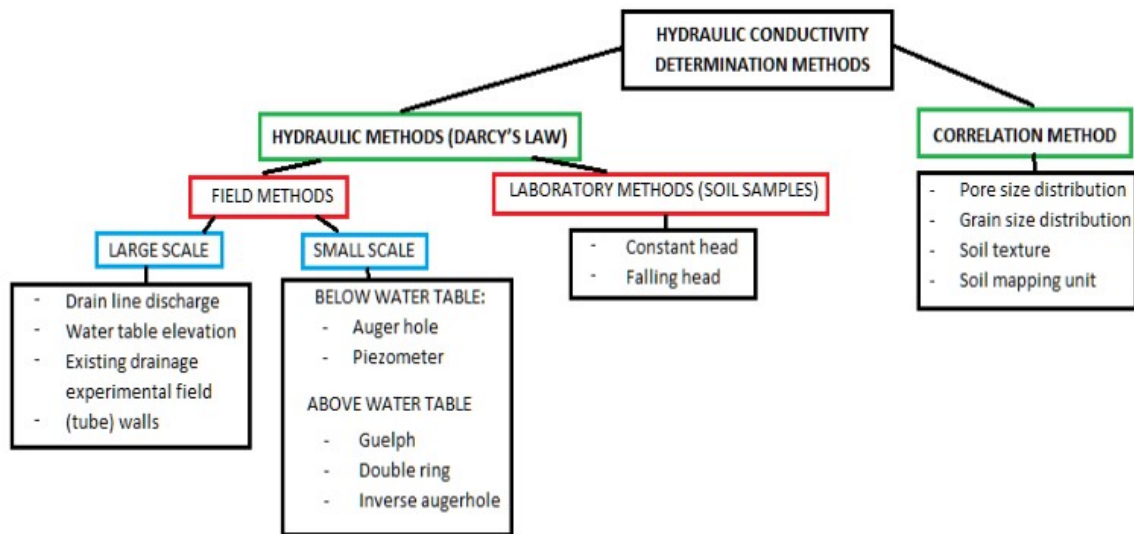


FIG 18 Overview of methods for the hydraulic conductivity determination (Ritzema 2006)

Quantitative laboratory measurements of hydraulic conductivity are typically made with an *permeameters* or *soil columns* (FIG 19), considered as other similar devices, inexpensive, generally simple and easy to be used. Those columns are made of a transparent material (generally plastic instead of glass, for safety reasons) in order to allow better observations in terms of preferential path formation, presence of air, or either flow paths and tracer dispersion while introducing a visible tracer (like a food dye). Columns are generally mounted on a stand that can easily allow changes on the orientation and elevation of the sample. Measurement of K requires that Δh or/and Q are kept constant. Therefore, two main types of tests could be performed: the Constant Head and the Falling Head.

For the **Constant Head** one, at the inlet section of the permeameter/column a device can be used to supply fluid keeping a constant water level (a constant input of water should be assured). Then, connecting the outlet flow to another constant device, the head difference Δh can be easily measured and fixed. While calibrating the experience for different types of sands is it possible that the heights should be adapted and regulated for each set up at different levels. The Constant Head test is used for slightly fine to medium and coarse-grained soils, and it's a test based on the assumption of laminar flow where the hydraulic conductivity is independent of the gradient. The experiment is generally considered in steady state conditions. The system is considered closed in the sense that there is no evaporation. The sample should be fully saturated and as boundaries conditions, also perfectly impermeable lateral boundaries can be assumed. The main disadvantage is that the measured value is considered valid only for the relatively small soil sample, so attention should be put while extending the values to larger scale samples. Furthermore this laboratory method is generally not suitable for samples with either extremely high or either extremely low hydraulic conductivities.

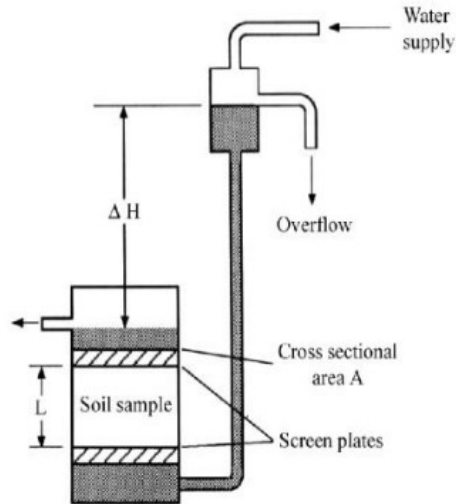


FIG 19 Constant head permeameter (Domenico and Schwartz 1990)

On the other hand, in case of **Falling Head** test, the water head at one of the sides of the column sample decreases with time. The falling head test is mainly used fine-grained soils such as fine sands and silts. The calculation of the hydraulic conductivity is then computed from the flow passing through the sample, and it is related to the head difference measured in time (Stibinger, 2014). Application of this kind of test are mainly related to very fine sands, silty loam and silty clay samples (Johnson et al., 2005). The main limit of this test is that the small sample area generally induces a large random error. Moreover, this laboratory method is only suitable in case of samples with very low hydraulic conductivities.

In the context of this work, a study was performed to investigate the effects of the size (and also the shape of the particles) of sand grains on the hydraulic conductivity. The two different lab tests are performed, and also 15 mathematical models are compared.

D) Longitudinal dispersivity

This parameter can be determined by a soil column tracer test, following the same procedure described above for the effective flow porosity estimations. The interpretation of those tests can be easily done by analytical solutions or by the same automated software already cited, which are able to optimize also the longitudinal dispersivity.

3. Columns preparation

In this paragraph the final set up of the column samples is presented. More details about previous trials, problems and progressive improvements are reported in **Annex II**. Possible extension and amelioration of the procedure are also reported.

3.1 Set up of samples

Column-samples preparation begins with the choice of the **filters** to insert in both the extremities of each column. The filter is necessary to avoid the sand to exit the column during the experiments and it shouldn't have a hydraulic conductivity lower than the tested material. The application of a multi-layer filter (composed by different materials) results to be the best choice. Filters choice is evaluated for each sand type, even if at the end similar set up were done for the 4 different columns. Two porous (plastic) stones of more or less one cm thickness were used in each sample. Highly porous and permeable disks/stones together with the other filter material, must be measured in thickness in order to really see the volume of the column filled by the sand (very important while performing test interpretation). The available material as filters were a squared plastic net, a sponge finer but still very permeable, and different filter papers. Those lasts were excluded because they were too fine compared to the granulometry of the studied sands.

Top filters were added in all the configuration:

- a) For the coarser sands 3to5, 1to2 and also N5, before the stones, four layers of squared plastic net with different orientation were introduced (cut in a circular shape).
- b) For N1 a porous disk in the upper end of the column is coupled with a circular layer of the porous/permeable sponge, to allow the sand not to exit and the sample to be more stable.

Concerning bottom filters:

- c) In samples N1, N5 and 1to2, it was decided to insert two porous stones with the finer permeable sponge (cut in a circular shape a bit larger than the column shape in order to allow the entire coverage of the section and to have borders fold to the sand side).
- d) When for the coarser sample 3to5 sand column the filter is made by 2 porous stones with in the middle the 4 nets layer.

Clear plastic columns 38 cm long and with an internal diameter of 10 cm, were filled by the previously characterized sands. An advantage to use narrow distribution uniform sands is that material will just randomly distributed to fill the column tube, while with a wide distribution of particle sizes it will tend to segregate by size during this procedure.

Different **procedure to fill the columns** were evaluated, in order to have as less air as possible trapped inside the system:

- 1) Sample composed in the way to have it immediately saturated while filling the column: a layer of around 5 cm of water have to be put in the column and then the sand should be inserted with a rotational movement by the help of a funnel.
- 2) Column saturated while filling, then drained (making the water not absorbed free to escape the column) and re-saturated from bottom.
- 3) Column filled with dry sand with the use of a funnel to allow a more uniform sand distribution, and then saturation of the sample from the bottom.
- 4) Column filled by dry sand with the use of a funnel to allow a more uniform distribution of the sand, and each 5 cm layer of sand inside the tube a light compaction (5 shots should be provided by the use of an apposite object in *FIG 24*). This light compacting procedure will allow the particles to arrange better and the sample to be more levelled. So normally less air will be trapped inside it, and the series of possible subsequent settlements is minimized. Once compaction is applied an alteration of the measured parameter may be recorded. It was thus decided only to go for a light compaction (less alteration and more representative of what could be found in a natural environment). The bulk density values can be also modified and especially increased while applying compaction.

At the end the best option resulted to be the 4th one (steps on *FIG 20*).

Valves to regulate the flow and so to open and close the column system were put both in the inlet and outlet side of each column. The presence of those valves allowed the samples to be isolated once the experience was over. Each junction (including the cap of the column, all the valves-tube-column connections, etc..) was sealed by the use of Teflon tape, in order to avoid, or at least minimize, the water losses.

After filling each column with sand, those are connected to the inflow/outflow plastic soft tubes (already saturated), and to the manometers or every kind of devices applied to measure the hydraulic heads.

Plastic anti-escape valves coupled with regulating flux valves (marked www.bucikle.de) were used to keep the system closed and to avoid water to exit the system at both of the two extremities of each column. Then transparent plastic tubes of 0.8 cm internal diameter (1cm external diameter) were attached both in inlet (for total length of 100cm including valves and tubes) and outlet section (for a comprehensive total length of 80 cm).

While **saturating the sample** with water or connecting the column already saturated to the water circulation system, it is important to try to minimize the air entrapment within the sample and the system as well. The trapped air in fact lowers measured hydraulic conductivity by obstructing fluid flow. And the compressibility of air implies also that the degree of obstruction can change with the pressure head: due to that relevant difference in results can be obtained. For all those reasons it is basically better to slowly saturate the sample from the bottom. In order to prevent out gassing within the sample, tap water should be equilibrated to ambient conditions before entering the system. This minimizes temperature effects on viscosity.

Steady-state flow conditions were established and the system was run for at least half an hour before taking all the experimental measures, in order to allow the majority of air to exit the system and to achieve as much as possible the stabilisation of the system.

During operation, column preparation and experiments implementation, each sample was rightly fixed to the support.

Observations:

- The presence of immobile small air bubbles was a constant and also the evidence of some preferential path and dead-end pores.
- The water circulating the system was not “dirty” (full of sand) once it reached the outlet section.
- The system achieved always a good stabilization and was able to provide reasonable results.



FIG 20 Funnel use, compaction, saturation and observation of the final columns preparation

3.2 Possible further improvement and extensions

Few possible further upgrading of the column set up are presented.

In case it is chosen to proceed with the soil-filling of the column with a simultaneous saturation, it would be easier to have a heavier filter in the bottom. To do so a non water reactive metallic (i.e. stainless steel) plate of few cm thickness and with a hole larger than the column flow inlet section, could be attached (glued) to the sponge filter and positioned at the bottom of the column (*FIG 21*). Then the water could be inserted in layer of around 5 cm and small quantities of sands can be added gradually to the column (like 1/10 of the water volume inside the column). With a glass or metallic stick a rotational movement can be also applied when the sand is inserted in order to facilitate the air to go out from the sample. Then few minutes need to be waited before adding the following amount of sand/water. It can be noted that the larger are the sand grains, the easier the air will goes out and less time should be waited to proceed with the following layer.

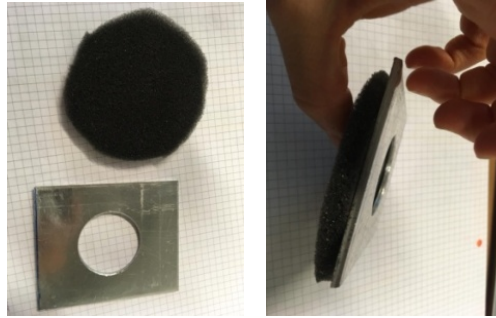


FIG 21 Metallic plate to apply to the filter

To solve the problem of air presence, washing of the system should be applied until a 1:1 ratio of Electrical conductivity is reached between the water entering the system and the one exiting. Or either Carbon dioxide can be applied to enhance air liberation (Behnke et al., 1963).

The equipment and the system can be putted in a high air pressured chamber in order to facilitate the air to move outwards of the column. But particular attention should be put to check if this will not induce high pressures in the column walls which can damage the system. (This application will not be very practical for a teaching experiments.)

Also a void-pump can be connected to the system in order to really be able to let all the air going out of the system. That will prevent the system to interfere with air, but from another point of view will be less representative of what could be found in nature.

3.3 Possible extensions

Many different types of soils and column samples can be analysed. As it is already said several procedures to prepare the sample can be followed. But also other extension can be though. For example the use of several type of sands in only one tube, as a mixed sample. The mix can be random or well-stratified. Even layers and mix of different soil types can be prepared: silt+ sand, gravel + sand, gravel + silt + sand + loess, etc .

Other orientations of the samples can also be evaluated: as for example the diagonal or the horizontal one, instead of the classical vertical one. The flow can also be provided from top to bottom, and many other types of filter can be tested.

Each experience will be able to add knowledge and consciousness on soil-flow-transport parameters behaviour.

4. Results of experiments performed on sand(s)

Having in mind the previous subdivision, hereafter are presented the experiments performed and the results obtained while characterizing the four types of available sand.

First of all few general measurements on the four columns are done, in order to facilitate further calculations.

4.1 Preliminary columns parameters evaluation

For all the column test described, it is necessary to preliminary collect some useful information to be able to compute the parameters estimation (Lepage, 2013). So, while filling and preparing each column-sample, several characteristic parameters of each column and the granular medium they contains were noted. *TABLE 4* is summarizing those characteristics.

Few additional observations on that should be done:

- The filters weight is calculated according to the information given in the *paragraph 3* concerning their composition for each column. It is considered that : one porous disk is equals to 22g, one layer of squared net is 1g and one layer of very permeable sponge material is 2g.
- Each column is weighted three times: empty, filled with dry sand, and also once it is saturated.
- Also the mass of dry sand inserted in each sample is determined.
- The saturation degree $S_{\text{saturation}}$ is always a bit lower than one due to the fact that it was impossible to remove all the air trapped within each sample. Also more of one third of the total volume of each sample is associated to the pore spaces, and that is normal in case of not very fine quartz sands.
- Volume of pores is obtained from total porosity and the volume of the column. Volume of voids is calculated from the weight of sand inserted in each column and the bulk density associated. Therefore the volume of pores (more theoretical) is always higher than the volume of effective voids for each sample.
- Water content of each sand/porous medium studied, is obtained by subtracting from the weight of saturated column, the weight of sand introduced and the weight of empty column (filters and tubes included).

Parameter	Unit	Description	Value
Lcolumn	m	With filters (Without filters)	0.38 (0.36)
W _{sand,dry}	g	Weight of dry sand 3to5 in column	4299
		Weight of dry sand 1to2 in column	4209
		Weight of dry sand N5 in column	4412
		Weight of dry sand N1 in column	4212
Wall filters	g	Weight of all filters, column 3to5	52
		Weight of all filters, column 1to2	50
		Weight of all filters, column N5	50
		Weight of all filters, column N1	70
W _{sand,sat}	g	Weight of saturated sand 3to5 in column	5407
		Weight of saturated sand 1to2 in column	5327
		Weight of saturated sand N5 in column	5531
		Weight of saturated sand N1 in column	5346
W _{sat,column}	g	Weight of saturated column with 3to5	6547
		Weight of saturated column with 1to2	6281
		Weight of saturated column with N5	6578
		Weight of saturated column with N1	6413
W _{column}	g	Weight of empty column+tubes and filters	1041
φ _{column}	m	Internal column diameter	0.10
V _{column}	L	Empty column volume	2.83
e	/	Water content of porous medium obtained by subtracting from weight of saturated column, the weight of sand introduced and the weight of empty column (from top 3to5, 1to2, N5, N1)	0.40
			0.34
			0.37
			0.38
S _{saturation}	/	3to5 sand saturation degree	0.95
		1to2 sand saturation degree	0.86
		N5 sand saturation degree	0.91
		N1 sand saturation degree	0.87
V _{pore}	L	V _{pore, 3to5} = n _{tot,3to5} × V _{column}	1.26
		V _{pore, 1to2} = n _{tot,1to2} × V _{column}	1.28
		V _{pore, N5} = n _{tot,N5} × V _{column}	1.33
		V _{pore, N1} = n _{tot,N1} × V _{column}	1.35
V _{void}	L	V _{void,N1} = V _{column} - V _{solid,N1}	1.14
		V _{void,N1} = V _{column} - V _{solid,N1}	0.95
		V _{void,N1} = V _{column} - V _{solid,N1}	1.05
		V _{void,N1} = V _{column} - V _{solid,N1}	1.07
V _{solid}	L	V _{solid, 3to5} = W _{dry sand,3to5} /p _{bulk,3to5}	3.10
		V _{solid,1to2} = W _{dry sand,1to2} /p _{bulk,1to2}	3.00
		V _{solid,N5} = W _{dry sand,N5} /p _{bulk,N5}	3.04
		V _{solid,N1} = W _{dry sand,N1} /p _{bulk,N1}	2.86

TABLE 4 Summary of columns preliminary measurements

4.2 Bulk density (ρ_{bulk})

Experiment description:

A very simple lab experiment (FIG 22) was performed to determine ρ_{bulk} : a glass with a volume of 0,35 L and a weight of 29.58 g was taken and accurately filled until the top (levelling with a ruler) every time with a different type of dry sand. Then the glass was weighted using a balance with a maximum capacity of 2 kg and a precision of 0.01 g (METTLER PM 2000, LMC 082). For the following calculation only an average/measured value is considered, but it must be said that those results are affected by an error of ± 0.01 g. Once all those weight were recorded, it was calculated the ratio between it and the glass volume. Densities obtained are reported in the TABLE 5.



FIG 22 Bulk density lab evaluation

Values of bulk densities can be lately recalculated in a very similar way also once all the columns are done (taking in account the volume of the empty column, the weight of the column filled, the presence of tubes/valves/filters, etc..). As will be shown in TABLE 6 those values are really close to the other one.

To weight the larger amount of sands and quantify the quantities inserted in each column it was used another balance: METTLER TOLEDO 656, with a maximum capacity of 32210 g and a precision of 1 g. Again, in the calculation only the average value was taken into account, because the range of variation is really small in comparison to the magnitude order of the measurements.

Results:

As it was possible to observe the values of ρ_{bulk} dry medium determined once the columns are set, are always very similar to the values of ρ_{bulk} previously determined in simple lab measurements. It is important to note that only the results of the final set up of the columns were considered (samples dry with layer of 5 cm and few shots for levelling and a bit compacting the sand). That's because the data obtained from the previous arrangements are really similar and do not produce too high variations in the results relevant for this section.

Observing the two reported tables it can be seen that in the first experiment, a scale of densities is measured, and in fact ρ_{bulk} is increasing while the grain size is decreasing. In column experiments, the values are not ordered in scale, that's because the samples analysed are bigger and maybe more error can be done. In further calculus, values of ρ_{bulk} from glass experiment will be considered, as they seems a bit more precise and logic.

Sand type	Volume Glass Container (L)	Weight of Container (g)	Weight of Container + Sand (g)	Sand (g)	ρ_{bulk} (g/cm ³)
3to5	0.35	29.58	515.73	486.15	1.39
1to2	0.35	29.58	519.99	490.41	1.40
N5	0.35	29.58	538.33	508.75	1.45
N1	0.35	29.58	544.37	514.79	1.47

TABLE 5 Results of bulk dry densities evaluation for all the four types of sands studied with glass experiment

Sand type	Column Volume (L)	Weight Column (g)	Weight Column + Filters + Dry sand (g)	Sand (g)	Filters (g)	ρ_{bulk} (g/cm ³)
3to5	2.83	1041	5407	4299	67	1.52
1to2	2.83	1041	5327	4209	77	1.49
N5	2.83	1041	5531	4412	78	1.56
N1	2.83	1041	5346	4212	93	1.49

TABLE 6 Results of bulk densities for all sands studied through column samples

4.3 Total porosity (n_{tot})

Experiment description:

This determination requires the knowledge of the actual density of the sands and the dry density of the granular medium.

The first one, given the lack of sand technical datasheets, is taken from the literature equals to 2.65 g/cm³. While the bulk density values used are the ones measured with the small volume experiment in lab. An average value of the total porosity is estimated.

Results:

The total porosities values are not substantially different comparing the four column, so generally it can be said that a value between 44 and 47 % of total porosity is estimated for those type of sands. Considering reference ranges from Morris and Johnson (1967), which

says that for fine sand the total porosity is generally varying between 26-53%, for medium sand between 29-49% and for coarse sand between 31-46%, the obtained values are reasonable. Moreover these results are considered reliable also according to the dimension of the systems studied and to the small influence of the light degree of compaction applied while preparing the samples.

Results are summarized in *TABLE 7*:

Sand type	Total porosity n_{tot} (%)
3to5	47.6
1to2	47.1
N5	45.2
N1	44.5

TABLE 7 Total porosity of all types of sand studied

4.4 Hydraulic conductivity (K)

In case of complex aquifer analysis, it must be said that laboratory testing using column (or permeameters), sometimes may not be a feasible and neither so reliable solutions, due to soil medium characteristics and variability in the real sites that cannot really be reproduced in a small scale lab test.

In order to do not waste time in collecting real soil samples, in many practical studies, especially for preliminary aquifer assessment, empirical relations appear to be a faster suitable and valuable alternative, even if they are not able to reproduce heterogeneity. In this documents, the results from 15 empirical formulae are presented. The validity of estimated empirical values is lately verified with the experimental data obtained from the sand column laboratory tests, especially the constant head ones.

a) Mathematical models and formula used:

Empirical formulae are often used in practice to quickly estimate the hydraulic conductivity of different kind of soils. Numerous relations based on dimensional analysis and experimental measurements have been published for the determination of K since the end of the 19th century (Siosemarde et al., 2014). Empirical relations have been derived for specific conditions and have their applicability limits (Kasenow, 2002; Vuković et Soro, 1992). General problems with the formulae are in determining the characteristic pore diameter (related to spherical shape of grains, see *FIG 23*) and expressing the effect of soil non-uniformity and the form of the appropriate porosity function which reflects the soil compaction rate (Riha et al., 2018).

Probably the first relation was proposed by Hazen (1892) and it expresses the simple linear dependence between hydraulic conductivity and soil porosity. In his formula, Hazen did not consider the effect of soil non-uniformity. This is also the case of the formulae proposed by Slichter (1899) and Terzaghi (1925). Kozeny (1927) proposed a formula that was modified by Carman (1937-1939) and lately again by Kozeny (1953). Then other formulas were proposed by Sauerbrey (1932), Krüger (1918), Zunker (1932), Zamarin (1928), Koenders and Williams (1992), and Chapuis et al. (2005) in which the characteristic pore diameter is directly derived from the effective grain size (indicated as D_e and in the majority of the cases considered equals to D_{10}) and porosity function $\chi(n)$ based on the analysis of typical sphere/grains configurations (VNIIG, 1991). Other generally less used formulae were proposed by Harleman (1963), Alyamani et Sen (1993) and Chesnaux et al. (2011). When the grain size is relatively well-defined is generally providing a lower uncertainty in resulting hydraulic conductivities estimations, while compared with more complex soils. Attention to the units must be taken while performing calculations to end up with consistent results for the comparison.

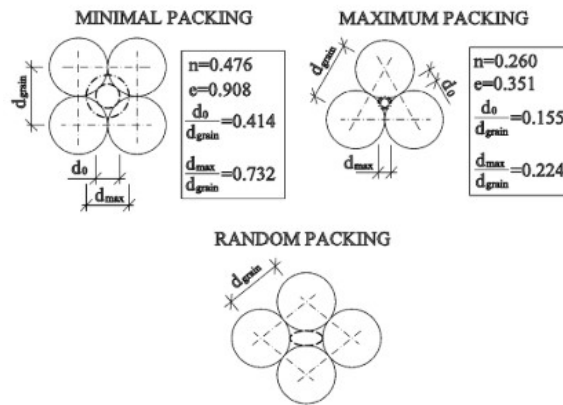


FIG 23 Schematization of the packing of spherical grains and possible pore size (Řiha et al., 2018)

A pre-dimensioning analysis while dealing with K determination, it is always useful in order to have an idea about the reasonable range of results that can be achieved. According to the type of sands, in terms of material and granulometry, a selection of formulas to apply has been done. Common input implemented and a table with all the achieved results are reported in **Annex III**. Details (brief description, explanation and limits) about the formulas used are given hereafter (Hussain et al. 2016).

- a) The *Hazen formula* was developed for a prediction of the hydraulic conductivity of uniformly graded loose sand with C_u less than 5, and an effective grain size (D_{10}) between 0.10 and 3.0 mm. Therefore it is normal that this formula can only provide reasonable results for the sand samples N1, N5 and 1-2.

$$K = 6 \times 10^{-4} \times \frac{\rho \times g}{\mu} \times [1 + 10(n - 0,26)] \times D_{10}^2 \quad (\text{XXX})$$

- b) The *Kozeny-Carman formula* is one of the widely used derivations for hydraulic conductivity calculations. This equation is not applicable for either soil with an effective size above 3 mm, or for clayey soil.

$$K = 8 \times 10^{-3} \times \frac{\rho \times g}{\mu} \times \left[\frac{n^3}{(1-n)^2} \right] \times D_{10}^2 \quad (\text{XXXI})$$

- c) The *Chapuis formula* is applicable for soils with D_{10} ranging from 0.03 to 3 mm, so potentially can be used for each of the studied sand type, even if for a large approximation will be done in case of the coarser sample.

$$K = 1219,9 \times \frac{n^{2,3475}}{(1-n)^{1,565}} \times D_{10}^{1,565} \quad (\text{XXXII})$$

- d) *Sauerbrey equation* can be used for soils with D_e up to 5.0 mm. It is ok for all columns, but it works better from the finest one until the 1-2 sample, because the 3to5 sample is actually related to a maximum granulometry of 5.6mm. The values of D_e are related to the 17%, and therefore could be extrapolated from the granulometric curves analysis.

$$K = 3,75 \times 10^{-3} \times \frac{\rho \times g}{\mu} \times \left[\frac{n^3}{(1-n)^2} \right] \times D_{(e)17}^2 \quad (\text{XXXIII})$$

- e) *Krüger formula*, where $C_K = 4.35 \times 10^{-3}$, n is porosity and D_e is effective grain size here equals to D_{10} . This is mainly valid only for the finest sand, so only N1.

$$K = 4,35 \times 10^{-3} \times \frac{\rho \times g}{\mu} \times \frac{n}{(1-n)^2} \times D_{10}^2 \quad (\text{XXXIV})$$

- f) In *Zunker expression* the C_{ZU} is an empirical coefficient that depends on the porous medium and it is generally equals to 2,4 for uniform sands with smooth and rounded grains (Kasenow, 2002).

$$K = C_{ZU} \times \frac{\rho \times g}{\mu} \times \left(\frac{n}{1-n} \right)^2 \times D_{10}^2 = 2,4 \times 10^{-3} \times \frac{\rho \times g}{\mu} \times \left(\frac{n}{1-n} \right)^2 \times D_{10}^2 \quad (\text{XXXV})$$

- g) *Harleman formula* has no particular recommendations and limits, but as the majority of the already cited ones it is mainly valid in case of fine samples.

$$K = 6,54 \times 10^{-4} \times \frac{\rho \times g}{\mu} \times D_{10}^2 \quad (\text{XXXVI})$$

- h) *Zamarin relation* has the empirical coefficient $C_{ZA} = 8.64 \times 10^{-3}$ and can be applied in all samples analysed in that work.

$$K = 8,64 \times 10^{-3} \times (1,275 - 1,5n)^2 \times \frac{\rho \times g}{\mu} \times \left[\frac{n^3}{(1-n)^2} \right] \times D_{10}^2 \quad (\text{XXXVII})$$

- i) The *Breyer formula* does not consider porosity and is often most useful for materials with heterogeneous distributions and poorly sorted grains with a uniformity coefficient between 1 and 20, and effective grain size between 0.06mm and 0.6mm.

$$K = 6 \times 10^{-4} \times \frac{\rho \times g}{\mu} \times \log \frac{500}{Cu} \times D_{10}^2 \quad \text{with } 1 < Cu < 20 \quad (\text{XXXVIII})$$

- j) *Slitcher formula* is most applicable for grain-size between 0.01mm and 5mm, so it can be used in all studied cases, but considering a larger degree of approximation for the 3to5 sand.

$$K = 10^{-2} \times \frac{\rho \times g}{\mu} \times n^{3,287} \times D_{10}^2 \quad (\text{IXL})$$

- k) The *Terzaghi formulation* is dependent on C_t = sorting coefficient, which ranges from 6.1×10^{-3} to 10.7×10^{-3} . In this study, two different values of C_t are used, according to the grain size and visible shape:

For sands with smooth finer grains

$$K = Ct \times 10^{-3} \times \frac{\rho \times g}{\mu} \times \left(\frac{n-0,13}{\sqrt[3]{1-n}} \right)^2 \times D_{10}^2 = 10,7 \times 10^{-3} \times \frac{\rho \times g}{\mu} \times \left(\frac{n-0,13}{\sqrt[3]{1-n}} \right)^2 \times D_{10}^2 \quad (\text{XL})$$

While for sands with coarse less rounded grains

$$K = Ct \times 10^{-3} \times \frac{\rho \times g}{\mu} \times \left(\frac{n-0,13}{\sqrt[3]{1-n}} \right)^2 \times D_{10}^2 = 6,1 \times 10^{-3} \times \frac{\rho \times g}{\mu} \times \left(\frac{n-0,13}{\sqrt[3]{1-n}} \right)^2 \times D_{10}^2 \quad (\text{XLI})$$

- l) *US Bureau of Reclamation (USBR) formula* is not based on the porosity value and it estimates K using D_{20} . The formula is most suitable for medium-grain sand with C_u less than 5.

$$K = 4,8 \times 10^{-4} \times \frac{\rho \times g}{\mu} \times D_{20}^{2,3} \quad (\text{XLII})$$

- m) *Koenders and Williams formula* is derived from the Kozeny-Carman equation and is related to χ = proportionality coefficient ($\chi = 0.0035 \pm 0.0005$) and D_{50} as the median grain diameter. It is normally applicable for silts, sands and gravelly sands, but in many case is not producing very accurate results. Two values are computed in association to this formula, respectively associated to $X=0,0030$ (a) and $X=0,0040$ (b).

In the statistical analysis after developed sometimes only one of this two values is considered.

$$K = \frac{1}{v} \times X \times n \times \left(\frac{n}{1-n}\right)^2 \times D_{50}^2 \quad \text{with } X = 0,0035 \pm 0,0005 \quad (\text{XLIII})$$

- n) The *Alyamani and Sen equation*, one of the well-known equations the grains dimension (D_{10} and D_{50}) and sorting characteristics, I_0 is the intercept (in mm). It estimates K is in m/day so the value has to be transformed while doing comparison analysis.

$$K = 1300 \times [I_0 + 0,025(D_{50} - D_{10})]^2 \quad (\text{XLIV})$$

- o) The *Naval Facilities Engineering Command Design Manual DM7 (NAVFAC)* proposed a chart to predict the saturated K value of clean sand and gravel based on e and D_{10} . The limitations described in this approach are :

$$0.3 < e < 0.7 + 0.10 < D_{10} < 2.0 \text{ mm} + 2 < C_u < 12 + D_{10}/D_5 < 1.4.$$

The results obtained with that are mainly ok for the finer samples until 1-2column.

$$K = 0,2272 \times (1,772189 \times 10^{11})^{\frac{n}{1-n}} \times [(D_{10})^{3,31917}]^{\frac{n}{1-n}} \quad (\text{XLV})$$

As it was possible to note from the results (and already knowing the results of the lab tests which will be presented after) the best estimations of all 4 sand types K -values are given by the Terzaghi formula, which is proved to be one of the most accurate in case of sand samples of the given granulometric size (Hussain et Nabi, 2016).

Through this analytical relation in fact is possible to make the difference between smooth/fine and coarse grains by the use of the sorting coefficient. The ranges of variation obtained considering all the results computed by the different empirical formulas are kind of big and so, the K (Terzaghi) was taken as the reference values in term of magnitude order for the following lab experiments. Values are resumed in *TABLE 8*.

	Hydraulic conductivity (m/s)		
	K(Terzaghi)	Kmin	Kmax
N1 (0.1-0.5 mm)	1.20×10⁻⁴	3.31×10 ⁻⁶	6.15×10 ⁻⁴
N5 (0.5-1 mm)	7.40×10⁻⁴	3.71×10 ⁻⁵	8.05×10 ⁻³
1/2 (1-2 mm)	2.18×10⁻³	1.15×10 ⁻⁴	2.88×10 ⁻²
3/5 (3-5.6 mm)	8.90×10⁻³	5.53×10 ⁻⁴	1.82×10 ⁻¹

TABLE 8 Results of analytical computation (Terzaghi K as the closest to the experimental ones; range of variation)

b) Experiment 1: CONSTANT HEAD PERMEABILITY TEST

Procedure and description:

- Prepare and assemble the column, being sure that all seals are air-tight (metallic and plastic valves to stop/open the flow, use of Teflon in junction, valves to seal the entrance and bottom of the column, tubes connections, etc...).
- Keep the column isolated from the system (valve closed), and saturate all tubes before connecting them to the sample. The water that is feeding the system can be distilled or simply tap-water. In the presented case, it is directly taken from the sink also to have already the right pressure to achieve the system stability (function of the Δh , the column dimensions and positions, the type of sand analysed, etc..). Otherwise, if no problem of high water pressure are registered, a system with an open water tank and a peristaltic pump can be implemented (allowing also water recovery/recirculation).
- Saturate all the system and the connection tubes before link all with the columns, and experiment one sample at a time.
- Fix the best constant difference of the heads Δh (measured with a meter) together with a flow as much as possible laminar. To do so, it must be determined the minimum water discharge associated to an optimal supplied flow rate.
- Let the system run once all is connected: when no more bubble of air are escaping from the column and the minimum quantity of them that is still trapped in the soil sample, the test can start and measurement of the collected water at the outlet section can be done using a graduated cylinder: $Q \text{ (ml/s)} = \text{Volume (L)} / \text{time (s)}$. Several outlet volume can be taken and average values can be calculated.

Observations:

All the experiments were performed at a constant room temperature (T) around 23.8°C. All the columns were always tested at the same elevation (the lowest available in the support structure). With the pump it was not always possible to allow a sufficient flow, therefore water was taken directly from the sink. In that way, it was not possible to re-circulate the water, but it was possible to collect the clean fraction discharged in some tank to other uses (also in further experiments).

To provide constant heads, the devices presented in Chapter 2 are used. It was possible to observe that, once the system was started and the constant head devices filled with water until the level required, the shape of the plastic was not anymore perfectly circular due to the weight of the water charge and to the strength/pressure applied by the additional strings used to stabilize and fix at the wanted height the device. Anyway in the calculation this variation of the shape was not be taken into account. So approximately the section was always considered circular. To have a better stabilization and equal conditions in both devices it was decided to keep the constant level in the larger section. The internal diameter of the larger circular section is considered 10 cm, while the one of the smaller cylindrical tube is 3.5 cm. The height of the device is 14 cm for the larger section, 13cm for the smaller one and the level of the constant head is around 12cm. While implementing the water

flow/circulation to the samples the minimum discharge should be achieved through the regulation of the inflow water. Every time the studied sample is changed, the different in h should be regulated to allow not to have a too fast flow. This should be a bigger problem when the coarser sample 3to5 sand is analysed. Normally the bottom device (outlet one) is kept constant as a reference for all the tests, but the upper-inlet one should be regulated. Knowing the granulometric size and based on the theory linked to K , it is possible to say that for the study of 3to5 sand the Δh will be lower than the one applied to N5 and N1, as this is the coarser sand type between the analysed ones. Otherwise the flow can be either too fast or either too slow (problem of difficult water constant circulation due to too high/low elevations).

To connect all column and water system devices some tubes were added and linked to the ones already set in the column: they are with an external diameter of 1.4 cm and an internal one of 1 cm. The length of tubes attached and discharging in the sink is for each tube of 250 cm; while the ones linked to the entrance and the exit of the column are both 170 cm long. The final scheme of the chosen design is reported together with the picture of the final set up in *FIG 24*.

Several tests were carried on for each column, in order to have a wider range of measurement to compare. Remembering that at least before each test it is better to let the system going for 30 minutes (in order to reach a stabilization once the minimal discharge and the optimal Δh are set), each test took one hour minimum to be done. Measurements of outlet flow rate were repeated for each test many times in order to asses that the system was stable. To measure the flow rate a graduated container with a maximum capacity of 2 litres, was used. Measure of time needed for the water to fill precise volume were taken and a medium value was used for further estimation of K , in case they were a bit different (always in very small ranges).

Calculation:

The value of the hydraulic conductivity K (m/s) is obtained through the *eq. (VII) in Chapter 1*. Attention should be put while taking measurement of the gradient and the outlet flow-rate, together with the conversion of the unit of measures.

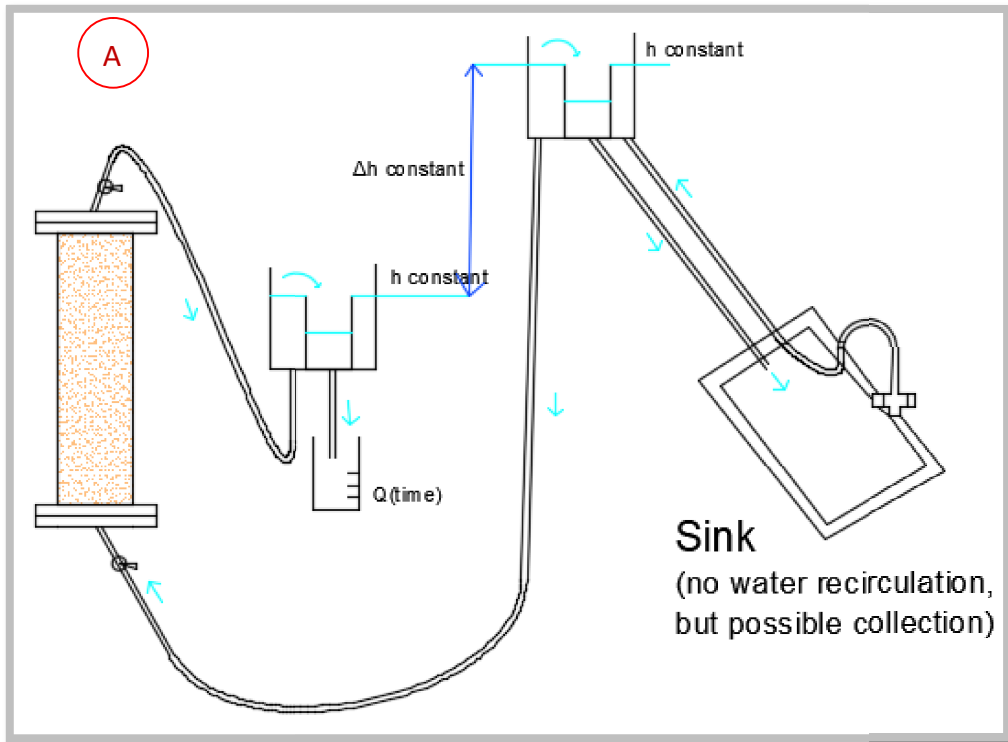


FIG 24 Final constant head set up : A schema and B real system used

Results and discussion:

The test was applied only in case of homogeneous sands, because the purpose of the experience was to characterize the parameter K associated to different grain size sands. But of course the experiment can be implemented in column filled by different soils/grain sizes and evaluation of mixed medium hydraulic conductivity can be done (those values will be maybe more closed to something that could be really be found in natural sites/aquifers).

Results of the most significant tests are listed in **Annex IV**. Here only a final summary of all the K-values estimated for each sample is reported and the range of variability of the results is highlighted in green in **TABLE 9**.

Also the average is calculated: as it was supposed, it is a scale of hydraulic conductivity values starting from the lowest value associated to N1 the finest granulometry ($K_{av,N1} = 2.94 \times 10^{-4}$ m/s), and gradually proceeding with N5 ($K_{av,N5} = 8.82 \times 10^{-4}$ m/s), 1to2 ($K_{av,1to2} = 2.13 \times 10^{-3}$ m/s) and arriving to the larger K of 3to5 ($K_{av,3to5} = 2.54 \times 10^{-3}$ m/s).

Hydraulic conductivity measured (m/s)			
N1	N5	1to2	3to5
2.64×10^{-4}	8.14×10^{-4}	2.47×10^{-3}	2.12×10^{-3}
2.45×10^{-4}	8.99×10^{-4}	2.16×10^{-3}	1.17×10^{-3}
2.25×10^{-4}	9.88×10^{-4}	1.99×10^{-3}	3.00×10^{-3}
2.17×10^{-4}	8.83×10^{-4}	2.05×10^{-3}	2.93×10^{-3}
4.28×10^{-4}	8.65×10^{-4}	1.82×10^{-3}	2.92×10^{-3}
3.84×10^{-4}	8.43×10^{-4}	2.30×10^{-3}	3.10×10^{-3}

TABLE 9 K-values calculated experimentally for each sand sample with CH test (range of variability min-max in green)

Results are reasonable in term of order of magnitude, which is perfectly in line with the range of hydraulic conductivity associated to sands, and K-values is gradually increasing going from the finer o the coarser sample.

Not a large difference is recorded, but this is normal, given the fact that all sands are made by quartz and are tested in column limited in dimensions.

c) Experiment 2: FALLING HEAD PERMEABILITY TEST

Procedure, description and observations:

The procedure is basically the same of the constant head test except the fact that no water is pumped into the system, and a decreasing Δh as to be monitored.

The water is allowed to flow through the soil specimen. The lower hydraulic head h associated to the reference outlet device as to keep constant, and so measure of the progressive decreasing of hydraulic head (at $t= t_0, t_1, t_2$) can be taken (Johnson et al., 2005). A high initial water head is preferable, especially in case of expected low hydraulic conductivities. All the experiments were performed at a constant room temperature (T) around 23.8°C. A scheme of the experiments is presented in FIG 25.

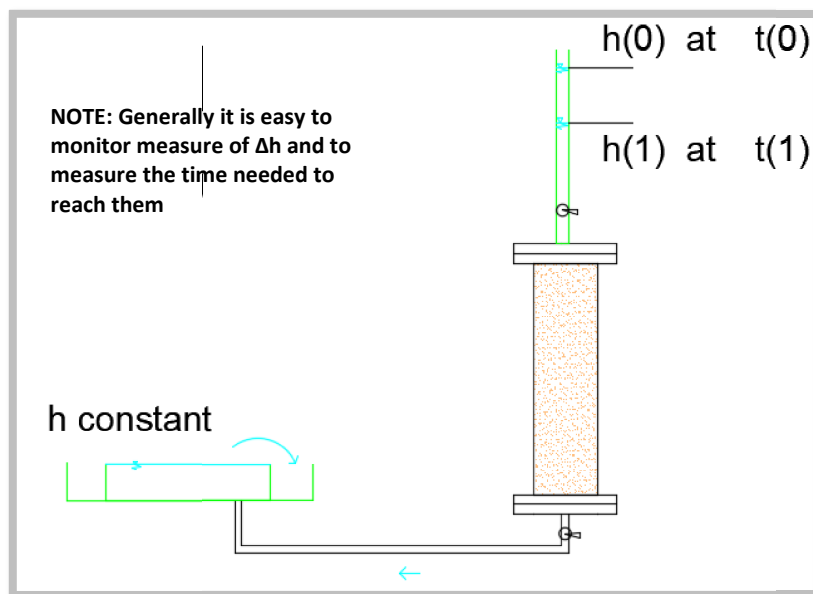


FIG 25 Falling head operational scheme

In the studied case, the reference level was fixed as the bottom of the inlet device used for constant head test and three different Δh were chosen to be monitored in time: top of external tube, half tube, tube empty.

The falling head test was repeated only once for each column, and basically it was chosen not to proceed with other measurement and implementation of the test because the results were not reliable.

Calculation:

The formula implemented to estimate the K-values in this case is:

$$K = \frac{a \times L}{A \times \Delta t} \times \ln \left(\frac{h_1}{h_2} \right) \quad (\text{XLVI})$$

where a is the inside cross sectional area of the water level monitoring device (m²); h₁ equals the distance to bottom of the control-hydraulic head device before the test (m) and h₂ is the distance to bottom of the beaker after a certain time (m). As the cross sectional area of the water level monitoring device is taken the area of the larger plastic circular tube minus the one associated to the internal tube.

Results:

Results obtained from the falling head experiments are considered non reliable mainly because they are not showing any relevant variation between the different granulometries of sand-samples analysed. Moreover they are not consistent with the one calculated with the precedent constant head tests.

Given those un-reasonable results together with the fact that this kind of test is mainly adopted in case of very fine particles (like for silt), which is not this case, it can be concluded that this falling head method doesn't work for the studied sands, and so those K-results will not be taken further into account.

d) Statistical analysis on empirically computed and measured K

Estimation of hydraulic conductivities of soils in terms of grading characteristics can lead to underestimation or overestimation unless the appropriate method is used. Differences between the results given by the empirical formulas and the ones obtained performing the laboratory tests are presented in statistical way. Mainly considering that the estimations are used only to have an idea about the order of magnitude of the K that should be encountered in the following experiences, results are not compared looking at a single unit precision.

Taking as the example the sand type N1, a bars graph reporting all the values associated to each models computation is done. Each empirical model is associated to the correspondent researcher(s) name(s) and to a symbolic ID composed by the letter M and a number from 1 to 15, in order to easily see and compare which methods are used in each sand type. Average (red) and median (blue) values resulting from the analysis are reported as straight vertical line (*FIG 26*).

For sand N1 it was decided to compare all the available models because they are all potentially and theoretically correct for the chosen sample. It can be observed in *FIG 26* that both K-median and K-average values are a bit underestimated, if compared with the one lately obtained in the lab by the Constant Head Permeability test ($K_{lab(N1)} = 2.17-4.28 \times 10^{-4}$ m/s).

Same analysis and graphs were done also for the other types of sand, and few general observation can be pointed out:

- The most accurate results in all case are related to Terzaghi and Chapuis methods, which were really able to be applied in all type of sands studied and were able to provide the same order of magnitude ranges founded lately in the constant head lab tests.
- Overall results showed that the hydraulic conductivities calculated by the Slitcher method are in all cases lower than from the other methods and from the effective values determined in lab. As well as the USBR model is providing a good result and match with the constant head K-estimations, only in case of N5, while for N1 and 1to2 samples is showing too low values and for 3to5 a too large estimation. On the other hand Breyer formula, Kruger expression and Alyamani and Sen one are correct only for the finer sample N1, while is relevantly overestimating in all the other cases. According also to other researches (Hussain et Nabi, 2016), (Vukovic et Soro, 1992) and (Cheng et Chen, 2007), those methods can be always considered inaccurate.
- Sauerbrey method is mainly effective in case of the intermediate ranges of sand granulometry studied.
- Hazen formula and NAVFAC one are also providing good results, especially while referring to the samples N1, N5 and 1to2. A bit overestimation of the 3to5 K is resulting in both of the cases. On the other hand Kozeny-Carman formula is able to provide other great results but mainly when the granulometric particle size is a bit larger.

- Zunker, Zamarin and Harleman formulas are providing good results mainly only for N1 sample. Then proceeding to larger grain size the K-values are generally again a bit over estimated.
- Koenders and Williams formula is contrarily showing more accurate results while looking at 3to5 sample, and is generally underestimating in the case of finer granulometries.

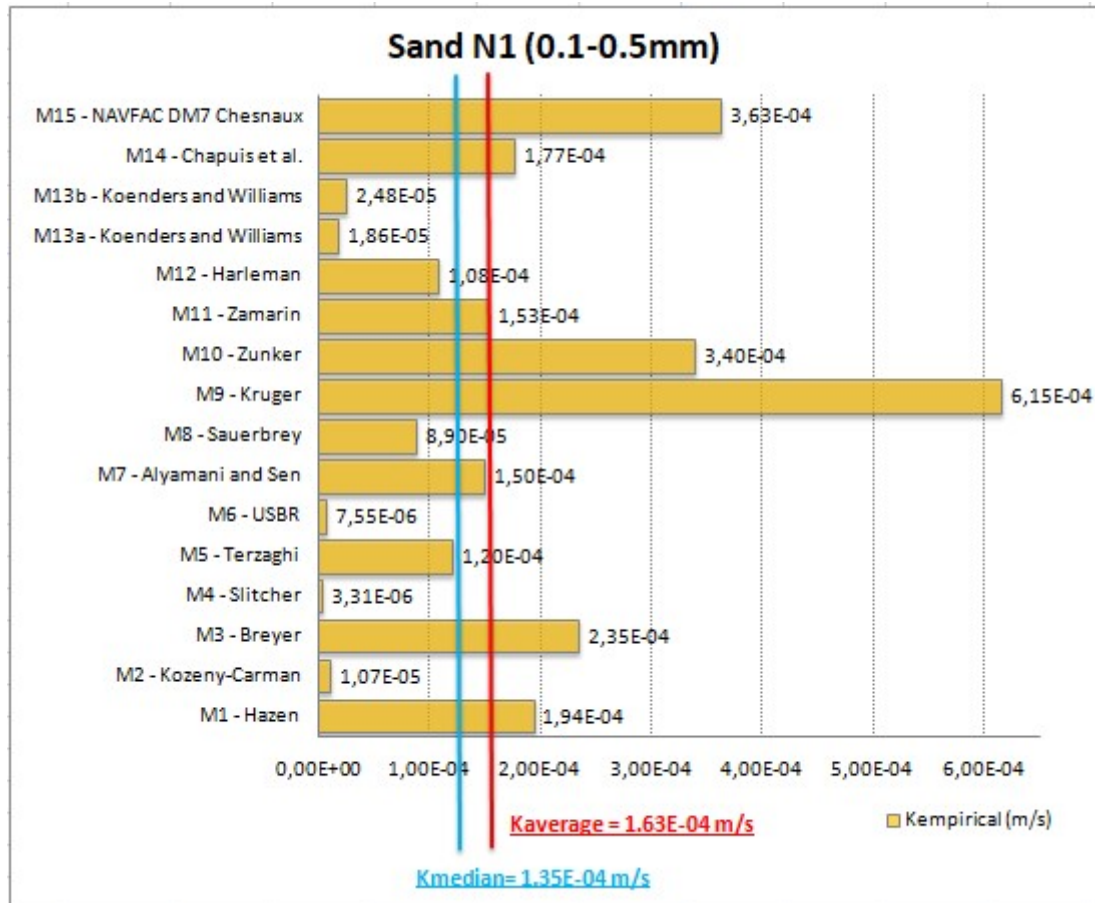


FIG 26 Statistics on N1 empirical K-values (all formulas)

All the graphs (similar to FIG 26) for the others sand samples N5, 1to2 and 3to5 are reported in the **Annex V**.

4.5 Effective drainage porosity ($n_{eff,flow}$) and longitudinal dispersivity (α_L)

Experiment: TRACER TEST (KCl)

Effective flow porosity and also longitudinal dispersivity can be evaluated by sand column ideal conservative tracer (behaving like water, and chemically non-interacting with the system) tests. Once the breakthrough curves from the tracer tests are obtained, and under several hypothesis and assumptions, the parameters can be evaluated by the use of some interpretation tools, such as TRAC.

Column conservative and ideal tracer tests were conducted in lab closed-flow experiments through KCl injections. The samples tested are the same already tested with permeability tests. The flow was a single-phase flow (only one fluid, water), occurring under saturated conditions. No additional transport phenomena are added to advection and dispersion (homogeneity of each sample can in fact be associated to low chemical reactivity).

The columns were set up vertically to provide a vertical flow from bottom to top (against gravity) driven by a peristaltic pump (WATSON-MARLOW 520S). The peristaltic pump was taking the water from a tank filled by tap water, and left open in order to have less variations of pressures, which can influence the pump functioning. This water reservoir was positioned below the column level (even if it can also be placed above to better simulate natural conditions).

The experiments were carried out at a constant water in-flow rate of 111.11 mL/min (provided setting the pump at $Q = 580$ mL/min). Given that value of flow rate applied, it was decided only to perform brief injection of tracer, and not continuous one.

Salts can be applied in tracer and ideal tracer tests. A known amount of salt can be added to a solution injected to a system and measured from an outlet point, by monitoring the changes in the electrical conductivity or/and by measuring samples water chemistry through ion chromatography or other analogue methods. Normally the cations are more subjected to sorption and other exchange processes, while the anions are the real tracer detected portion. Mainly selected anions such as Cl(-) and Br(-) are recognised to be transported un-retarded as conservative tracers (Nowamooz, 2015).

Saline solutions can be easily and economically monitored by electrical conductivity (EC) probes and loggers. Unfortunately, the use of EC as a tracer test measure for interpretation can lead to an erroneous parameterisation of the investigated porous media, mainly because reactions between solute and matrix are in the majority of the cases a-priori neglected or underestimated (Nowamooz, 2015). Furthermore these “low-cost” techniques only provide information on the total concentration of ions in solution, so to resolve the ionic composition of the aqueous solution they must be coupled with lab specific analysis.

Here it was used Potassium Chloride KCl, which is a salt easily soluble and globally non-reacting with quartz sand. In fact, anions Cl- are un-reactive and relatively inert with respect to quartz at almost neutral pH due to the low point of zero charge of quartz, and since the

affinity of cations K^+ to quartz surfaces is also negligible, it can be assumed that the subsequent experiments will not be influenced by previous KCl transport (Nowamooz, 2015). In case of quartz sands, it is in fact demonstrated that the sorption potential of potassium chloride is relatively low (Knutsson, 1968).

The brief injections were done through the second branch/entrance of an Y-device (FIG 27). This device was equipped with a cap that could allow to open and close the entrance. Tracer tests were conducted injecting everytime a solution made by tap water and dissolved KCl: similar values of concentration and initial EC of the solution, but different mass injected (following literature examples). Data are resumed in TABLE 10.

The injected volume is limited by the volume of the syringes used to perform brief injections (maximum of 50 ml or 30 ml). Small losses, due to the injection through the Y-device (implementing and removing syringe), are already taken into account. After the injection the Y-device branch is every time re-closed, as it is before, and the water-flow continues until the end of the experiment. No air should be introduced in the system.

The columns were saturated with tap water and washed in open-flow mode until the EC of the effluent was stable (generally ranging between 225 and 250 $\mu S/cm$, and a bit lower for the first test, while higher in case of second or third test on the same sample).



FIG 27 Brief injection of tracer: syringe manually pressed

SAND	Mass Injected KCl (g)	Mass Injected Cl- (g)	Volume injected (ml)	Concentration (g/L)
N1	7.7	3.7	50	154
N5	6	2.9	45	133
1to2	4.7	2.2	40	118
3to5	3.2	1.5	25	128

TABLE 10 Data of injections on different samples

The outflow device is equipped with an EC-probe (HACH CDC401 SN180452587016) reported in *FIG 28*. The probe was directly connected to a data logger (HACH HQ40d): so the data were automatically collected and no manual observations and notes were needed. Before start the recording, the probe was correctly calibrated. Measurements of the electrical conductivity at the outlet point were taken every 30 seconds and were after used to estimate the K⁺ and Cl⁻ concentration. The EC recordings start always some time before the injection in order to see the stabilization of the system and check the probe functioning.

Samples of outflow-water were taken regularly in order to determine the correlation between EC values and ions concentration through lab analysis (again *FIG 28*). In details, after the injection, and once the EC value monitored by the probe starts to increase, water samples were taken each time step Δt of 30sec. Then after the peak, a larger step was used, such as 3, 5 or even 10 minutes close to the end of the test. Each test is supposed to last after 1h30min after the injection, so around 2h for each test were taken into account, including the time to put in place all the equipment and activate the system. Few water samples were taken also before the injection: they are analysed in order to have an idea about the background ions concentration values. A fast renewing of the volume that is sampled is also assured in order to have more reliable results (no influence with previous volume).



FIG 28 Probe to monitor the EC-values, and water sampling during tracer test

The mixing is supposed to be complete between the injection point and the entrance of the column: the length of Y device + tubing before column entrance is about 15 cm. If the mixing is not well provided of course the tracer will mainly pass to only the half side of the column in which it is injected, but this cannot be eye-visible in case of salts (while it is in case of fluorescent or coloured dyes).

All the connection tubes (between Y-devices, column in/out, pump) are plastic transparent tubes, softer than the ones used for the CH tests, and with an internal diameter equals to 8 mm. Especially in the connection between the injection point and the outflow section, the tubing must be shortened to the possible minimum length (still practical) to avoid a large impact of void volumes and too long time of delay in the measurement. A scheme of the whole system is reported in *FIG 29*.

When a column should undergo to another test, it is better to let the system running just with the in-water-flow, in order to really reach the initial EC-value of the previous experiment. Few times the pore volumes, meaning around 2h and 30min of effective test after the injection, could be the minimum to completely wash the system and come back to the initial configuration. Otherwise the background value changes and it must be taken into account in the interpretation.

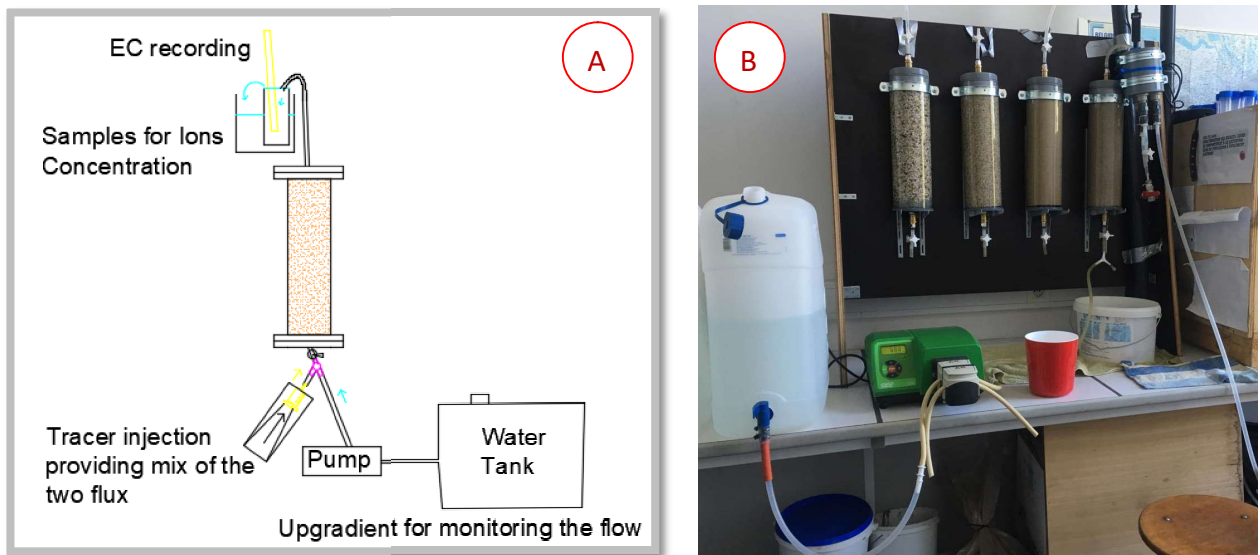


FIG 29 Implementation of tracer test: A) the scheme and B) the practical set up

Pre-dimensioning:

A fast pre-dimensioning of the test was done with the software TRAC (BRGM, 2011), in order to have an idea about the time needed and the mass of tracer to use. A reasonable and feasible test, being in the didactic purpose and considering the measures of the studied system, should show some tracer arrival (beginning of the breakthrough curve) after few minutes and the return to a value close to the initial reference (i.e. zero in case of zero background concentration) in few hours maximum.

A comparison between available formulas in TRAC for 1D Brief Injection was done: *Infinite* vs *Semi-Infinite* porous medium (FIG 30). Theoretically, both can be right in the studied case because, considering the tubing before the column entrance, is not completely true that the KCl is immediately forced just to move upwards together with the flow. Practically speaking, the difference in the results is in the first salt detection time and in the shape of the curve: faster arrival and steeper slopes before the peak are recorded for the **Semi-Infinite** case. Thus, this last is chosen as the most representative formula, and the time needed to do the experiment, injecting an example quantity of tracer, is estimated to be appropriate in term of breakthrough curve: first arrival in few minutes, peak reached before 15 minutes, and ending tail of BTC achieved after 45 minutes. Therefore, also the interpretation of all performed tracer tests was done through the use of TRAC with the Semi-Infinite formula (good fit of the breakthrough curves was always reached).

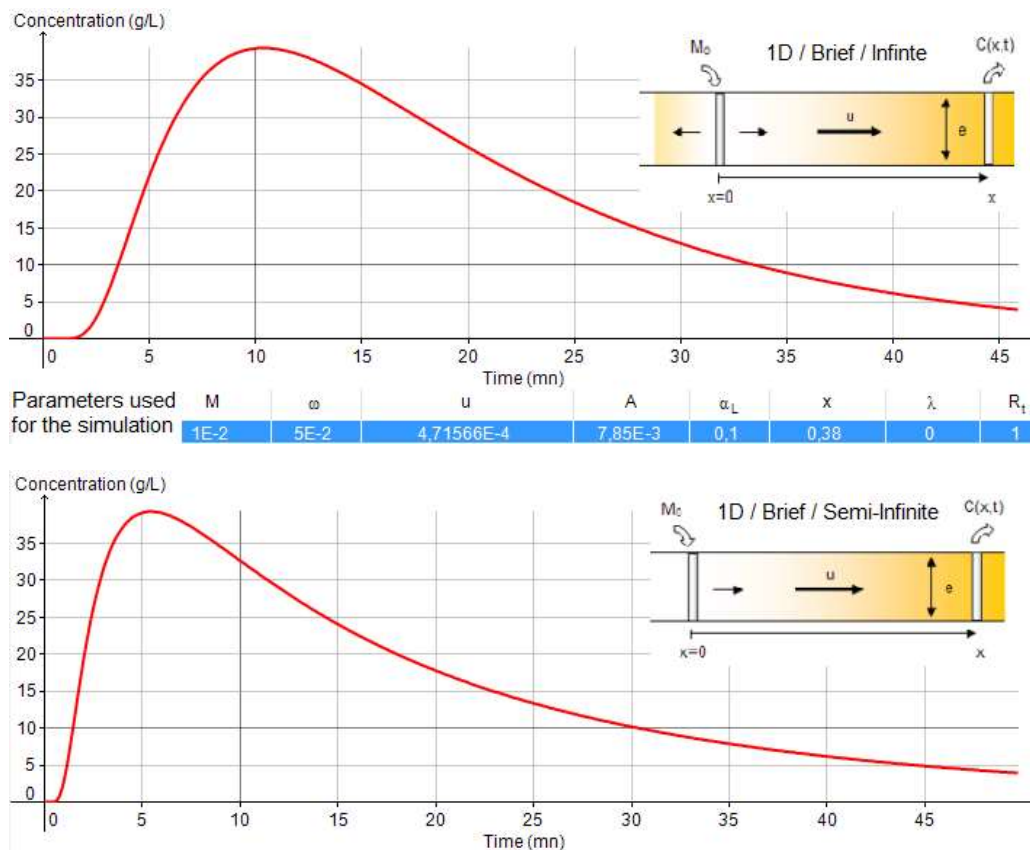


FIG 30 Pre-dimensioning of the KCl tracer test for sand-columns: A) Infinite and B) Semi-infinite (selected)

EC measurements, ions concentration and breakthrough curves analysis:

The probe recording EC values ($\mu\text{S}/\text{cm}$) every 30 seconds for a test duration up to 2hours. Simply using those measurements in a graph EC vs time, sort of breakthrough curves were immediately obtained. From those, was possible to observe that, after about 5 minutes the initial constant values of EC start to increase rapidly reaching a peak, in the interval of time between 10 and 25 minutes (depending on the type of sand studied, basically quicker in the case of coarser grains, while slower in case of finer granulometry). The decrease of EC-values in all the recorded breakthrough curves was always more gradual and after more or less 90min the constant initial EC was re-established.

Given the fact that water samples were regularly taken for each test, a comparison between the values measured by the probe and the one detected in the lab was done. Bad correspondence of values is indicating the presence of an error, maybe related to an incorrect calibration of the probe, or to the presence of precipitate, or even to a not enough recirculation of the system. This happened in the first test performed in N1 sand. In fact,

from lab analysis the results show the presence of precipitate (occurred probably during transport and handling of samples before the analysis in the lab).

Moreover, another important problem was the renovation of the water within the collected samples, that was not that efficient. In the following tests in fact, the system was improved re-positioning the probe and facilitating the water outflow from a first collecting backer.

It is noticed, while collecting water samples that the water was less transparent/clean in correspondence of higher EC-values, especially in case of sand-column N1 and N5. That could be associated to the fact that those sands are fine-grained so they have more fine particles creating turbidity and which increase the value of EC (higher conductivity).

The results obtained by lab analysis confirm the efficiency of the improvement, showing almost a perfect correspondence, especially in case of test 4 (1to2 sand) and 5 (3to5 sand). Generally the shape of those obtained EC breakthrough curves become larger but less high going from finer to coarser sands. To validate lab measurements of concentration of [Cl-] and [K+], EC lab (T = 25°) and EC probe (T = 23.8°) have been compared (FIG 31 and 32). For sand 1to2 and 3to5 the match is definitely ok: linear tendency passing through 0, and with R² equals almost one. While for the first test performed on sand N1 was not the case, for the reasons already cited.

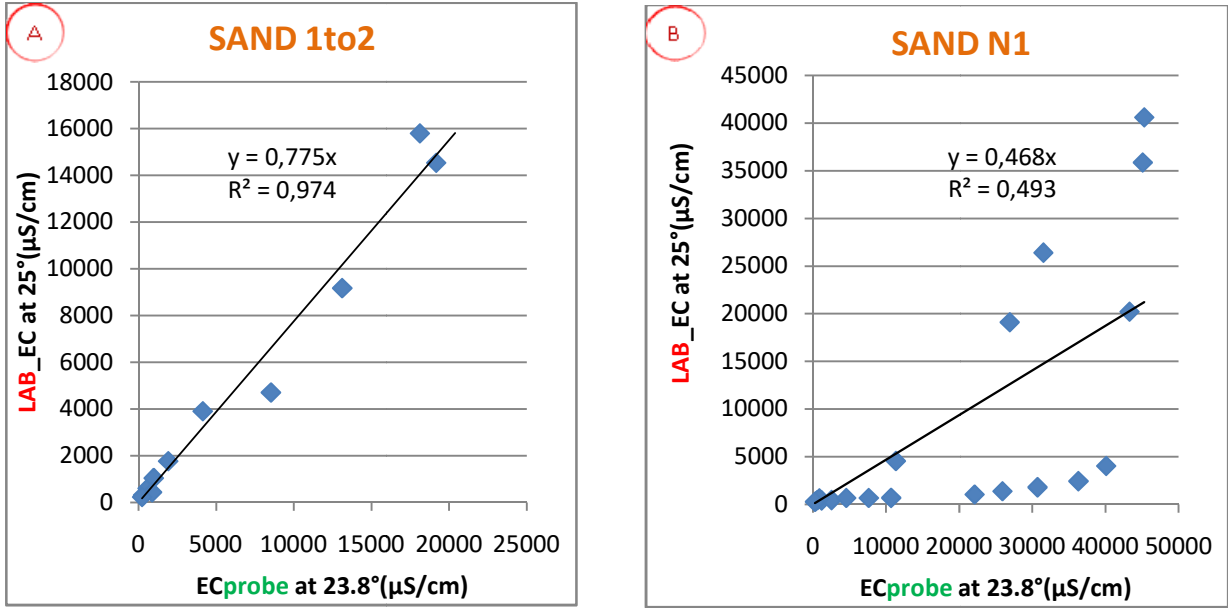


FIG 31 Correspondence of EC values (Probe vs Lab analysis): sand 1to2 (A) and N1 first test (B)

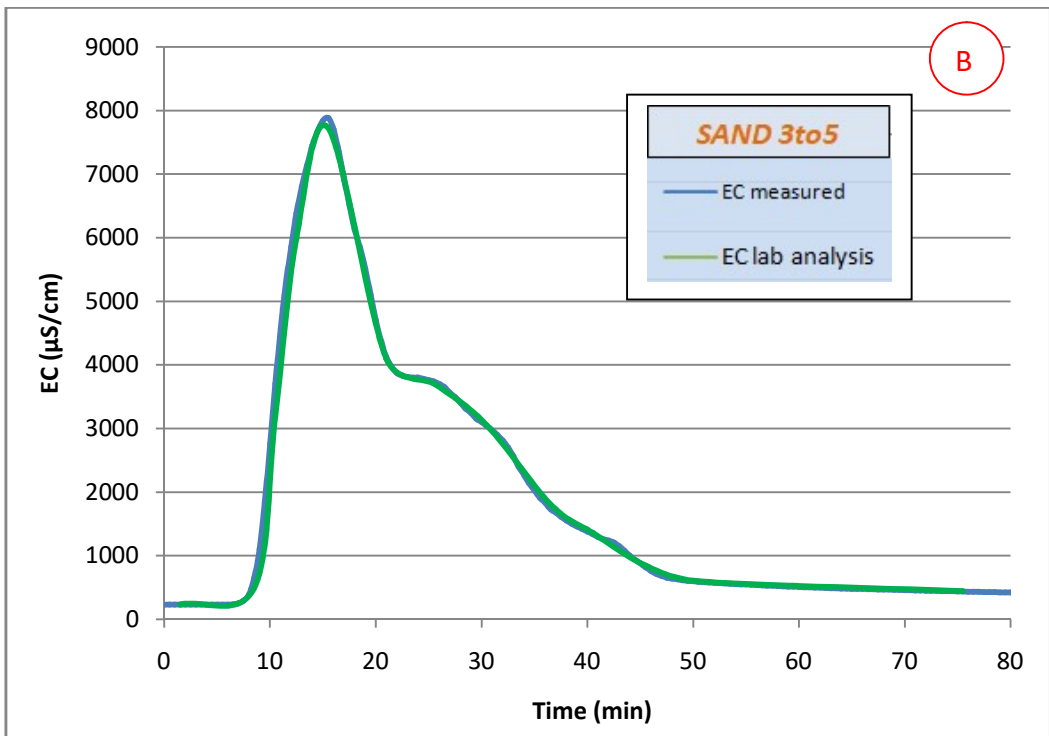
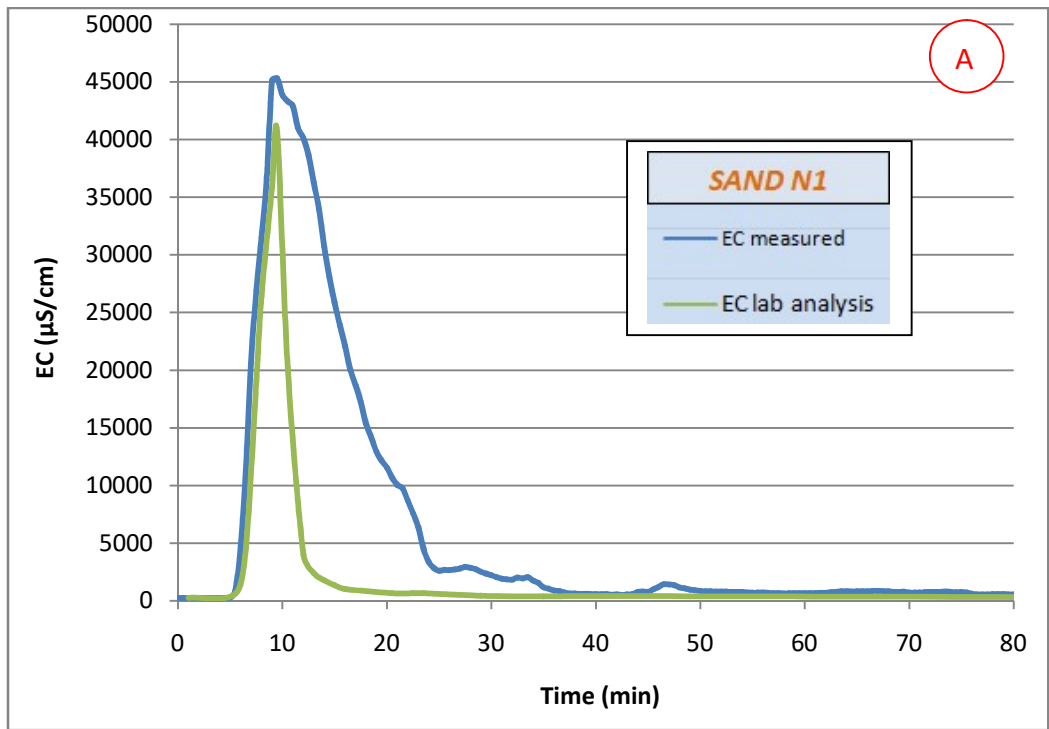


FIG 32 EC-Curves comparison between lab and probe measurements after injection: test1 N1sand (A) and test5 3to5sand (B)

Based on water samples lab analysis results, to really demonstrate that both of ions Cl⁻ and K⁺ are representative for this tracer test, a comparison in term of concentrations breakthrough curves is shown (FIG 33). In all the performed tests it is observed that the behaviour (therefore the shape of the arrival curve) is basically the same qualitative speaking. From lab analysis, other data associated to several ions concentration are available. Comparing them for the four types of sand analysed, a common behaviour was found: the shapes of the curves displayed over time is always the same. That means that no interaction between the saline solution injected and the soil analysed took place.

In terms of meq/L, a quantitative, but still not so substantial, difference it is shown. Similar studies generally report more evidence of this expected difference of ion concentration (Steyl et Marais, 2014; Mastrocicco et al., 2011). This is due to the difference in the molar mass associate to K ions (39.0983 g/mol) and Cl ions (35.453 g/mol). The conversion between mg/L and meq/L is done according to the formula (source <http://www.nafwa.org>):

$$\text{meq} = \text{mass (g)} / \text{atomic weight (g/mol)} * \text{valence (/)} \quad (\text{XLVII})$$

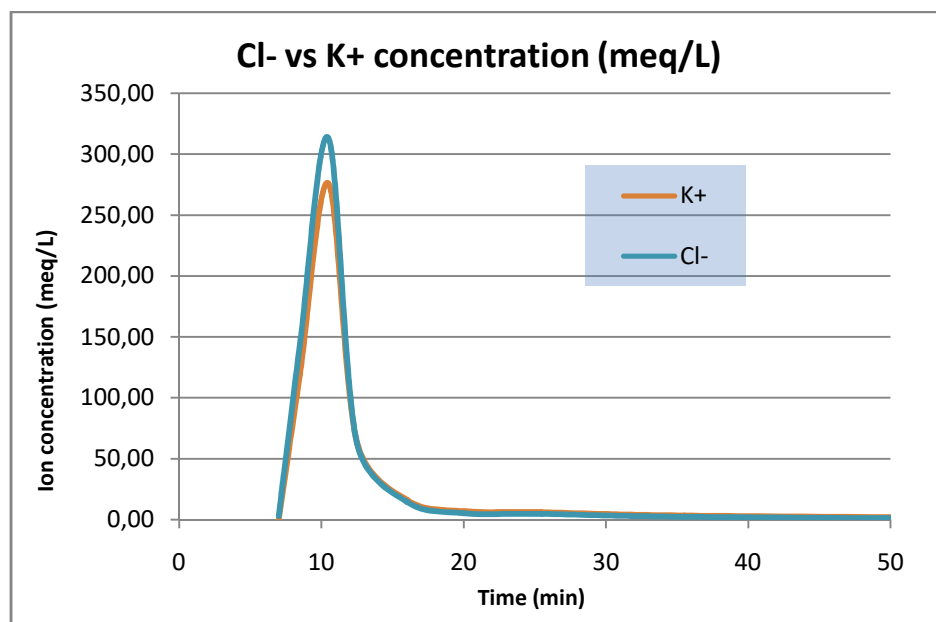


FIG 33 Ion concentration: comparison Cl⁻ and K⁺ breakthrough curves (sand N1, second test)

The EC profiling should be analogue to the ion concentration breakthrough curve shape. Therefore a correspondence between the two values was studied: an analogous X-Y graph was drawn, and the linear relation between [K⁺] or [Cl⁻] and electrical conductivities was pointed out. Normally it is supposed to be a linear relation and through this expression it is possible to convert the curves. Comparison was done with both the series of data of EC, the ones measured directly with the probe and the one stated in the lab.

In case of bad correspondence with probe measurements, only the lab analysis results were further consider for the interpretation (case of N1 and N5 sands). While when good relations with the probe recordings were possible, it was decided to consider the larger dataset linked to probe measures for the generation of more detailed breakthrough curves that can allow a better parameterization. When this reasonable linear relation is found, it is both for [Cl⁻] and [K⁺]. And actually there are not big differences in terms of coefficient of direct proportion: ranges between 0.22 and 0.29 when concentration values are in mg/L, and 0005-0.007 when they are expressed in mmol/L (mass concentration × molar mass = molar concentration). Furthermore, the correlation coefficient R² (representing the goodness-of-fit measure between the observed values of the outcome variable and the fitted ones) is always > 0.95 (FIG 34 and 35).

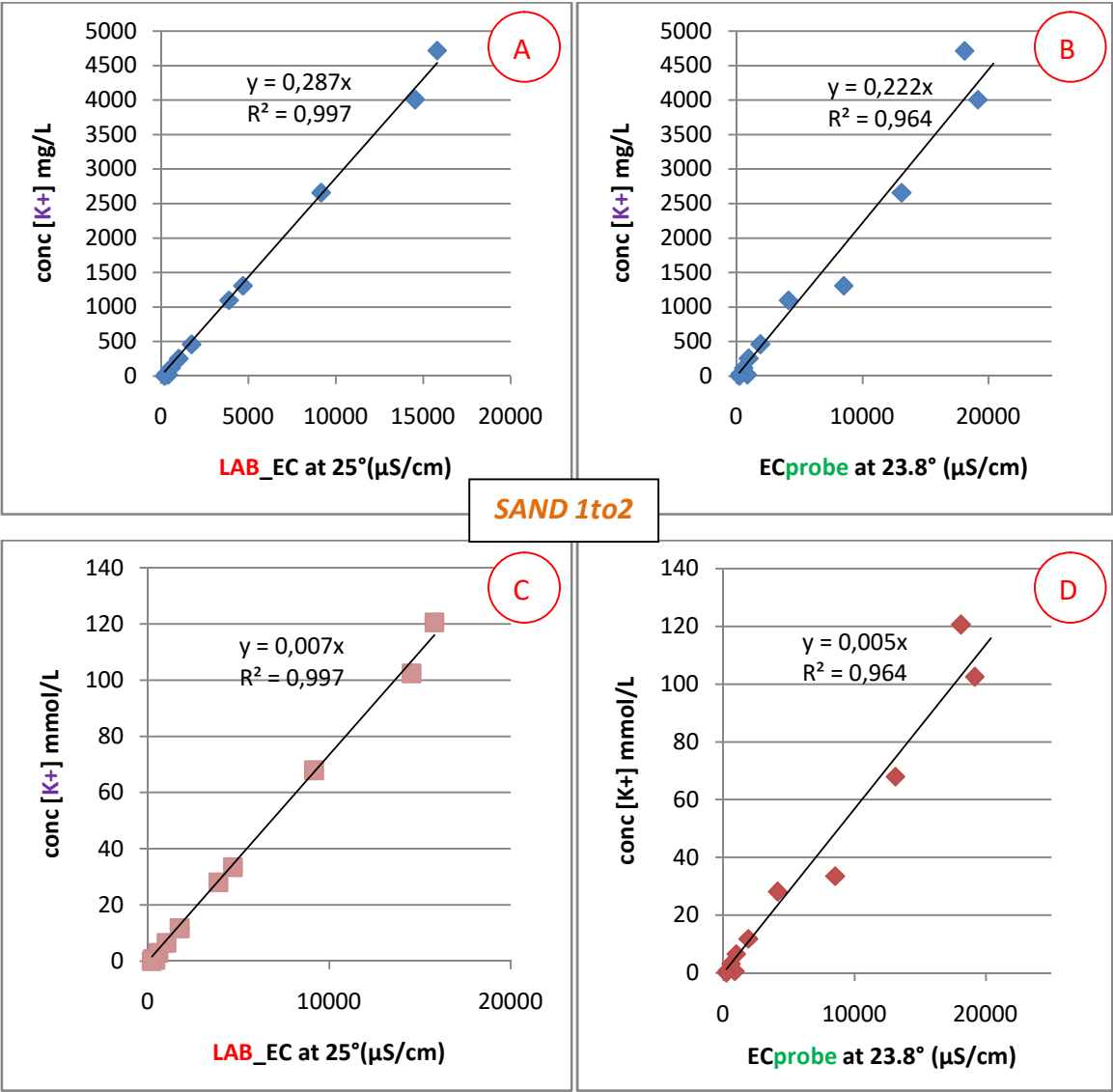


FIG 34 Linear correspondence between EC and concentration[K⁺]: case of sand 1to2 (A;C-EC,Lab vs mg/L, mmol/L; B;D-EC,Probe vs mg/L, mmol/L)

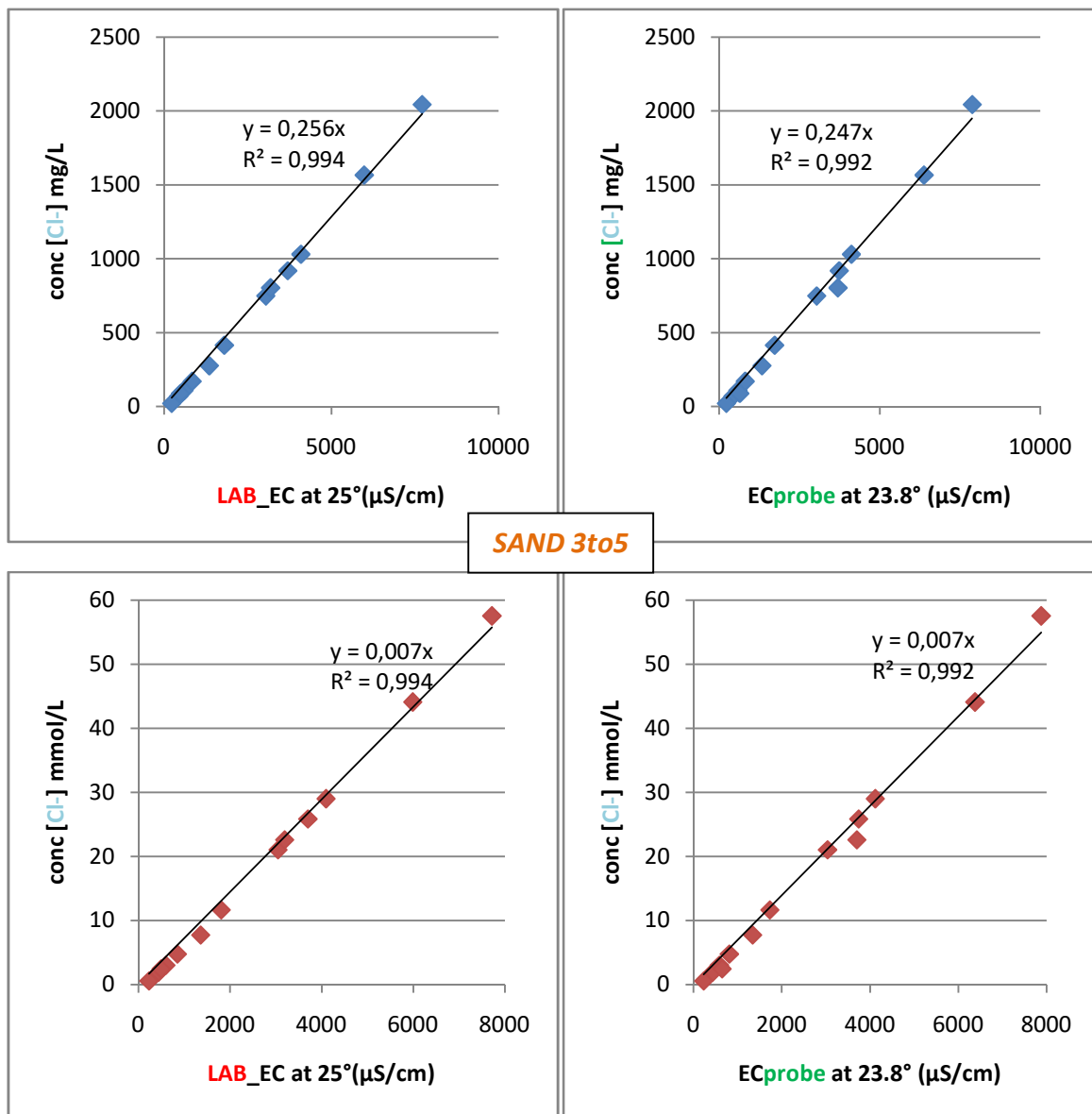


FIG 35 Linear correspondence between EC and concentration[Cl-]: case of sand 3to5
(A;C-EC,Lab vs mg/L, mmol/L; B;D-EC,Probe vs mg/L, mmol/L)

The easier tests to interpret are the ones associated to the coarser sands, due to the fact that there is no differences between the restitution curve of EC from the probe and EC from lab analysis (good linear correspondence, no formation of precipitate supposed). Before the estimation of flow/transport parameters, a basic analysis in term of first arrival time and peak are done by the use of Excel, only looking at those breakthrough curves. The comparison between the four sand-columns is carried on looking at the “ Δt measured between the first increment in EC recorded and the instant associated to the maximum peak”. Results are reported in TABLE 11: this Δt is generally and reasonably larger for finer sand samples (slower flow, lower permeability) and it is decreasing looking at bigger sand grains size.

Measure of EC are taken every 30seconds so, for that reason the time values are approximated to minutes or half minutes (time estimations can be considered affected by a small error).

Column	Test ID	Arrival time of Cl- (min)	Peak time (min)	Δt (1 st Arrival - Peak) (min)
N1	T2 T6	5	30.5	25.5
N5	T3	5	15.5	10.5
1to2	T4	5	14	9
3to5	T5	5	12.5	7.5

TABLE 11 Tracer tests summary of analysis on first tracer arrival and peak time

Given the fact that, the quantity of tracer (in grams) differs from one case to another, the concentrations are impacted. So the comparison of the breakthrough curves (FIG 36) was done in terms of concentrations normalized by the injected mass of tracer [mg/(L x injected mass of tracer)].

While doing this comparison all the tests are analysed starting from the moment of the injection and as it can be seen the first arrival has always been recorded after more or less 7 minutes.

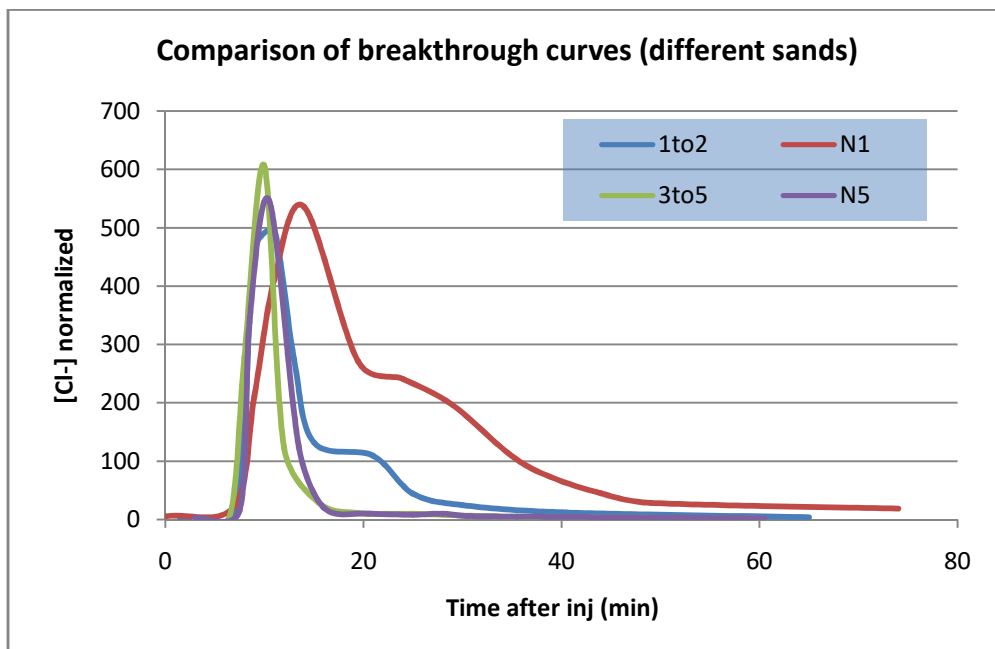


FIG 36 BTCs normalized comparison between the different sand samples

TRAC interpretation: parameters estimation

Using TRAC, once the data and parameters are inserted to find the best curve fitting, in the same time of the breakthrough curve a recovery curve is draw. To do so TRAC is computing the calculation of this percentage of recuperation rate of each sample taken through the formula:

$$TR (\%) = \sum_{i=1}^N \frac{\Delta t \times q \times C_i}{C_0 \times V_{tracer}} \times 100 \quad \text{where } N=n^\circ \text{ of samples taken} \quad (\text{XLVIII})$$

Where C_0 , C_i are the concentration at time zero and i , V_{tracer} is the tracer volume. The values of those recovery rates are always around 100% looking at both investigated ions concentration. Those estimation of are done according to the roughly estimated volume of tracer actually injected into the column (obtained by considering the small losses of the volume of tracer solution remaining in the syringe itself, attached to the walls and the rubber in the piston, the one remaining in the "Y" after the injection phase, and the one lost during the removal of the syringe).

While doing the interpretation with TRAC, some hypothesis were taken into account:

- First of all, all tests were interpreted starting from the injection time, so removing the minutes before the entrance of the tracer in the system, in which only the functioning of the probe was checked and the system was stabilizing.
- Then it was considered the so called "delay time" associated to the tubing length which is included in the system to be able to perform injection and collect samples, and which is enlarging the total length of the water path to reach the collection point. This time correction was applied simply subtracting from the time measured by the stopwatch, the time it took the tracer to traverse the two branches of the "Y" device and the outlet pipe of the column. This was calculated considering the velocity of the input flow (related to the tube section) and the length of the tubes connected. Moreover, tubes and valves effects are not negligible, even though their application is reduced to the minimum. Thus, it is approximately obtained the actual time of transporting the tracer through the column: knowing the Q_{in} provided by the pump, the tubes plus the 2 branches of "Y" plus the valves length (15 cm inlet + 15 cm outlet) and the tube internal diameter (0.8cm), this time is estimated to be around 12 seconds, rounded in excess to 15 seconds taking in account the time needed to re-circulate the water at the outlet point (sampling and monitoring point) and the dispersion.
This time of delay was enough to allow interpretation and good optimization of the curves (in fact the efficiency coefficient values of all the interpretations are around 0.85 and 0.95, which means quite a good fitting between data and simulated values).
- The length of porous medium was maintained constant: $x = 0.38$ cm, which is the entire column length.
- Other constant inputs were the Darcy's velocity, the mass of tracer introduced (different for each test and associated to the Cl-).

Few examples of the graphs produce during interpretation of breakthrough curves with TRAC are reported (FIG 37 and 38). It must be said that, when low number of samples were analysed, it was possible to reproduce less defined BTCs, and so a bit less precise parameters estimation was carried on. That is the case of simulation applied directly to EC lab analysis data, when no good linear correspondence with probe's measure was found (coarser sands, precipitate presence). All the figures are in *Annex VI*.

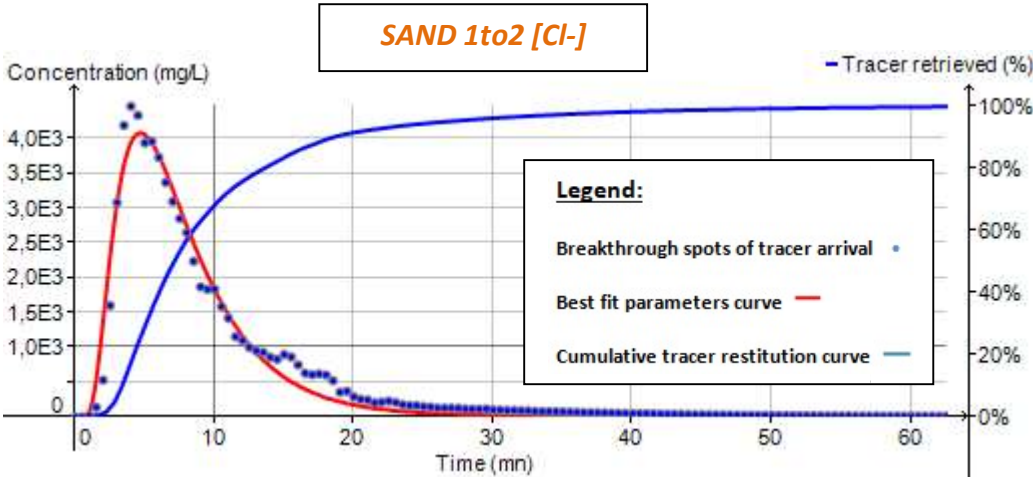


FIG 37 Interpretation of breakthrough curve of Cl- ions concentration (mg/L) in 1to2 sand

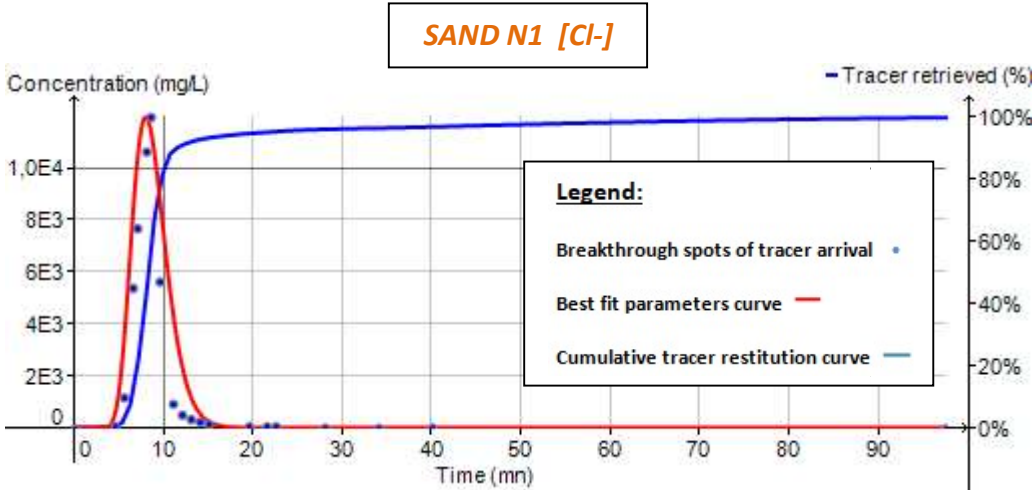


FIG 38 Interpretation of breakthrough curve of Cl- ions concentration (mg/L) in N1 sand (second test)

All approximations and trials allow to end up with ranges of variation of the investigated longitudinal dispersivity and effective drainage porosity referred to lightly compacted samples (results in TABLE 12). Those estimations may vary considering other grade of compaction.

In general, the obtained results are considered reasonable regarding the types of material studied, and are confirmed by the literature. In fact, according to lab studies conducted to estimate dispersivity, Wierenga and Van Genuchten (1989), and Costa and Prunty (2006), suggested that, both in saturated and unsaturated soils, the parameter depends on the travelled distance. In fact, longitudinal dispersivity values found for sandy soil in saturated conditions are around few cm, similar to what was achieved by Khan and Jury (1990) and Kasteel et al. (2009), Kanzari et al. (2015).

Looking at the *TABLE 12*, few things can be highlighted:

- Adjusted $n_{\text{eff,flow}}$ values were always \ll than n_{tot} , except for sand 3to5 where $n_{\text{eff,flow}}$ is 39% and n_{tot} equals 47.6%. This can be justified taking in consideration the size of the grains (quite big to be a sand) and the relative small dimension of the column system.
- Looking only at $n_{\text{eff,flow}}$ ranges, they are consistent for N1, N5 and 1to2 sands, in terms of scale, from the smaller value of to the larger one. In general the smaller value is associated to the hypothesis in which all system length from injection point to recovery one is considered, while the larger one to the hypothesis where only real column length is taken in consideration, as it is logical. Also an average value is determined and the scale is again respected. To really understand which is the correct value for each sand, additional experiments will be helpful. For example a tracer test in a 3D sand box will return a value which is expected to be within each range determined and which can therefore help to be closer to the representative effective value of the parameter (that probably is not the average one).
- The longitudinal dispersivity coefficient α_L is gradually changing together with the increase of granulometric particles size. There is one order of magnitude of difference between the N-sands and the 3to5 coarser one, as it is also for the hydraulic conductivity. Dispersivities are known to increase with increasing transport distance and scale of the experiment. Lateral scale of the experiment is generally playing a significant role in the determination of this parameter. In coarse-textured soils, lateral water redistribution may take place across relatively larger distances, which explains the larger dependency of dispersivity on lateral scale of the experiment especially in coarse soils (Vanderborgh et Vereecken 2007).

	Sand-column N1	Sand-column N5	Sand-column 1to2	Sand-column 3to5
K average (m/s)	2.94×10^{-4}	8.82×10^{-4}	2.13×10^{-3}	2.54×10^{-3}
K range (m/s)	$2.17-4.28 \times 10^{-4}$	$8.14-9.88 \times 10^{-4}$	$1.82-2.47 \times 10^{-3}$	$1.17-3.10 \times 10^{-3}$
α_L (m)	0.01	0.013	0.04-0.05	0.09-0.11
$n_{\text{eff,flow}}$ (%)	20 - 22	22 - 23	26 - 30	38 - 40
$n_{\text{eff,flow}}$ average (%)	21.5	22.5	28	39
n_{tot} (%)	44.5	45.2	47.1	47.6

TABLE 12 Summary of estimated parameters by the use of TRAC for all sands tested

Chapter 4

Modelling of 3D physical sand tank

The 3D physical sand tank is financed by the University of Liège mainly as a teaching support, in fact it will be used for teaching hydrogeological processes. Thus, pumping test and tracer test will be implemented such as exercises for students.

In this section, a numerical model based on GMS-MODFLOW-MT3DMS (by USGS, version 1.0, year 2000) of the sand tank is developed in order to simulate water flow and solute transport within the sand tank previously described in *Chapter 2*. With this numerical model, once it is calibrated, it is possible to design different exercises.

The objective of this section is therefore to have a fully functional numerical model of a flow-transport, ready to be calibrated. Implementation of the conceptual model is provided together with some useful tips for the model functioning. Problems encountered and points of attention are highlighted. A sensitivity analysis on the influence of each parameter change is then performed.

1. Conceptual Model

The numerical model aims to simulate the **hydrodynamic behaviour** of an **unconfined homogeneous saturated sand aquifer**. An unconfined aquifer is defined as an aquifer whose upper water table is at atmospheric pressure, and so it is able to fall and rise: groundwater is in direct contact with the atmosphere through open pore spaces of the overlying soil, which, in this case, is sand.

In this study, only a **forward modelling** is performed: $y = f(x,a)$ where x , meaning the model inputs which can be from observations and future scenarios, a , that represents the group of all parameters, and f model geometry, grids, BC's and initial conditions, allow to determine y , the ensemble of hydraulic heads and flow. Direct modelling is mainly used for predictions.

[If sand parameters have to be calibrated, an **inverse approach** should be used (meaning $y = f(x,a)$ where system configuration (f and x), observed heads and flow (y) are used to calibrate a , the ensemble of parameters. The objective is to estimate the input parameters in order to better characterize the properties of the medium. Calibration is in fact based on the minimization of the difference between observed data and simulated ones.]

The constructed model should allow to reproduce and study the reaction of the sand tank system, once external stresses (pumping and tracer injections) are applied. The first step is to reproduce a groundwater flow model and then a transport model in which groundwater fluxes computed in the flow model will be used as boundary conditions to compute tracer fluxes between cells. Fundamental attention is the choice of cell size and number of layers.

The conceptual model is upstream of any numerical choice, including the discretization with a finite difference grid. It translates the reality, which is here the sand box, into a "simplified system" that will be modelled, through mathematical concepts (type of equations solved, boundary conditions, etc.). Developing the conceptual model, all the information required to make the link between the "plans" of the sand tank and its further discretization are pointed out. Starting from the setup of the sandbox, explanations of how each component will be considered in the model are given. Then, time scenario will then depend on type of simulation performed.

Even if the tank is supposed to internally be 1440 mm long x 830 mm thick x 800 mm height, the portion that is useful to be modelled is only the one really filled by sand (and not all the box due to flow stabilization and pressure issues). Thus, it was decided to focus on a **1200 mm (length) x 800 mm (thick) x 700 mm (height)** package of sand, and **two additional line-column-cells, one at each of the two opposite extremities** of the longer side of the tank. Those last were added in order to allow the prescription of constant heads (water reservoirs) both in the entrance (up) and in the exit (down) sections.

To avoid problems linked to prescription of constant head lower than the bottom elevation of upper layer cells, the dimensions of the **grid is 1 cm (X) x 1 cm (Y) x 35 cm (Z) cell**, for a total of 19.520 cells in only **2 layers** of sand. This grid allows to reduce troubles with code calculations induced by the presence of dry cells as a consequence of pumping/drawdown. The dimension of the cells is more accurate in XY plane, instead in Z direction, because the number of layers is not so important reproducing simulations of steady state flow, basic pumping and tracer tests, where no variations in K are considered.

In particular, for the **FLOW MODEL**:

The model aims to reproduce and visualize aquifer behaviour in all directions (vertical, horizontal and transversal flow components). The porous medium is supposed to be homogeneous, so even a 2D horizontal model can be implemented. But, choosing to set more than one layer (at least two), it is more realistic to implement a numerical 3D model, even if no difference in K should be implemented.

The water flow through the sand tank is performed by creating a hydraulic head difference Δh between the inflow and outflow reservoirs. During the test, the hydraulic gradient is controlled using Constant head devices (presented in *Chapter 2* and used also in columns experiments) directly connected through the drainage holes in the two small water reservoirs at the boundary of the sand tank. At least one well, located in the centre of the system, is necessary to following reproduce a pumping test.

The BC's to implement are (*FIG 39*):

- In the two opposite in/up and out/down sides of the tank, the hydraulic heads set in the water reservoirs (by the constant head overflow devices) are imposed (Dirichlet). Those are responsible of the constant flow within the sand. It is important to note that, while simulating an unconfined aquifer, those hydraulic heads should be imposed lower than the total height of the sand because otherwise all the system will be flooded. Therefore not all the sand results completely saturated.

- At the lateral borders, meaning the two sides of the box in which no constant heads are imposed, no explicit BC is specified. Therefore, no flux (Neumann) is chosen by default from the software, which is actually the great representation of impermeable boundaries.
- The bottom of the tank is considered impermeable too, therefore again no flux is automatically imposed (Neumann).
- On the top boundary, starting heads should be firstly set equal to the top grid elevations but once the first flow simulation is run, they can be imposed equals to the obtained hydraulic heads.
- Pumping rate applied (and time of pump functioning) should be also implemented at the correspondent well and time.

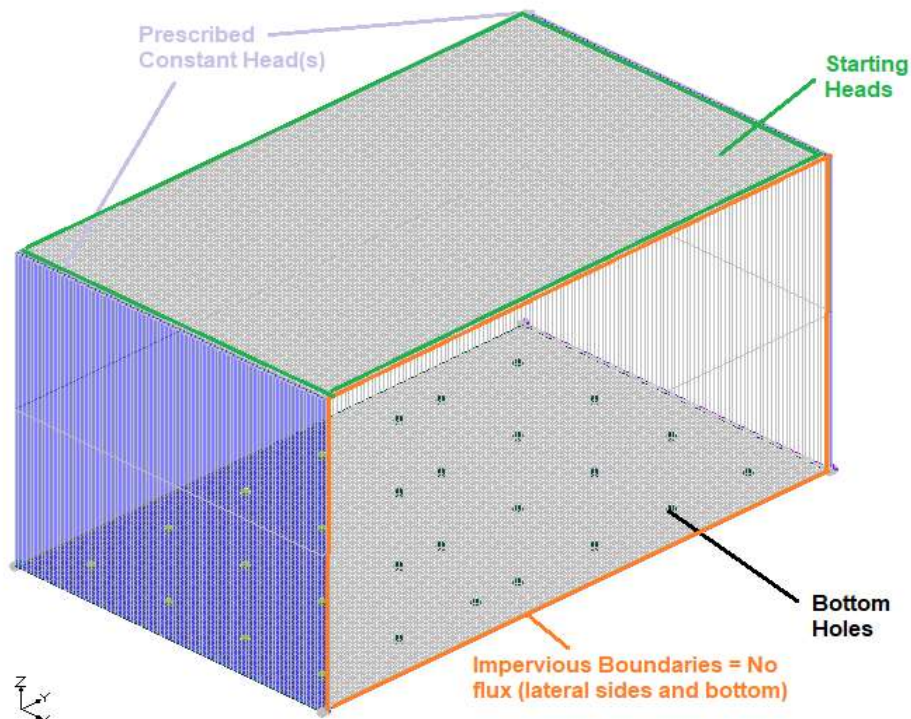
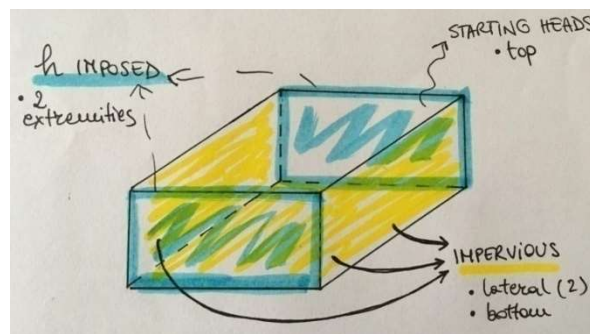


FIG 39 BCs of FLOW numerical model of physical 3D sand tank

And for the **TRANSPORT MODEL**:

It is used to simulate tracer tests. The injection well is set in the upper side of the system and the observation well, needed to monitor tracer behaviour, is located down-gradient. The model derives from the flow one, and so it is again 3D. Thus, it can reproduce more results in terms of compound spreading.

The BC's and inputs are:

- Water heads in the two opposite boundaries are taken from the flow model, together with the flow within the system.
- Hydrodynamic diffusion-dispersion mass flux through the lateral boundaries and the bottom one, is set equal to zero (Neumann), in order to reflect their imperviousness.
- No background concentrations are imposed in the system.
- The specified concentration injected (Dirichlet) is implemented only at the specific injection well and at a determined time. In the other parts of the system any concentration is specified.

2. Numerical implementation

For the construction of the numerical model it is used the code MODFLOW-MT3DS 2000 (Parallel version 1.0), through the interface of GMS 10.3. Explanations on how concepts are translated into numerical input are given.

The conceptual approach is followed and several coverages are implemented: boundaries of the system (sand tank + constant head reservoir space), boundary conditions (imposed heads for flow), sand characteristics (hydraulic conductivity, and in case of transient variations also specific yield and specific storage), wells and observation points. In this way, soil characteristics result to be associated only to a polygon (not inserted by the use of the "material set" tool).

Between the four types previously tested in columns, it is assumed that the quartz sand N5 will be used to fill the tank. An homogeneous and saturated medium is studied. Therefore it is immediately possible to implement in the numerical model the associated parameters determined through previous column experiments.

Hydraulic conductivity differences are not specified (not influent in the model functioning) for sand and constant head reservoirs, neither for the very permeable mesh/material used to confine the sand and control the flow within the medium, will be represented.

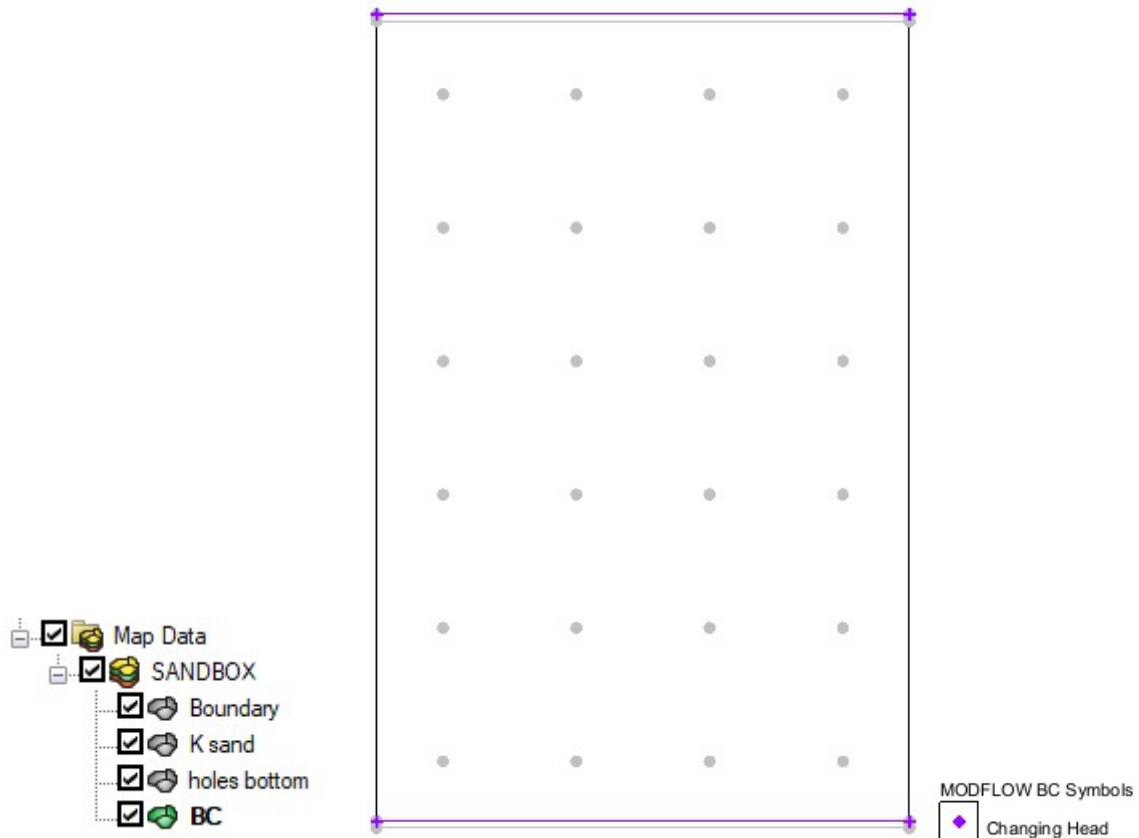


FIG 40 Conceptual model implementation through coverages in GMS

When implementing well(s), location(s), tube characteristics (screen position) and depth are specified. To simplify the model, no differences in K between the inside of a well, the plastic wall of it, and the surrounding sand are also assumed. Furthermore, only punctual wells are represented (just one-cell-column) even if they normally have a diameter ranging from 1 to 6". This strong assumption means that no physical representation of boreholes are implemented. But it is acceptable because a screen is imposed all along the tube.

Therefore **value of K** (and also **total porosity**, **effective porosity** or specific yield, and storage coefficient) results to be **the same everywhere**. For the selected N5 sand those values are: **$K = 8.82 \times 10^{-4}$ m/s**, **$n_{tot} = 45\%$** and **$n_{eff,flow} = 22\%$** .

Regarding the **FLOW MODEL**:

The equilibrium under steady state conditions is characterized by a stable constant flow imposed by constant head reservoirs, in both the two extremities of the sandbox. Those water levels are imposed in all the cells of the two line-columns outside the real sand delimitations. [Note: Given the fact that constant heads should only be imposed in the extreme sides, the IBOUND array, which is used to identify specified head boundaries, should be correctly implemented: values in all the grid should be >0 (equals to +1) meaning that the heads should be computed as part of the simulation, except in the lateral constant

head sections where values are <0 (equals to -1) because of the 1st type of boundary condition].

Especially while performing pumping tests, particular attention should be done to face the problem of having dry cells (too fast de-saturation).

Initial conditions to specify, mainly refers to the hydraulic gradient imposed, the hydraulic heads resultant from the constant flow, and the specification concerning the pump functioning (pumping rates and time). The useful packages selected to perform MODFLOW simulations are listed in TABLE 13. Drain and recharge are not needed.

Packages for FLOW simulations	
LPF	Layer Property Flow package
WEL	Well package
CHD	Constant Head package

TABLE 13 Packages implemented in MODFLOW for the flow model

Stresses are defined by the use of stress periods (time interval of input) and each stress period is divided into time steps (time interval of head calculation). For transient problems, the final head in each stress period will become the initial condition for the next stress period. Usually it is run a first steady state configuration, to generate a reasonable initial condition to begin transient analyses. In these last also the storage coefficient is specified: the obtained values of S_s ranges between 9.8×10^{-6} and 10^{-4} m^{-1} , and they are perfectly in line with the reference of Domenico and Mifflin (1965) and Batu (1998).

To verify if the flow model is providing reasonable results, it is evaluated the Flow Budget: the % of in-out water losses should be closer to zero, meaning that in and out water flow should not be substantially different.

Regarding the **TRANSPORT MODEL** (FIG 41):

Once the flow issues are investigated by MODFLOW, new simulations can be run by MT3DS to analyse transport mechanisms. Particular attention is put on the condition imposed by the **Peclet number** (described in *Annex I*). According to the parameters determined for N5 sand, the **longitudinal disperivity** α_L should be set equals to 1.3 cm. But, according to the choice of having cell size $\Delta x = 1 \text{ cm}$ and to the fact that this parameter is really scale dependent, in order to have more regular BTCs, it is reasonable to set it up to an higher value, such as 10 cm.

The aims of this model is also to reproduce and monitor the variations of tracer concentrations, after injection. [Note: IC-BOUND array is the visualization of involved cells in the transport process: all cells are set equals to +1, meaning that they are variable concentration cells]. Initial conditions to specify are the constant flow heads and the injected concentrations when and where they are implemented.

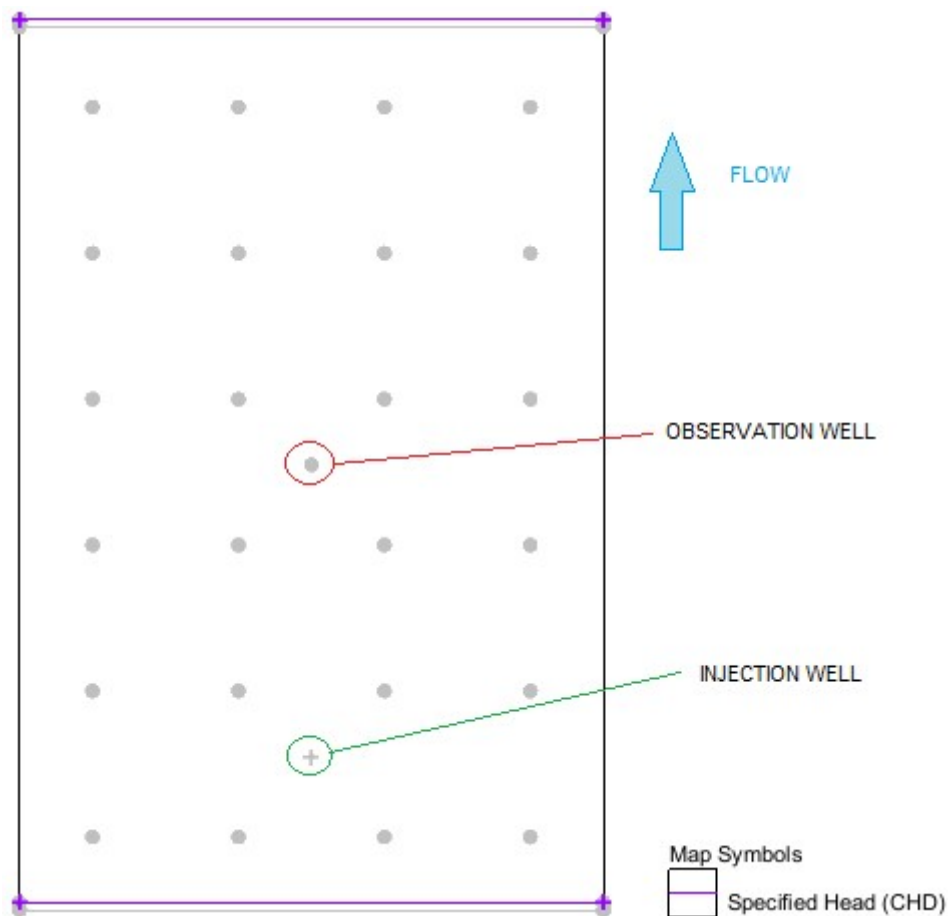


FIG 41 Tracer injection model coverage visualisation (without grid) in GMS

Injections are applied in a well located in a central position close to the higher water level section of the model: coordinates are $x = 0.40$ m and $y = 0.21$ m. The well is passing through both the layers but injection are performed in the top one. An observation well is then located down-gradient: coordinates $x = 0.40$ m and $y = 0.61$ m. Both elements are visible in *FIG41*.

As the tracer is supposed to be ideal and conservative in the simulation performed, no chemical reactions are specified (therefore this package is not chosen while selecting the basic transport packages to use for MT3DS simulations), and neither retardation and degradation are considered. The focus is mainly on advection and dispersion mechanisms.

Between Standard FD, TVD and **MOC solution** (brief explanations of all methods in *Annex I*), the last one is supposed to be the most representative and reliable one.

In *TABLE 14* are reported some information of the **solver** used, both for flow (MODFLOW) and transport (MT3DS). Those specifications are implemented in order to reach a more precise convergence of the models and to not encounter problems on particles number while simulating transport. To qualitatively check simulation results for transport, it is reasonable that a certain spreading of the plume will be visualized.

SOLVER COMPLEMENTARY INFORMATIONS			
Flow	PCG package (Preconditioned Conjugate-Gradient)	Head Change Criterion	0.0001
		Residual Criterion	0.00001
Transport	Advection package	MXPART (max number of particles allowed)	750000
		NPMAX (max number of particles per cells)	50
		NPMIN (max number of particles per cells)	2
		Threshold relative concentration gradient	0.00001
	Dispersion package (considering sand as a structureless, natural, homogenous, non compacted porous medium)	TRPT (ratio between horizontal lateral- transverse and longitudinal dispersivity)	1
		TRVT (ratio between vertical lateral-transverse and longitudinal dispersivity)	1

TABLE 14 Flow (MODFLOW) and Transport (MT3DS) simulation solver characteristics

3. Simulations performed

The sandbox will normally take time to stabilize in terms of flow, once heads are imposed (even several hours for a small dimension tank (Chao et al., 2000)). Therefore the first simulation to be performed consists of modelling a sort of “natural groundwater flow in the sand tank under a prescribed hydraulic gradient”. The system is supposed to be in equilibrium. Once the steady state flow is determined, other type of experiences can be numerically simulated and dimensioned for practical demonstrations. This phase begins with simple pumping and tracer tests. To do so, different pumping-injection-monitoring wells are placed in the sand tank.

It is important that all the experiences will be able to be performed in one afternoon, in order to be practically shown to students.

3.1 Steady state flow

The main objective of the exercise is to set the range of variations of different variables (mainly flow rate and hydraulic heads) to support the correct dimensioning of experiments that will be done in the future.

Trial of different gradients is done, in order to find out a maximum flow rate that should exit the feeding water tank, and thus roughly dimension the circulation pump that has to be implemented in the system. It is decided to impose three different Δh , from the lower to the higher heads difference (doubling and tripling the initial one), to compare the $\hat{Q}_{in/out}$ flow obtained in each configuration. Results are tabled in *TABLE 15*.

$H_{up} ; H_{down}$	Δh (cm)	Gradient (%)	$\hat{Q}_{in/out}$ (m ³ /s)
68; 61 cm	7	6%	2.60E-05
68; 55 cm	13	11%	4.60E-05
68; 48 cm	20	17%	6.75E-05

TABLE 15 Results of steady state flow simulations

As it is expected the flow rate $\hat{Q}_{in/out}$ value increment is proportional to the increment in Δh .

The maximum flow rate that can be push through the sandbox is not known, but it will be mostly limited by the device used to set the water levels (feasibility: consistent flow, reasonable time and visible results) and not primarily by the circulation pump. Furthermore, if the imposed gradient will be too large, other inflow devices to feed the water tank should definitely be added (i.e. additional tubes).

So, it will be possible to assume an entering flow rate of 1 or 2 liters per minutes, and that should also be the maximum pumping rate for the pumping test, otherwise the sand box will remain empty.

In conclusion, the **imposed heads** used also for the following experiences, are **0.68 m** at the entrance (up) section and **0.61 m** at the exit section, thus a $\Delta h = 7 \text{ cm}$ and **gradient** of approximately **6%**. The **flow rate** $\hat{Q}_{in/out}$ is $2.60 \times 10^{-5} \text{ m}^3/\text{s} = 1.56 \text{ L}/\text{min}$, moving towards the lower water level (*FIG 42*).

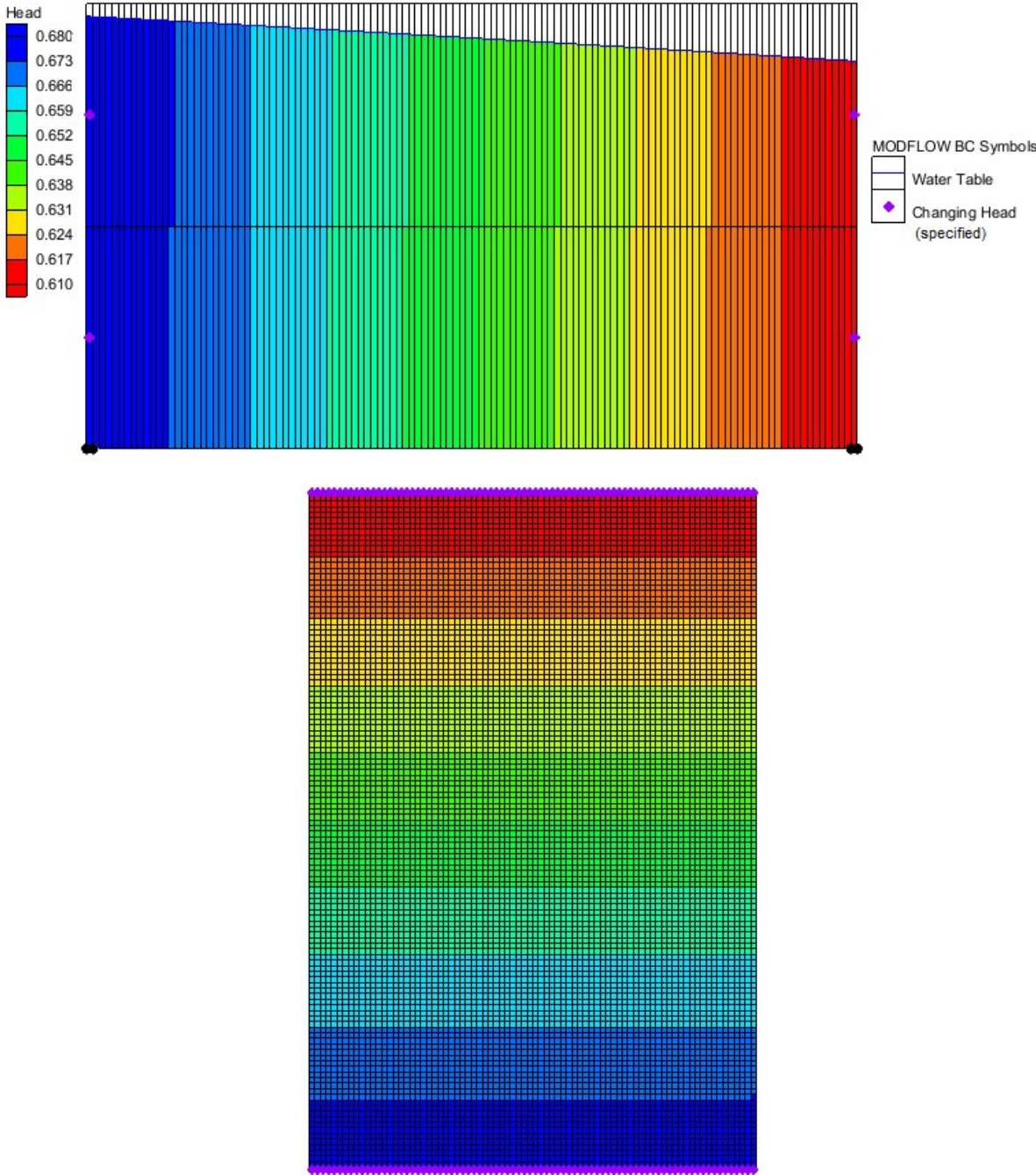


FIG 42 Steady state flow ($\Delta h = 7 \text{ cm}$): lateral and top view, grid visualization

3.2 Pumping Test

Water is pumped from a well in a central position of the sand tank. Therefore, a radial flow towards the central well is simulated and, starting from a stable water level, it reflects a change in the shape of the piezometric surface.

Water levels in the model are monitored through control piezometers (graduated tubes) installed in correspondence of the “holes” at the bottom of the box. [Note: Measurements on the model dimensions, such as the distance between the pumping well and the outer edges of the sand, and from the centre of the well to each of the control points, are taken in order to better quantify the radius of influence and the drawdown].

Basically, drawdown are measures of the water-level response while performing a pumping test. Generally, an higher drawdown is calculated in correspondence of surrounding pumping well portion of upper layer. While a lower one is computed in bottom and further portions. Drawdown (automatically calculated in MODFLOW) have to be really measurable and visible to have a “useful” experiments to show to students. Therefore, at least those measures have to be not lower than 0.5 cm.

Critical flow rate and influence radius are important while dimensioning the test: in fact, based on the position of the monitoring points, it can be determined the pumping rate which allow to observe a maximum drawdown of few cm at the outermost point (larger distance from the central well). Few others helpful tips are:

- To set reasonable pumping rate(s) which are not completely drying up neither the entire system, neither the well itself.
- In all simulations, it must be assured that water level at the extremities of the tank stays fixed at specified levels (constant head imposed for the steady state flow).
- Two types of tests are performed: the short-duration step test and a long duration constant test. The last one is called steady-state pumping test, and practically speaking in the real experiments, it should be conducted at the end of the step-transient test, once water levels in the manometers are again stabilized (the well should be rested between the step test and the constant-rate one to allow for the water level to fully recover the steady state undisturbed configuration). Numerically speaking, to simplify the implementation, two separate simulation, not influencing each other, are done.
- Furthermore, the water through the well should not be pumped at a rate higher than the manufacturer’s recommended capacity for the well screen to avoid damages of the well itself.
- Attention should be put while determining the optimum pumping rate both for the constant rate pumping test and the step test: a visible and measurable drawdown has to be reached, in order to quantify the effect of the experiments (mainly in terms of drawdown and influence radius). The pumping rate Q_{pump} must be prescribed all along the pumping well (screen length). Pumping rate references are taken from similar experiences on physical aquifer models, described by Liu et al. (2007), Illman et al. (2010), Suski et al. (2010), and Zhao et al. (2015).

- Pumping tests can be implemented both in steady state and transient conditions. For constant pumping rate long duration test, a steady state problems is enough representative of the configuration (FIG43): in fact water levels will reach a new stabilization. While, in case of transient step test, the experiment aims to observe continuous changes in water levels to monitor the alternance of different transient and steady state phases (FIG44): here all steps, should be long enough to reach an equilibrium with the water level imposed.

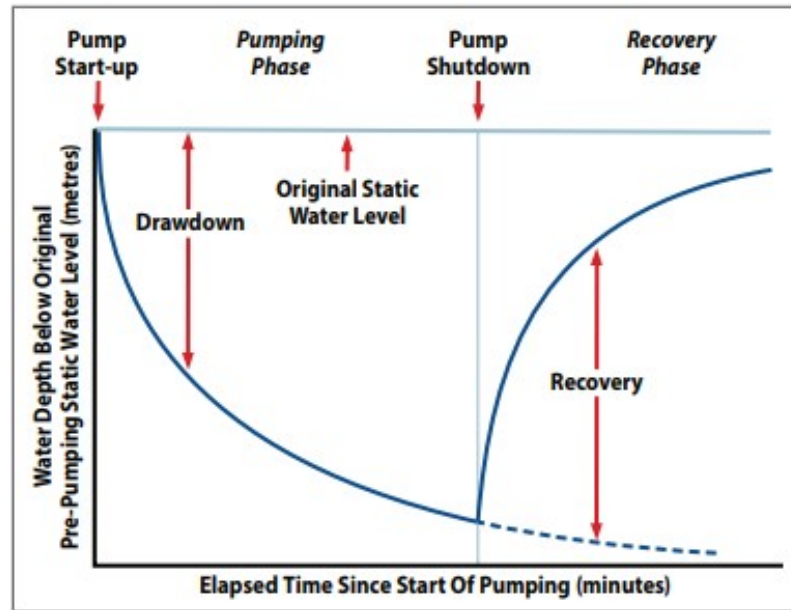


FIG 43 Graph showing the different phases of a constant rate (British Columbia, 2007)

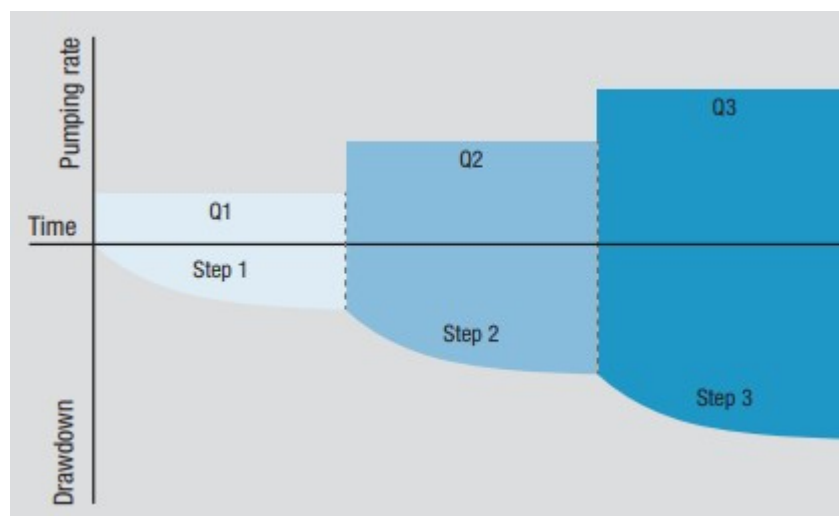
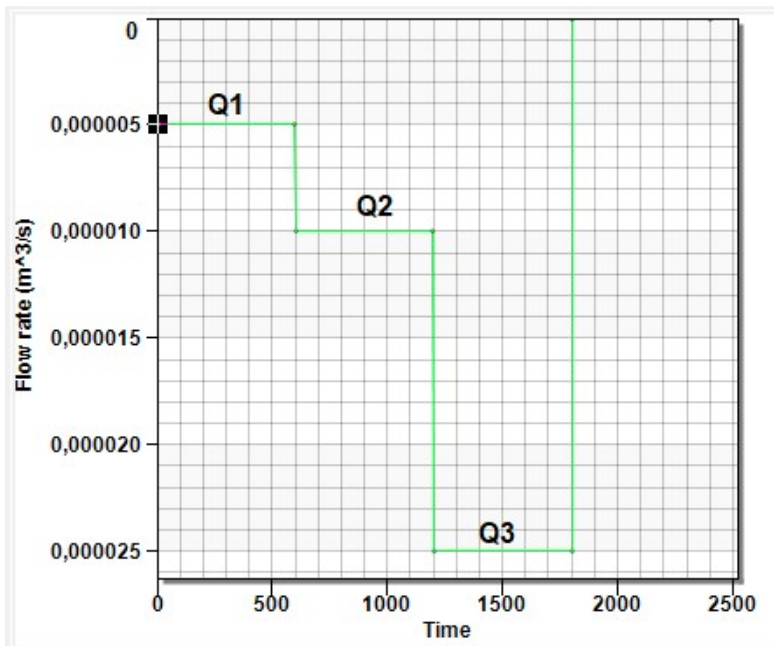


FIG 44 Pumping step test: typical series of pumping rates (Everett, 1995 modified)

During the design and implementation of a **three STEP PUMPING TEST** (FIG45) adopted to the model dimension (scaled down compared to real aquifer tests), the focus is on step pumping rates and lengths :

- a) It is chosen to apply three different increasing subsequent pumping rates. This increment influences a bit the time needed to reach a steady state condition for each step simulated. Anyway, for this simulation, that time is never overcoming few minutes. In order, the applied pumping rates are $Q_{1\text{pump}} = 5 \times 10^{-6} \text{ m}^3/\text{s}$, $Q_{2\text{pump}} = 1 \times 10^{-5} \text{ m}^3/\text{s}$, and as last $Q_{3\text{pump}} = 2.5 \times 10^{-5} \text{ m}^3/\text{s}$, which equals the maximum allowed according to the steady state flow set. [Note: It can be said that while dimensioning the Q_{pump} to apply, it is found that values of the order of magnitude of $10^{-4} \text{ m}^3/\text{s}$ are showing problems linked to flooding/drying of many cells, both close to the well and far away. For this reason, $Q_{3\text{pump}}$ value could be considered as “critical” and maximum to apply to not empty the system.]
- b) While, looking at the steps length, it mainly depends on the number of steps compared to the total time available for the test (not more than one afternoon, as a substitution activity of a frontal lesson). Thus, 10 minutes are used as step length. Ideally, the water level in the well will approach equilibrium at the end of each step, but this cannot always be achieved. Even if the water level has not reached equilibrium at the end of each step, but it is still slowly falling, the results from the test are representative and reliable. The total duration of the experiment includes also the time needed for the system to re-stabilize the steady state previous equilibrium.



Q _{pump}	(m ³ /s)	(L/min)
Q1	5.00E-06	0.30
Q2	1.00E-05	0.60
Q3	2.50E-05	1.50

T _{step} (min)	T _{step} (s)
10	600
Total duration	
40 / 60	2400 / 3600
considering recovery of stable flow	

FIG 45 Step test implemented

It is used always the numerical model with 2 layers: results of water head variations, increasing drawdown and radius of influence are summarized in following figures and tables. Lateral view are always associated to pumping well position (central section). Figures concerning drawdown along vertical direction are not presented, because the grid is not refined enough to represent them correctly.

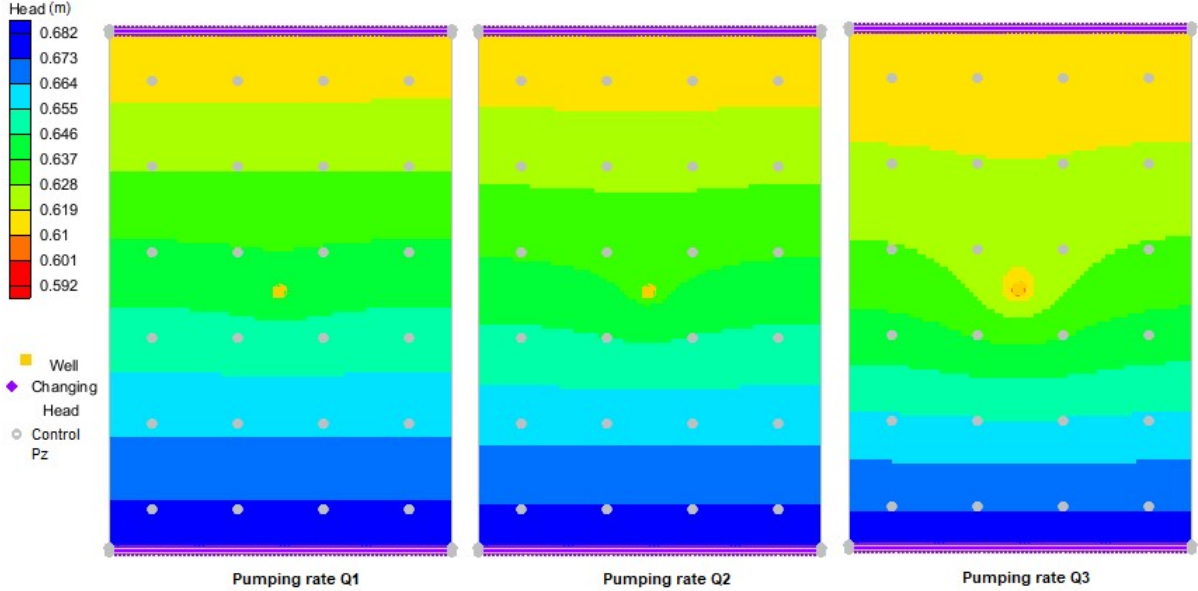


FIG 46 Step pumping test: heads variation

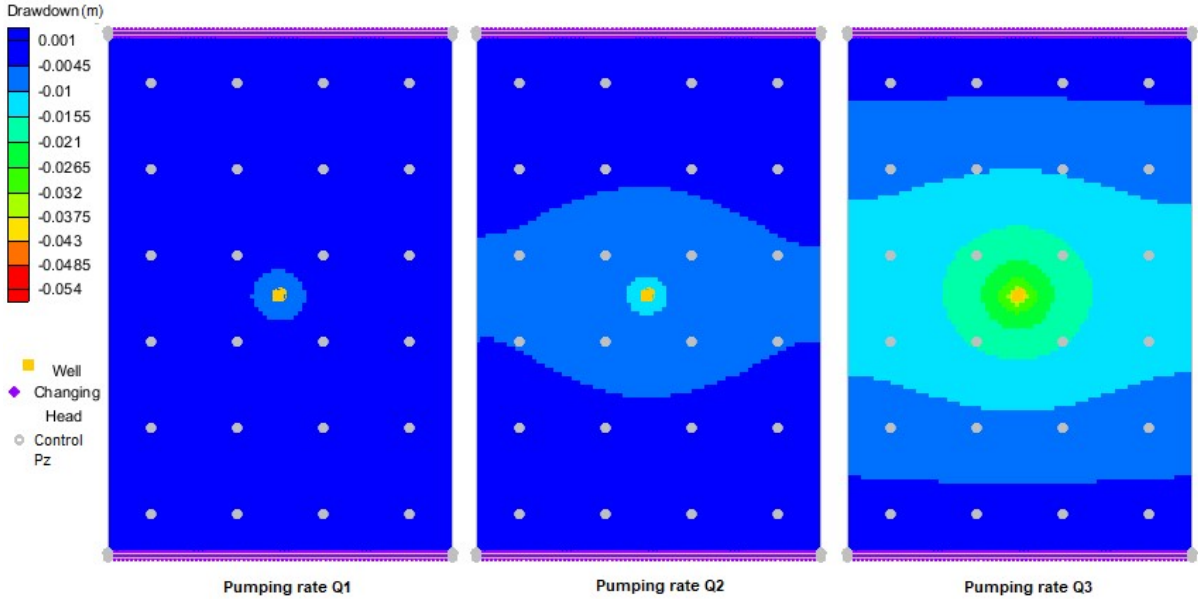


FIG 47 Step pumping test: Drawdown variations

Only results associated to equilibrium steady state phase are reported. As it is possible to see, the system is varying with the time and following “steady state” configurations are reached. The more consistent variation of water levels (*FIG46*) are recorded while passing from Q2 to Q3, and generally seems to induce higher heads difference in the down-gradient portion of the system. In *FIG48*, it is possible to visualize the variation of the water table passing from 2nd to 3rd step.

Concerning the drawdown, in *FIG47* it is reported the correspondent system top view of the series of variations associated to heads of *FIG46*. Those drawdown variations allow to better evaluate the influence radius, and visualize how the pumping test influence is symmetric, considering the well as the centre of the radial flow. *TABLE16* summarises the influence radius rough evaluation, according to the drawdown quantification for the higher pumping rate Q3. As it could be seen in *FIG47*, starting from the Q2, laterally all the system is involved and the limit is imposed by system dimensions.

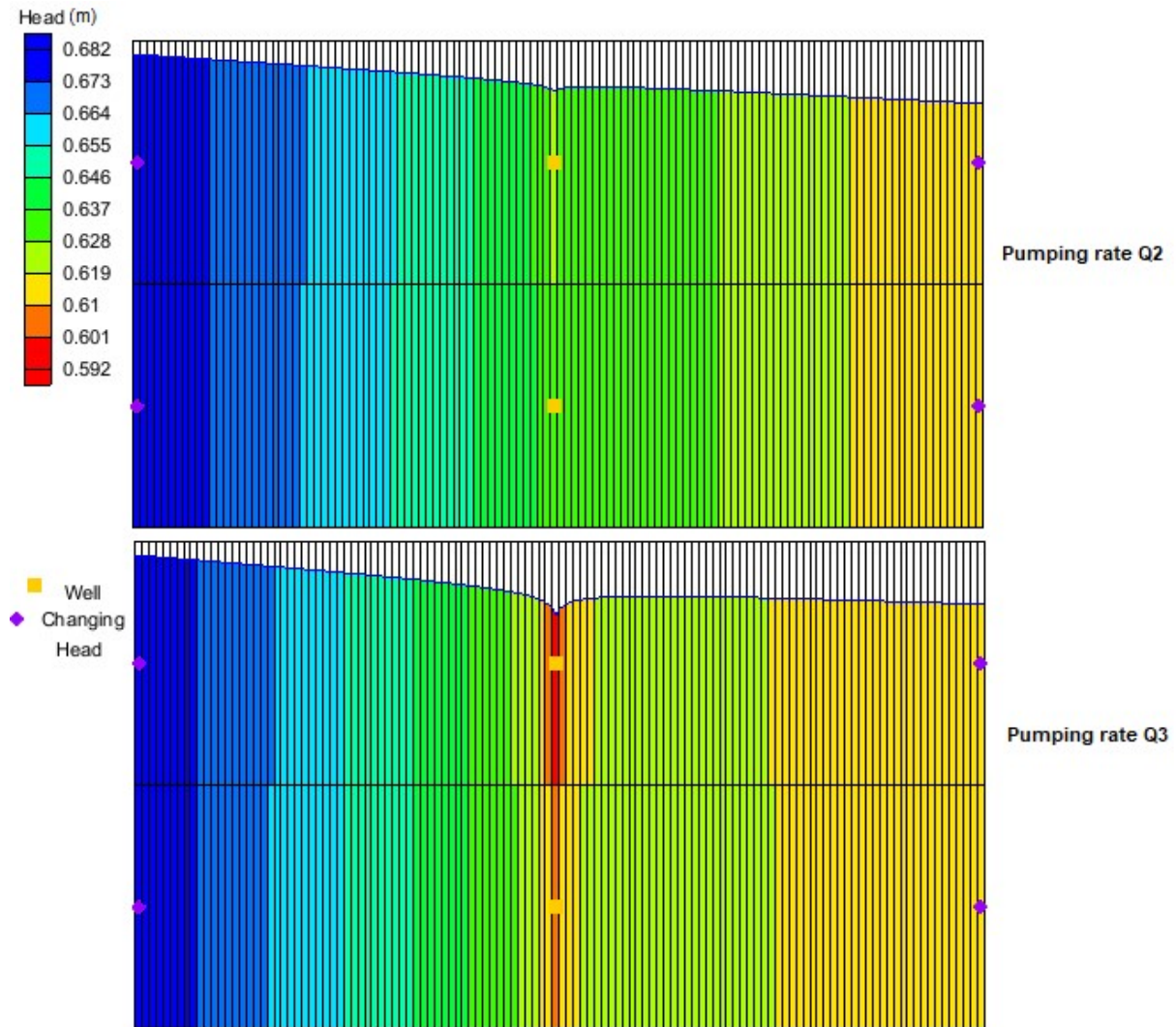


FIG 48 Step pumping test: water table variation passing from Q2 to Q3

To estimate the influence radius, control piezometers correspondent to the holes in the bottom of the tank are considered. Roughly the location of the pumping well and those piezometers (real diameters influence), is supposed to be referred to few cells surrounding the center of each specified point.

	Influence Radius (cm)	Drawdown (cm)
Q3	10	between 4 and 2.5
	30	between 2.5 and 1.5
	50	between 1.5 and 0.5

TABLE 16 Step pumping test: influence radius and drawdown for higher pumping rate

Based on those results, also simulation of **CONSTANT PUMPING TEST** are performed. Results concerning problems and maximum drawdown values are in **TABLE 17**. A comparison between different Q_{pump} applied on the 2 layers model is done (additional images of analogous simulations with the 7-Layers model are reported in **AnnexVII**: there it is more visible how the presence of too many dry cells leads to lack of values and troubles on computation). It can be seen that more variations of head are recorded in correspondence of higher Q_{pump} , as it is reasonable.

According to those results, the pumping rate $2.50 \times 10^{-5} \text{ m}^3/\text{s}$, seems to be again the most reasonable choice: it allows to register interesting water table variations without reaching complete de-saturation of any portions of the system. [Moreover, the numerical simulation is running fast, and computations are not time consuming.]

Q_{pump} (m^3/s)	Problem	Drawdown max at control pz
2.50E-04	many dry cell	empty system
6.50E-05	few dry cell	around 8 cm
2.50E-05	no dry cell	around 3.5 cm
1.00E-05	no dry cell	around 1.5 cm
2.50E-06	no dry cell	too small, not visible
1.00E-06	no dry cell	too small, not visible
2.50E-07	no dry cell	too small, not visible

TABLE 17 Different pumping rates applied on the 2 Layer Numerical Model

3.3 Tracer Test

The majority of tracer tests performed on physical sandy aquifer models at laboratory scale are used to investigate the effect of travel distance and the longitudinal dispersivity along the sandy material (Kim et al., 2002). In the studied case, the injection value used are only trials, and are taken from the literature, looking at similar experiences. They are mainly related to the substance that is used as tracer, to their detection and solubility limits. Thus for example in case of fluoresceine a reasonable concentration to inject can be considered $100 \mu\text{g/l} = 0.1 \text{ mg/l}$ (Jose et al., 2004), for bromide solution and a food colouring dye is 151.5 mg/l (Illman et al., 2012) and for a solution of KCl is around $10 \text{ g/L} = 10000 \text{ mg/L}$ (Kim et al., 2002).

The purpose is to investigate other groundwater flow and transport properties along the homogeneous isotropic medium of sand, using a **conservative ideal tracer**. In particular, it is chosen again the conservative tracer Cl^- , as for the column tests, because it is able to reproduce water behaviour without activating any chemical reaction within the investigated sand system. Cl^- tracer is delivered as a KCl salt. [Other analogous simulations can be performed considering substances such as uranine, or other salts with ions non reactive with quartz sands, such as KBr.]

In all the cases of simulations implemented, the **hydraulic gradient** imposed in the tank is around **6%**, causing a stable **flow** of $2.6 \times 10^{-5} \text{ m}^3/\text{s}$. It is used an injected concentration equals to $C_{\text{inj}} = 150 \text{ mg/l}$, in order to achieve visible results in a reasonable and useful time. The **injection flow rate** is around **0.01 L/min**, which is in line with the experiments founded in Illman et al., 2012.

Brief injections are associated to an **injection time** $T_{\text{brief,inj}} = 10 \text{ minutes}$, while **continuous injections** have a $T_{\text{continuous,inj}} = 3 \text{ hour}$ (stress periods definition). The duration of the performed analyses and their relative breakthrough curves BTCs is varying between the different tests, and it is never overcoming 3 hours. To display a quite detailed BTC, it is generally chosen to record results every minute.

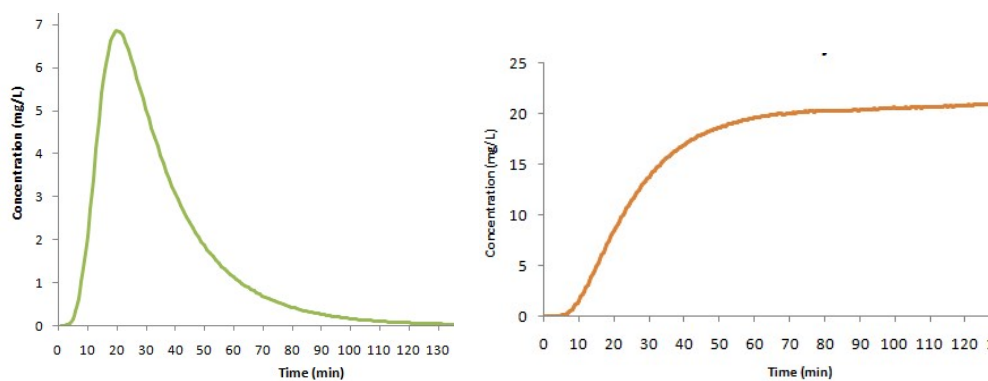


FIG 49 Examples of results associated to brief and continuous injection breakthrough curves numerically obtained

FIG 50 is reported in order to show why it is chosen to set up the coefficient of longitudinal dispersivity to an higher values than the one determined for the N5 sand column-sample, and why it is used the MOC method. Firstly, using $\alpha_L = 0.013 \text{ m}$, uncommon and unexpected curve shapes are recorded, both for TVD and MOC solutions, and both in case of continuous and brief injection: the main reason could be associated to the cell dimension. In fact, between Δx cell (0.01m) and the value of longitudinal dispersivity (0.013m), there is a too small difference, which can produce numerical oscillation and unreliable results. So, finally it is set $\alpha_L = 0.10 \text{ m}$. And it is chosen the **MOC method** because is quite effective in eliminating numerical dispersion while preserving concentration peaks (in fact curves are always reaching a bit higher concentration levels). Furthermore, as it is possible to notice, while performing the same kind of test and analysing the same minute of time (FIG 50), the MOC simulation is presenting a smaller plume (in all dimensions) and a slower advancement and spreading of the tracer.

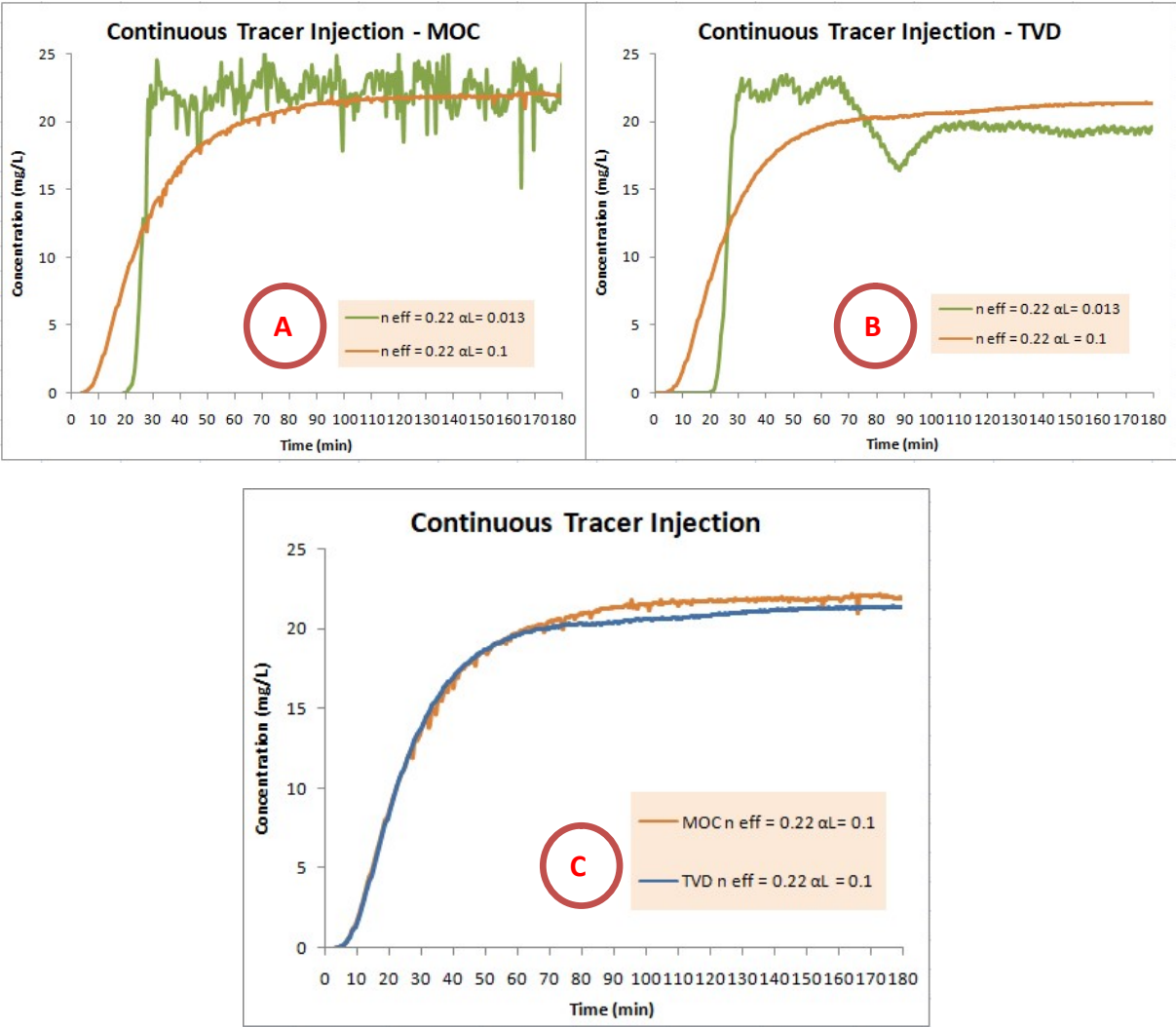


FIG 50 Comparison BTCs continuous tracer inj (A-MOC, B-TVD, C-Comparison) correcting the value of the dispersivity

TABLE 18 resumes results of two different tracer tests, according to the implemented parameters, that could be feasible as experiment/exercise to reproduce in the real sand tank during lessons.

Type of Test	Cinj (mg/L)	Tinj (min)	First arrival (min)	Peak/Stabilization (min)	End (min)
Brief injection	150	10	25	35	60-70
Continuous injection	150	180	8.5	after 120	180

TABLE 18 Results of main ideal tracer tests with N5 sand

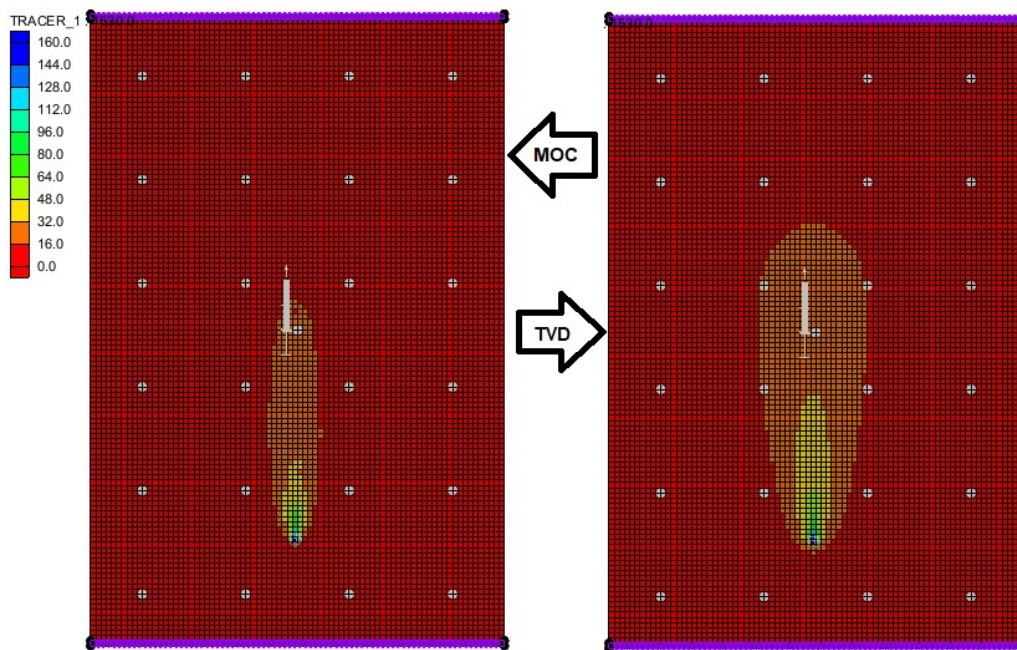


FIG 51 Continuous tracer injection with MOC and TVD advection solution (plume comparison at min 25, red background corresponding to zero concentration)

While increasing the hydraulic gradient within the system (FIG 52), a faster tracer first arrival is recorded (few minutes each increment of 7 cm in Δh , following the same steady state flow simulations presented in paragraph 3.1). In case of continuous injections, the BTC is stabilizing sooner at a constant value, so the first slope of increasing arrival tracer concentration is steeper and steeper while increasing the gradient. Analogous results are registered in case of brief injection, when the peak is reached before and the shape of the restitution curve is thinner and with a smaller tail. The result is that, while applying larger Δh , faster simulations, and normally also real experiment, can be generated.

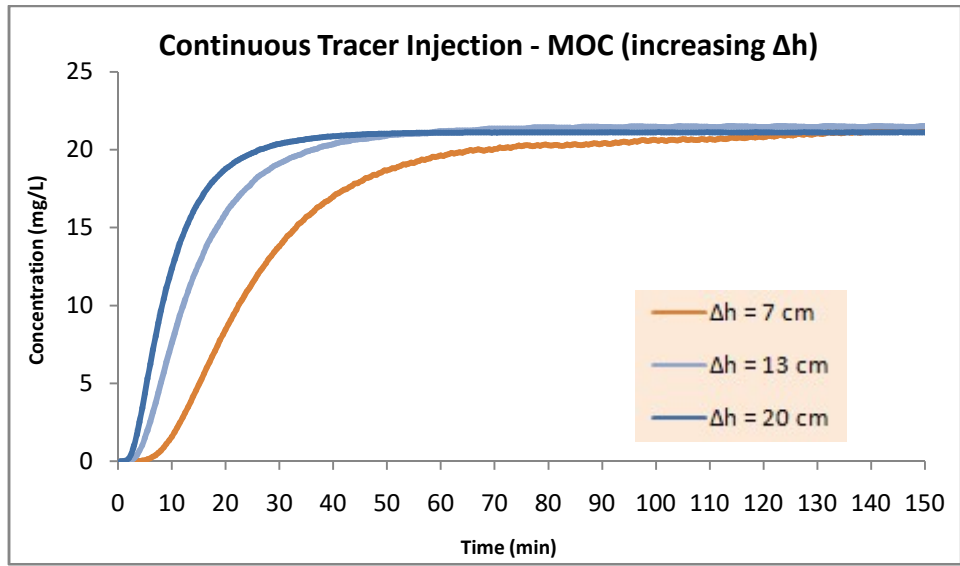


FIG 52 BTCs continuous injection simulated applying increment in prescribed Δh (MOC solution used)

4. Sensitivity analysis

A simple sensitivity analysis on the main parameters is performed and summarized hereafter by points. Parameters are changed one by one. The study in fact aims to study the influence of a change in each of the sand characteristics (such as K , $n_{\text{eff,flow}}$ and α_L) on the functioning of the model and on its reaction to external stresses.

- a) First of all a comparison in term of **hydraulic conductivity** between different types of sand and also extreme cases (such as the highest 10^{-2} m/s for gravel or cobbles, and the lowest 10^{-11} m/s for unfissured clay) is done.

First of all, changes in K are supposed to reflect variations of the shape of the water table/surface (FIG52). Given the fact that, K for N5 is really closed to the other ones determined for the other types of sands, no real differences are visible. By computations, it can be seen that mainly at the order $\frac{1}{10}$ of mm, those variations really occur. But even imposing higher hydraulic gradients and flow in the system, those changes are not really visible.

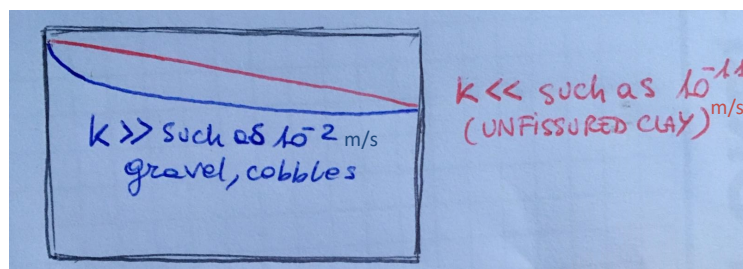


FIG 53 Change in water surface in relation to variations of K (m/s)

K changes also influence the results of all pumping test. In fact, as it is reported in FIG53, for the same pumping rate applied, different values of K are associated to different drawdown (gradual decreasing scale, results in TABLE 19): higher values of K (as for example $K_{3\text{to}5}$) correspond to smaller variations of hydraulic heads, while lower K (like K_{N1}) are associated to larger water level (and water surface shape) variations.

Sand Type	K (m/s)	Drawdown (cm)
N1	2.94×10^{-4}	between 8 to 0.5
N5	8.82×10^{-4}	between 4 to 0.5
1to2	2.13×10^{-3}	lower than 0.5
3to5	2.54×10^{-3}	lower than 0.5

Constant Q_{pump}	
(m^3/s)	(L/min)
2.50E-05	1.50

TABLE 19 Comparison of results of constant pumping rate test due to changes in K value

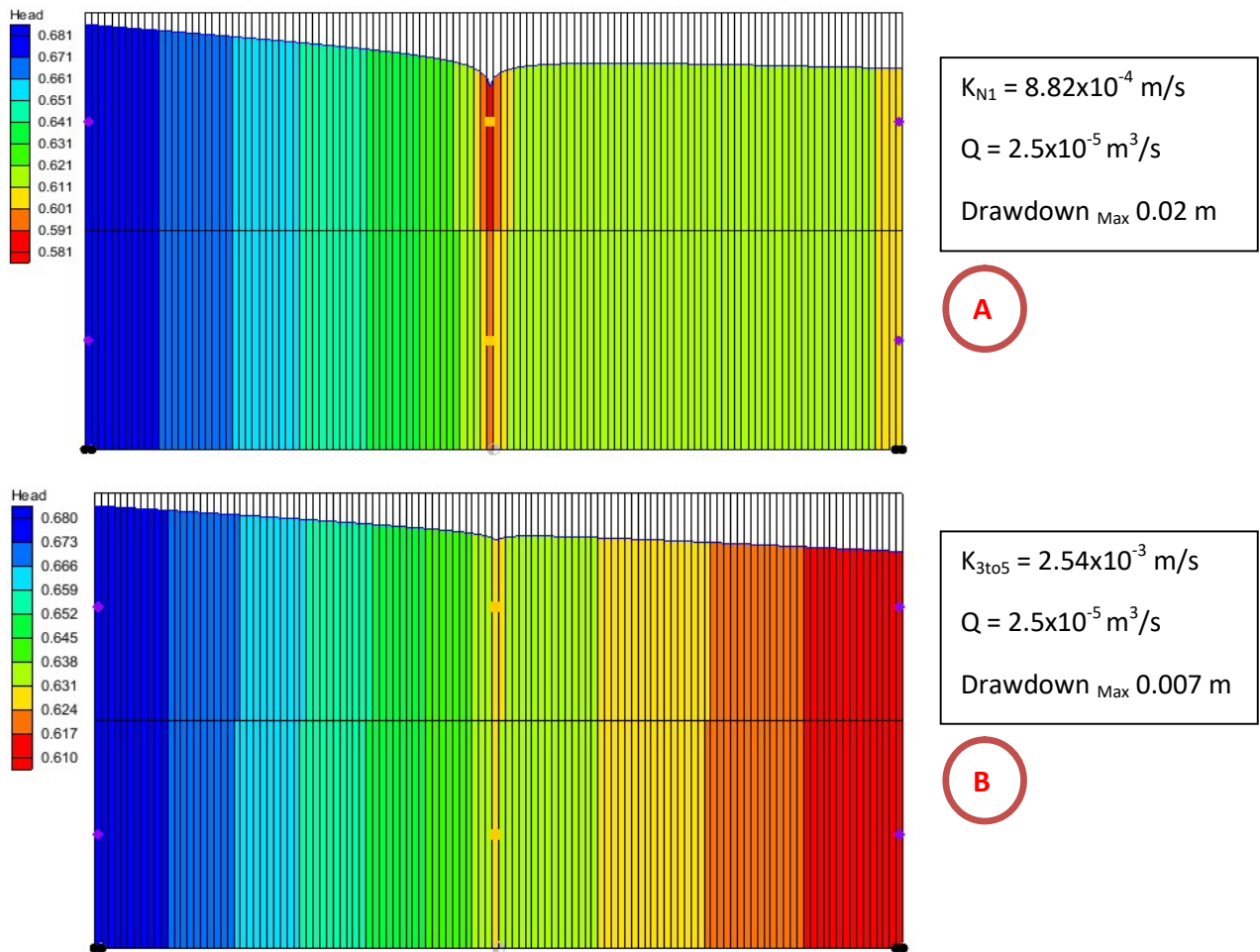


FIG 54 Head comparison while varying K value (A for K_{N5} , B for K_{3to5})

Obtained results are reasonable thinking about the meaning of K, directly linked to the velocity at which the water is flowing in the system: as faster it flow, less variation in hydraulic heads will be registered, in case of a stable flow system.

K_{3to5} and K_{1to2} are not so different, thus also the drawdown variations are almost the same. In terms of influence radius an opposite behaviour than the drawdown, is recorded: in fact, for a fixed pumping rate, while increasing K in the system, the influence radius is increasing too, even if the difference in water heads is diminishing.

Concerning tracer test simulations, variations of K do not have visible influence on final results.

- b) Then, only referring to sand N5, a change in the **effective drainage porosity** is applied. The main changes in system behaviour are affecting tracer test simulations. When the parameter $n_{\text{eff,flow}}$ is set equals to a lower value (such as 0.5 in *FIG54*), the time of tracer first detection is anticipated. Furthermore, the breakthrough curve in case of continuous injection, is reaching more rapidly the concentration peak values at which is stabilizing. On the other hand when $n_{\text{eff,flow}}$ is larger (such as 0.30 in the same graphs as before), a delay is recorded in the first arrival time, and also in the curve stabilization (which is also around lower values). In the same figure also the comparison of the different BTCs associated to different $n_{\text{eff,flow}}$ while increasing from 0.013 to 0.1 m the value of α_L are shown: to this last configurations, more defined and reliable BTCs are obtained. In fact, in case of MOC solution, less oscillation of values are recorded and differences in the arrival tracer concentration can be better visualize and monitored (different shapes and slope).

Different is the case of brief injection: here the restitution curve for lower $n_{\text{eff,flow}}$ is taller, thinner and it begins many time before the others. For larger $n_{\text{eff,flow}}$, the curve is shorter, wider and dalyed in time. To have an ideas about those time variations it can be said that for $n_{\text{eff,flowN5}}=0.22$ (value determined in sand column) the first consistent arrival is around 9 minutes, while in case of $n_{\text{eff,flow}} = 0.05$ it is at 2 minutes and for $n_{\text{eff,flow}} = 0.30$ it is at 13 minutes. In *FIG55* it is possible to visualize those changes, also in terms of peak concentrations.

[Comparison are done also using TVD method: analogous results are obtained. The graph is shown at the end of **Annex VII**].

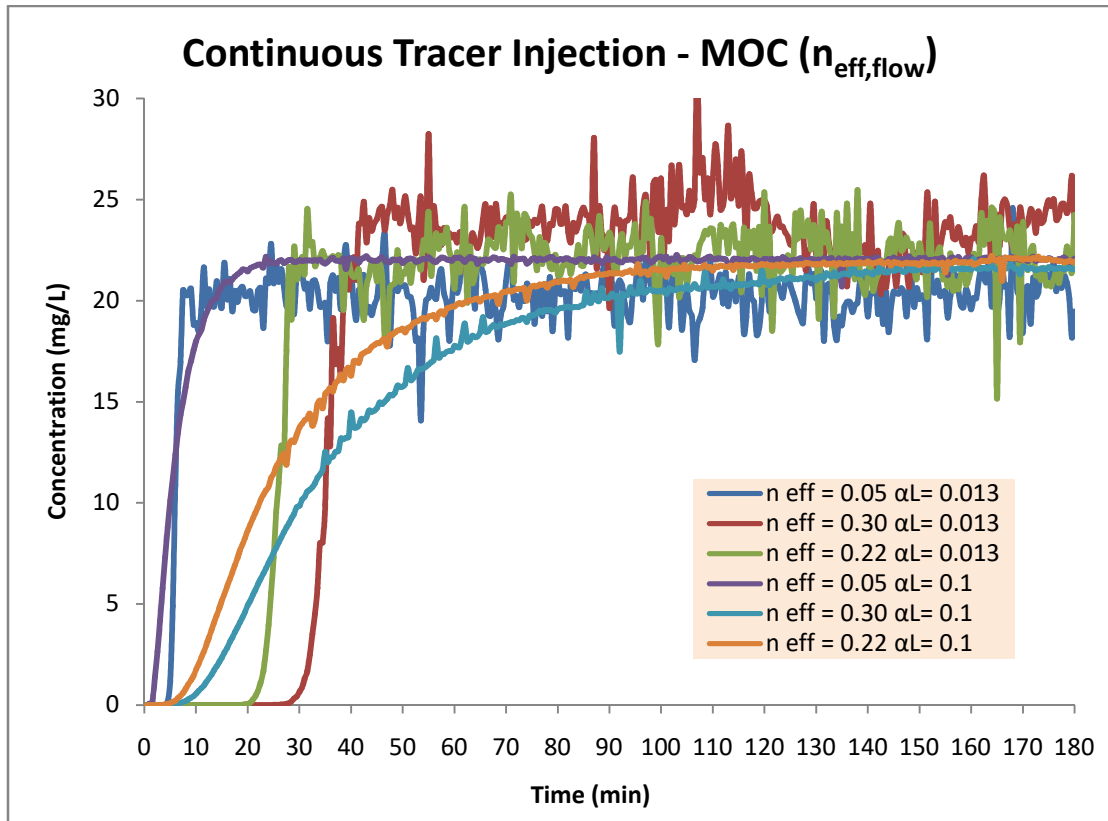


FIG 55 BTCs for Continuous tracer injection MOC (changes in n_{eff} and α_L)

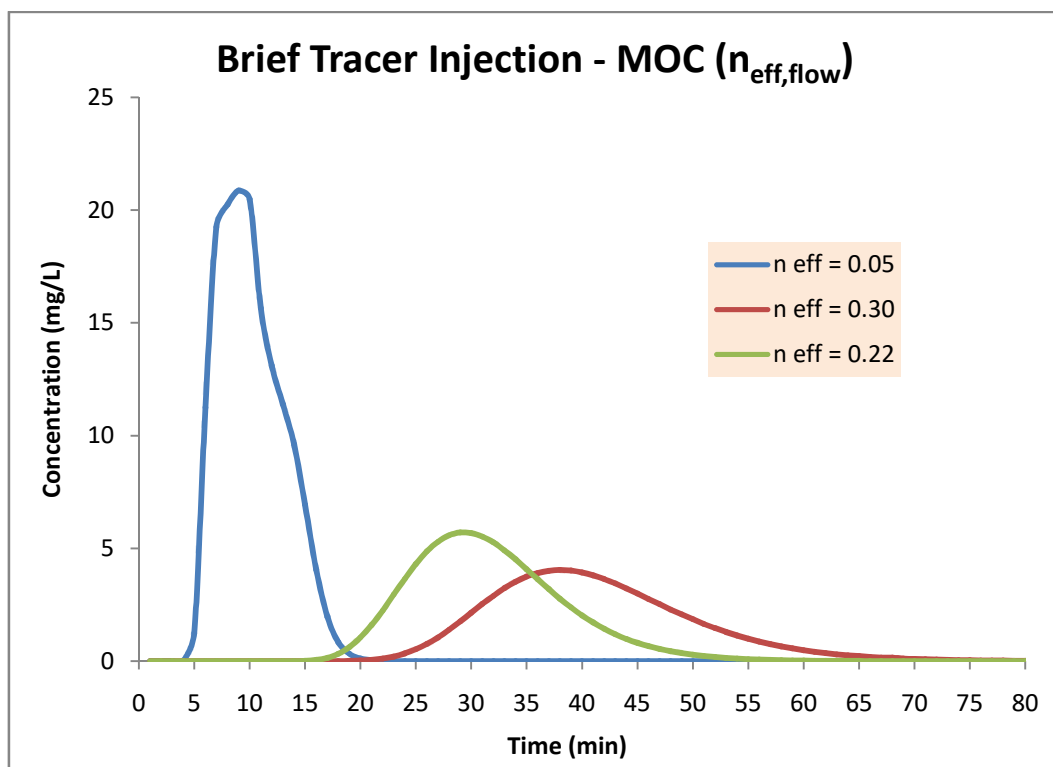


FIG 56 BTCs for Brief tracer injection, MOC solution, and changes in n_{eff}

Chapter 5

Conclusions

The final objective of this work was to carry on all the preliminary studies needed to have a lab scale 3D sand aquifer that can be used to illustrate different teaching aspects of hydrogeology: hydrogeological concepts, flow and transport processes, hydrogeophysics, groundwater modelling etc. To reach that final objective it was needed to proceed by steps :

- (1) Firstly to really design and construct the 3D physical model;
- (2) Then to select a porous material to fill it and pre-characterize this aquifer material in the lab (for example by column experiment);
- (3) And finally to develop a 3D model at the scale of the physical model as a support to pre-dimensioning and interpreting experiments.

This was the guiding thread between the different aspects of the work, and to conclude the main results obtained in each phase are presented while navigating across the different aspects.

By column experiments, reasonable and logical results were obtained in term of sand parameters characterization. The main trends highlighted were:

- Generally all values of hydraulic conductivity, total porosity, effective drainage porosity and longitudinal dispersivity are gradually increasing going from the finer to the coarser sample
- Only the bulk density is reasonably showing the opposite behaviour increasing while decreasing the granulometry.

This characterization allowed to make the choice of the type of sand to implement in the 3D tank: N5 resulted to be a good compromise between the four (not too fine to show problem of filters interferences, neither too coarse and therefore too permeable to simulate real aquifer example).

Confirmation of this choice comes from the results given by the simulation obtained after with the numerical model implemented by the use of GMS-MODFLOW-MT3DS. It is a functional flow-transport model of the unconfined homogeneous saturated sandy aquifer, able to reproduce and study the reaction of the sand tank system, once external stresses are applied. Here are briefly summarized few main applications and numerical simulations performed:

- Firstly a STEADY STATE FLOW : the aim was to set the range of variations of different variables (mainly flow rate and hydraulic heads) to support the correct dimensioning of experiments that will be really and physically done in the future. The maximum flow rate that can be push through the sandbox is not known, but it will be mostly

limited by the device used to set the water levels or more practically either by the holes for in/out flow connections.

- Then DIFFERENT PUMPING TESTS: Assume an entering flow rate of 1 or 2 liters per minutes, it is taken also as the maximum pumping rate for the pumping test, otherwise the sand box will remain empty. While performing a STEPS TEST: different increasing subsequent pumping rates Q1 Q2 Q3 are applied. Those steps, should be long enough to reach an equilibrium with the water level imposed. While, in case of CONSTANT TEST: only one pumping rate is applied for a longer time. Interesting water table variations without reaching complete de-saturation of any portions of the system should be reached. Those experiments were useful also in order to evaluate drawdown and to estimate the influence radius (control piezometers correspondent to the holes in the bottom of the tank were considered).
- TRACER TEST, both with brief and continuous injection. Reasonable results in term of test feasibility in few hours and enough concentration to be detected (clear breakthrough curves).

Therefore a useful primary pre-dimensioning of experiments was done through the numerical model implementation.

The following steps are to really activate the sand box and put in practice the experiments to see and determine the difference with the pre-dimensioning phase. And then the numerical model calibration and optimization can be done. Once this is achieved, scenarios analysis could also be performed.

The sandbox physical model is generally classified as a "Prototype Model" (and not a Reduced one) because no scale computation in term of ratio between tank dimension and sand grains diameters were carried on. This kind of model aims to reproduce a general behaviour observed in nature, under certain ranges of conditions. And it can be really useful to explain concepts behind phenomena.

Annex 0

Physical model additional images

Additional images related to different configurations available in the field of 2D physical models are here inserted.



FIG 57 Different examples of 2D physical aquifer model: landfill presence and different geological structures (<https://www.realscienceinnovations.com/groundwater-models.html>, consulted in April 2019)

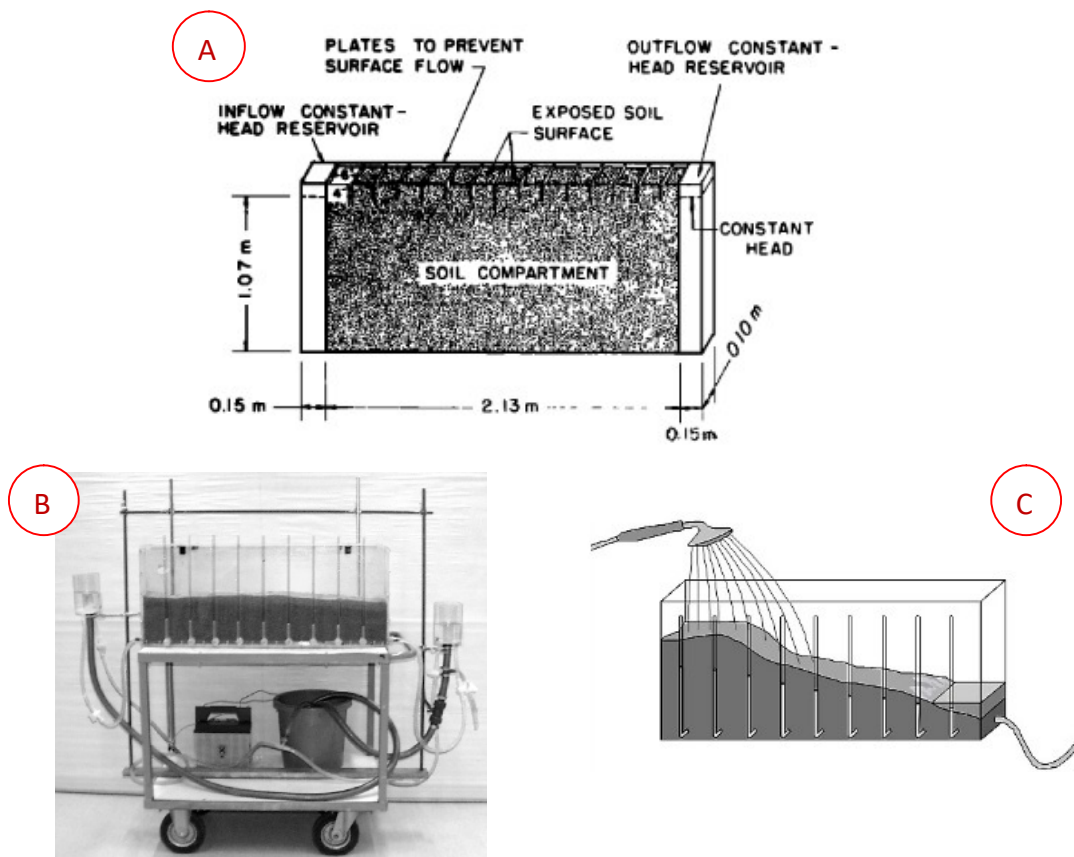


FIG 58 Sand aquifer for classroom demonstrations and example of streamflow generation (A-Silliman et Simpson, 1987; and B-C- Rodhe 2012)

Annex I

Basics of solute transport solving methods used

Solving transport equation is never a simple operation. The presence of both, partial derivatives of 1st and 2nd order, within the same equation, can cause relevant numerical dispersion, artificial oscillation and requires more memory and computational capacity.

The majority of numerical methods used to solve advection-dispersion-reaction equations can be classified as (MT3DMS Manual, 1999):

- a) **Eulerian**, when the transport equation is solved by approximating differential equations with differential equations (finite differences approximate derivatives). It has a fixed grid. This approach is mass conservative and offers the advantage of a fixed grid. It handles dispersion problems effectively, but for advection-dominated problems this method may be susceptible to excessive numerical dispersion or artificial oscillation. To overcome it, restrictively small grid spacing and time steps are generally required. Within those approaches, there are :

1. The STANDARD FINITE-DIFFERENCE METHOD (FD)

The advection term at any finite difference cell, (FIG59) can be approximated by the concentration values at the cell interfaces. It can be either upstream or central-in-space weighted. Because of the dual problem of numerical dispersion and artificial oscillation, the standard finite-difference method is only suitable for solving transport models not dominated by advection (for example when the physical dispersivity is large or the grid spacing is sufficiently fine).

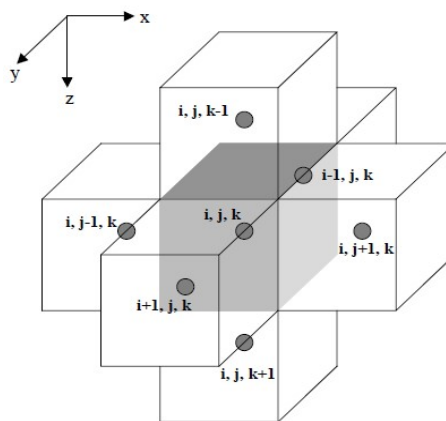


FIG 59 Cell and its interfaces identification: Standard finite-difference method (MT3DMS Manual, 1999)

Furthermore, concentration calculated at a given node should be more influenced by concentration at upstream node (considering an advective transport) than by concentrations at other neighbouring nodes. In eq. (XLIX) concerning the forward

procedure, σ indicates the upstream coefficient (ranging between 0 and 1), that is generally higher than 0.5 in order to create the upwind weighting. To solve this equation, the flow direction should be already known.

$$\frac{\partial C}{\partial x} \approx \frac{(1 + \sigma)C_{(x-\Delta x)} - (1 - \sigma)C_{(x)}}{\Delta x} \quad (\text{XLIX})$$

2. The **THIRD-ORDER METHOD (TVD)**

It is a solution technique called “Total Variation Diminishing”, which has the property that the sum of concentration differences between adjacent nodes diminishes over successive transport steps. This scheme is mainly used to solve advection-dominated transport problems. In the MT3DMS code is implemented the TVD scheme based on the ULTIMATE algorithm, Universal Limiter for Transient Interpolation Modelling of the Advective Transport Equations (Leonard, 1988).

Compared to the standard finite-difference method described previously, TVD is generally much more accurate in solving advection-dominated problems, although its greater computational load. On the other hand, compared to some Lagrangian or mixed Eulerian-Lagrangian methods such as the MOC method of characteristics (which are explained as follows), TVD is not as effective in eliminating numerical dispersion while preserving concentration “peaks”. Anyway, TVD mass conservation property together with smaller memory requirements, make TVD schema other time the best compromise between the standard finite-difference method and the particle tracking based Lagrangian or mixed Eulerian-Lagrangian methods.

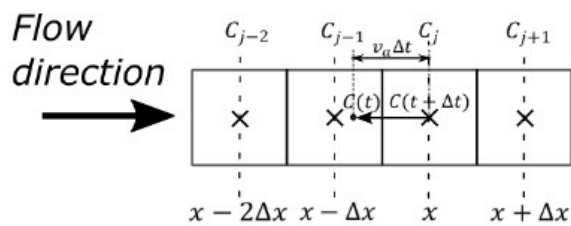


FIG 60 TVD schema of operation (Dassargues, 2019)

- b) **Lagrangian**, when transport equations of advection and dispersion are solved either in a deforming grid through particle tracking, either by random walk method. This approach provides an highly efficient solution to advection-dominated problems virtually free of numerical dispersion. However, without a fixed coordinate system, the method can lead to numerical instability and computational difficulties. Also the interpolation of velocity needed in particle tracking can lead to local mass balance errors and anomalies (LaBolle et al., 1996).

- c) **Mixed Eulerian-Lagrangian**, which attempts to combine the advantages of both Eulerian and Lagrangian approaches by solving the advection term with particle tracking and the dispersion-reaction terms with an Eulerian method. However, some of those procedures, such as the MOC method of characteristics, do not guarantee mass conservation, and may not be as computationally efficient as a pure method.

3. The METHOD OF CHARACTERISTICS (MOC)

In this operative solution, a set of moving particles are tracked forward during each time period. An intermediate concentration for cell m , equal to the weighted average of the concentrations of all particles in the cell, is computed (FIG61). This intermediate concentration accounts for the effect of advection alone during a time increment Δt , and it is used to calculate changes in concentration due to dispersion and other processes over that time increment.

One of the positive features of the MOC technique is that it can be considered virtually free of numerical dispersion. On the other hand, the major drawback of the technique is that it can be slow and requires a large amount of computational memory when it is necessary to track a large number of moving particles, especially in 3D. The MOC technique can also lead to large mass balance discrepancies because the discrete nature of the particle tracking does not guarantee local mass conservation at specific time step (in MT3DMS mass discrepancy is mitigated through the use of consistent velocity interpolation schemes and higher-order particle tracking algorithms). When mass balance issues are present, it is more convenient to use the TVD scheme or the standard finite-difference method if numerical dispersion is not a central concern of the investigated case.

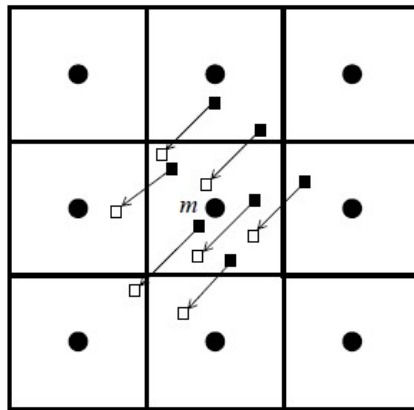


FIG 61 Illustration of the method of characteristics (MT3DMS Manual, 1999)

$$\frac{\partial C^v}{\partial t} \approx \frac{C_{(t+\Delta t)}^v - C_{(t+\Delta t)}^{v*}}{\Delta t} \quad (L)$$

In eq. (L) the variable $C_{(t+\Delta t)}^{v*}$ represents the intermediate volumetric concentration at time $(t+\Delta t)$ (Zheng, 1990).

All of these three techniques were employed to numerically simulate tracer test experiments on the studied sandbox, and results have been compared, following some guideline studies that have compared the performance of these transport solvers in case of stable systems (Mehl et Hill, 2001; Goswami et al., 2011).

Results that will be lately shown, present differences in the plume monitoring in the 3D investigated configuration. The experiment is simulated using alternatively the FD method, the MOC or the TVD, always with an homogenous conductivity field. The first method was never able to produce any kind of reliable results while more similarities were recorded between the other two techniques.

Peclet and Courant Numbers

Numerical resolution of the transport equation leads to numerical dispersion, roughly defined as the difference between simulated quantities and real ones. This loss of accuracy is evaluated through two dimensionless main tools, which influence time and space discretization:

- 1) The ***Peclet Number*** (Pe) is the ratio between advection and dispersion. It is simplified and reflects the fact that the cell size Δx should be equal or smaller than the longitudinal dispersivity α_L of the medium. This is necessary in order to have a gradient between the cells. The formula to calculate this Peclet Number (Pe) is reported below and it has to be lower than 1 to say that the model is providing good results:

$$Pe = \frac{v_{eff,flow} \times \Delta x}{\alpha_L \times v_{eff,flow}} = \frac{\Delta x}{\alpha_L} \leq 1 \quad (LI)$$

- 2) The ***Courant Number*** (Cr), which concerns the fact that the advection movement which is taking place during a time step, should be equal or smaller than the cell size. The formula to calculate it is reported as follows and to have an acceptable results and minimize the dispersion, it is better to keep this number lower than 1. This index is automatically set and optimized by the software once simulations are performed.

$$Cr = \frac{v_{eff,flow} \times \Delta t}{\Delta x} \leq 1 \quad (LII)$$

Annex II

Column preparation preliminary stages

Regarding the preparation of the columns, as it was said, several procedures were tested and progressive improvements were applied to solve the encountered problems.

The first important choice regards the filter: they can be selected differently for each sand sample, depending on the sands characteristic and feasibility of the experiments. Other differences between the sequence of trials concern the different procedures applied while filling each column with sand. Hereafter is presented a brief summary of the trials, together with problem and improvements.

1st Trial

Filters: it was decided to use for all the samples only a bottom filter composed always by two porous disks and in the middle four layer of squared net (disposed in four different orientation in order to have smaller size pores). The four “net-layers” were cut as squared to easy set the different orientation and to be sure to cover all the bottom of the column, also having borders fold to the sand sample side. Each portion of the filter was weighted and taken in consideration during soil bulk density estimation. In the end/top side of the column a layer of few little stones is disposed to assure that the sands will not move out of the column during the water circulation.

Filling procedure: all column were prepared filling sand simultaneously with water by layer of about 5 cm.



FIG 62 Filters bottom of the column: porous disks, net (4 layers to have a more consistent strata- grey in the figure), very permeable sponge material (black in the figure)



FIG 63 Top of the column: little stones used to keep the sands unable to go out from the system during the experiments



FIG 64 On left side it is shown the column preparation: first layer of water and then sand added;
On the right picture the final four columns of the first trial is presented

Problems:

- Preferential paths: the water was free to circulate through preferential paths within the column samples, and those were visible even by eye as holes and channels in the middle of the sand grains. This phenomena mainly happened with the two finer types of sands (N1 and N5).



FIG 65 Preferential paths visualization and similar correlated problems

- Finest sands moving and escaping the system, allowing the additional continuous formation of more water/air layer inside the sand sample within the column (complete decomposition of the sample). This happened mainly with N1. Therefore the stones positioned in the upper section are not enough to keep the system stable when water is circulating (and not only while applying the suction necessary to start the system).
- The presence of air presence within the samples: bubbles of air trapped in filters and not displacing when water is provided. This again was mainly a problem linked to the finer granulometries tested, especially around the bottom filter.



FIG 66 Sand N1 escaping the system while applying water circulation



FIG 67 Air bubbles and channels not filled by water in the finer sand samples plus bubbles of air entering the system together with water

2nd Trial

Filters: for sands 3to5, 1to2 and also N5, only the stones were left, and no filters were added. While for sand N1, another porous disk in the upper end of the column was inserted together with four layers of squared net, to allow the sand not to move out and the sample to be more stable.



FIG 68 Improvement of second and third trial in column preparation: changes in upper filters and hammer use to help air to exit

Filling procedure: it was decided to open the samples and refill them until the top with quantity of sands that had left the system in the previous trial. Then all samples were drained and slowly re-saturated from bottom. Moreover, to help the air displacement, an hammer was used to shake the sample. So generally more air was exiting the system and

less bubbles remain trapped. No air was seen in the tubes meaning that the system was working properly.

Problems:

- Some bubbles of air were still trapped and visible in all the columns, but especially in N5 and N1, where they were again the cause of preferential paths. While in the other two samples they were simply not moving so not really influent for the test results.
- Some grains were still going out from the samples: mainly at the beginning of the connection with the water circulation system for all sand samples, but also after in the case of N1.



FIG 69 Problem of the second trial: still air bubbles trapped and sands exiting the system

3rd Trial

Filters: top filters were added in all the configuration, as it is explained:

- e) For the coarser sands 3to5, 1to2 and also N5, before the stones, four layers of squared plastic net with different orientation were introduced (cut in a circular shape).
- f) For N1 the porous disk in the upper end of the column is maintained but coupled this time with a circular layer of the porous/permeable sponge, to allow the sand not to exit and the sample to be more stable.

Also the bottom layer filters are modified in all the configurations: in all sample it was decided to insert two porous stones with the finer permeable sponge (cut in a circular shape a bit larger than the column shape in order to allow the entire coverage of the section and to have borders fold to the sand side).

Filling procedure: the columns were prepared with a dry sand and then saturated slowly from bottom. [In this context, measures of saturation speed, time needed, related to a specific input flow rate can be taken. They can allow additional estimations of the porosity: those values can be affected by a large error, due to human evaluations. Anyway the obtained values were not so different from the ones previously shown.

Problems:

- Presence of air bubbles inside the samples, but not moving (immobile). For that it was considered not to be a real problem for parameters estimation tests. In fact to eliminate all the air is almost impossible without appropriate devices (such as void pump) because even during days of system inactivity, some reaction will occur within the water (especially because it is not pure water the one used but is the one coming from the sink), and liberation of air will constantly take place.
- Furthermore with the sponge as bottom filter it can happen that some grains will undergoes the porous disks and cause effect in the flow. This mainly happens while putting water before the sand in the column.



FIG 70 Third trial characteristics (filters details)

4th Trial

The main difference of the fourth and the 3rd one is the compaction applied while filling the columns. And the fact that for the coarser sample 3to5 sand column basically nothing change from the first set up for the bottom filter: 2 porous stones with in the middle the 4 nets. While for the other three samples and all the upper filter all was kept as same as it was set in the third trial.

Details and observation on this 4th Trial are already discussed in the paragraph concerning the column preparation final set up.

Annex III

Empirical formulas for K estimations: observations

For the computation of K- values by the chosen analytical relationships, some common inputs are necessary (summarized in TABLE 20). The kinematic viscosity is obtained as a ratio between dynamic viscosity or just viscosity and water density. In general, standard values associated to a 20° temperature are considered and approximated.

INPUT FOR EMPIRICAL CALCULATION FOR ALL SANDS			
ν kinematic viscosity (m ² /s)	g (m/s ²)	ρ water (kg/m ³) at T of 20°	μ viscosity (kg/m s) at T of 20°
0.000001	9.81	1000	0.001

TABLE 20 Constant Inputs of empirical formulas (source: <https://www.engineersedge.com> consulted in April 2019)

Finally, TABLE 21 reported below, resumes the empirical formulas and the results for each column of type of sand tested. The researchers names are sometimes highlighted in green just to put in evidence the formulas founded in several other studies of hydraulic conductivity estimations linked to granulometry, while dealing with sands.

Researcher/Organization	Year	K formula	Specimen (gradation)	Kempirical (m/s)
Hazen	1892	$K = 6 \times 10^{-4} \times \frac{\rho \times g}{\mu} \times [1 + 10(n - 0,26)] \times D_{10}^2$	N1 (0.1-0.5 mm)	1.94E-04
			N5 (0.5-1 mm)	2.56E-03
			1/2 (1-2 mm)	8.90E-03
			3/5 (3-5.6 mm)	4.82E-02
Kozeny-Carman	1927-53	$K = 8 \times 10^{-3} \times \frac{\rho \times g}{\mu} \times \left[\frac{n^3}{(1-n)^2} \right] \times D_{10}^2$	N1 (0.1-0.5 mm)	1.07E-05
			N5 (0.5-1 mm)	1.10E-04
			1/2 (1-2 mm)	3.22E-04
Breyer	1964	$K = 6 \times 10^{-4} \times \frac{\rho \times g}{\mu} \times \log \frac{500}{C_u} \times D_{10}^2$ with $1 < C_u < 20$	N1 (0.1-0.5 mm)	2.35E-04
			N5 (0.5-1 mm)	4.20E-03
			1/2 (1-2 mm)	1.81E-02
Siltcher		$K = 10^{-2} \times \frac{\rho \times g}{\mu} \times n^{3.287} \times D_{10}^2$	N1 (0.1-0.5 mm)	3.31E-06
			N5 (0.5-1 mm)	3.71E-05
			1/2 (1-2 mm)	1.15E-04
			3/5 (3-5.6 mm)	5.53E-04

Terzaghi	1925	$K = 10,7 \times 10^{-3} \times \frac{\rho \times g}{\mu} \times \left(\frac{n-0,13}{1-n}\right)^2 \times D_{10}^2$ sands with smooth grains $K = 6,1 \times 10^{-3} \times \frac{\rho \times g}{\mu} \times \left(\frac{n-0,13}{1-n}\right)^2 \times D_{10}^2$ sands with coarse grains	N1 (0.1-0.5 mm) smooth	1.20E-04
			N5 (0.5-1 mm) coarse	7.40E-04
			1/2 (1-2 mm) coarse	2.18E-03
			3/5 (3-5.6 mm) coarse	8.90E-03
USBR	1951	$K = 4,8 \times 10^{-4} \times \frac{\rho \times g}{\mu} \times D_{20}^{2,3}$	N1 (0.1-0.5 mm)	7.55E-06
			N5 (0.5-1 mm)	1.76E-04
			1/2 (1-2 mm)	9.02E-04
			3/5 (3-5.6 mm)	1.13E-02
Alyamani and Sen	1993	$K = 1300 \times [I_0 + 0,025(D_{50} - D_{10})]^2$	N1 (0.1-0.5 mm)	1.50E-04
			N5 (0.5-1 mm)	3.76E-03
			1/2 (1-2 mm)	1.50E-02
			3/5 (3-5.6 mm)	1.35E-01
Sauerbrey	1932	$K = 3,75 \times 10^{-3} \times \frac{\rho \times g}{\mu} \times \left[\frac{n^3}{(1-n)^2}\right] \times D_{17}^2$	N1 (0.1-0.5 mm)	8.90E-05
			N5 (0.5-1 mm)	8.53E-04
			1/2 (1-2 mm)	2.40E-03
			3/5 (3-5.6 mm)	1.14E-02
Kruger	1918	$K = 4,35 \times 10^{-3} \times \frac{\rho \times g}{\mu} \times \frac{n}{(1-n)^2} \times D_{10}^2$	N1 (0.1-0.5 mm)	6.15E-04
			N5 (0.5-1 mm)	8.05E-03
			1/2 (1-2 mm)	2.88E-02
			3/5 (3-5.6 mm)	1.82E-01
Zunker	1932	$K = Cz u \times \frac{\rho \times g}{\mu} \times \left(\frac{n}{1-n}\right)^2 \times D_{10}^2 = 2,4 \times 10^{-3} \times \frac{\rho \times g}{\mu} \times \left(\frac{n}{1-n}\right)^2 \times D_{10}^2$ for uniform sands with smooth and rounded grains	N1 (0.1-0.5 mm)	3.40E-04
			N5 (0.5-1 mm)	4.44E-03
			1/2 (1-2 mm)	1.59E-02
			3/5 (3-5.6 mm)	1.00E-01
Zamarin	1928	$K = 8,64 \times 10^{-3} \times (1,275 - 1,5n)^2 \times \frac{\rho \times g}{\mu} \times \left[\frac{n^3}{(1-n)^2}\right] \times D_{10}^2$	N1 (0.1-0.5 mm)	1.53E-04
			N5 (0.5-1 mm)	1.67E-03
			1/2 (1-2 mm)	5.07E-03
			3/5 (3-5.6 mm)	2.38E-02
Harleman	1963	$K = 6,54 \times 10^{-4} \times \frac{\rho \times g}{\mu} \times D_{10}^2$	N1 (0.1-0.5 mm)	1.08E-04
			N5 (0.5-1 mm)	1.80E-03
			1/2 (1-2 mm)	7.76E-03
			3/5 (3-5.6 mm)	6.57E-02
Koenders and Williams	1992	$K = \frac{1}{v} \times X \times n \times \left(\frac{n}{1-n}\right)^2 \times D_{50}^2$ with $X = 0,0035 \pm 0,0005$	N1 (0.1-0.5 mm)	1.86E-05
			N5 (0.5-1 mm)	9.79E-05
			1/2 (1-2 mm)	3.06E-04
			3/5 (3-5.6 mm)	1.45E-03
			N1 (0.1-0.5 mm)	2.48E-05
			N5 (0.5-1 mm)	1.31E-04
Chapuis et al.	2005	$K = 1219,9 \times \frac{n^{2,3475}}{(1-n)^{1,565}} \times D_{10}^{1,565}$	1/2 (1-2 mm)	4.08E-04
			3/5 (3-5.6 mm)	1.94E-03
			N1 (0.1-0.5 mm)	1.77E-04
			N5 (0.5-1 mm)	1.09E-03
NAVFAC DM7 Chesnaux	2011	$K = 0,2272 \times (1,772189 \times 10^{11})^{\frac{n}{1-n}} \times [(D_{10})^{3,31917}]^{\frac{n}{1-n}}$	1/2 (1-2 mm)	2.54E-03
			3/5 (3-5.6 mm)	8.19E-03
			N1 (0.1-0.5 mm)	3.63E-04
			N5 (0.5-1 mm)	3.38E-03
			3/5 (3-5.6 mm)	1.97E-02

TABLE 21 Summary of all empirical computation formulas and results

Annex IV

Constant Head Permeability Test Results

Each estimation of a K value is associated to a precise type of sand and the sample studied. The sample associated at each trial are called Sample 1, 2, 3, 4 and the majority of results reported hereafter refer to the fourth one, which is the best one. But it is possible to point out that, except from some values reported in red (associated mostly to sample one and two, the worst set up), the others are really close one to each other, within each sand type.

Furthermore for each test the variable typical value to insert as input in the K Darcy's formula are reported: they are the outflow rate Q and the constant head difference. The two constant inputs are :

- The length of the column 36 cm because over the total of 38 cm, 2 cm of filters were considered and excluded for the implementation
- The areal section of the column equals to: $\pi (10/2)^2 = 78.5 \text{ cm}^2$

Average K values are also reported and a reasonable scale is resulting: larger values are associated to the coarser type of sands, and gradually they are decreasing going to the finer sample.

Hydraulic conductivity average (m/s)			
N1	N5	1to2	3to5
2.94E-04	8.82E-04	2.13E-03	2.54E-03

TABLE 22 Average K values from CHPT

		CONSTANT HEAD METHOD			
Sample	Sand type	Test n°	K measured (m/s)	Q(t) out L/s	$\Delta h_{top-top}$ (cm)
Sample 1	N1 (0.1-0.5 mm)	Test 1	4.28E-04	6.77E-3	72.5
Sample 2		Test 2	3.84E-04	6.07E-3	72.5
Sample 3		Test 1	2.64E-04	3.00E-3	52
Sample 4		Test 2	2.45E-04	2.78E-3	52
Sample 4		Test 3	2.25E-04	2.82E-3	57.5
Sample 4		Test 4	2.17E-04	2.72E-3	57.5
Sample 1	N5 (0.5-1 mm)	Test 1	3.30E-04	3.10E-3	43
Sample 2		Test 2	5.20E-04	5.50E-3	48.5
Sample 3		Test 1	8.14E-04	7.68E-3	43
Sample 4		Test 1	8.99E-04	1.11E-2	51.5
Sample 4		Test 2	9.88E-04	1.12E-2	51.5
Sample 4		Test 3	8.83E-04	8.19E-3	42.5
Sample 4		Test 4	8.65E-04	8.02E-3	42.5
Sample 4		Test 5	8.43E-04	1.06E-2	57.5
Sample 1	1/2 (1-2 mm)	Test 1	2.47E-03	1.05E-2	19.5
Sample 1		Test 2	2.16E-03	9.20E-3	19.5
Sample 2		Test 3	5.20E-04	8.79E-3	48.5
Sample 3		Test 1	1.99E-03	1.65E-2	38
Sample 4		Test 2	2.05E-03	1.16E-2	26
Sample 4		Test 3	1.82E-03	7.96E-3	20
Sample 4		Test 4	2.30E-03	1.13E-2	22.5
Sample 1	3/5 (3-5.6 mm)	Test 1	2.12E-03	9.00E-3	19.5
Sample 1		Test 2	1.17E-03	1.02E-2	40
Sample 2		Test 1	3.53E-03	1.04E-2	13.5
Sample 2		Test 2	3.00E-03	8.85E-3	13.5
Sample 3		Test 1	2.93E-03	1.28E-2	20
Sample 4		Test 2	2.92E-03	1.27E-2	20
Sample 4		Test 3	3.10E-03	1.52E-2	22.5

TABLE 23 Resume of the principal and most representative values for each sand type studied

Annex V

Statistical analysis on empirical K

In this Annex are shown all the statistical graphs related to the empirical evaluation of K, for sand type N5, 1to2 and 3to5 (cited in *Chapter 3*).

There are always two different graphs for each sand type because a selection of the greater estimations was done. The first is reporting the analysis comparing all the models computed, while the second is referring to the operated selection. The criteria to chose the representative formulas for each type of sand are in line with what is reported in Hussain et Nabi (2016) studies.

Each empirical model is associated to a symbolic name composed by the letter M and a number from 1 to 15, in order to better see and compare which are used in each sand type.

Average (red) and median (blue) values are reported as straight vertical line. The Lab experimentally determined K values are respectively ranging between:

$$K_{(N5)} = 8.14-9.88 \times 10^{-4} \text{ m/s}$$

$$K_{(1to2)} = 1.82-2.47 \times 10^{-3} \text{ m/s}$$

$$K_{(3to5)} = 1.17-3.10 \times 10^{-3} \text{ m/s}$$

Generally the value determined by the Constant Head Permeability Test (reported above) is a bit closer to the median, while the average is always a bit higher.

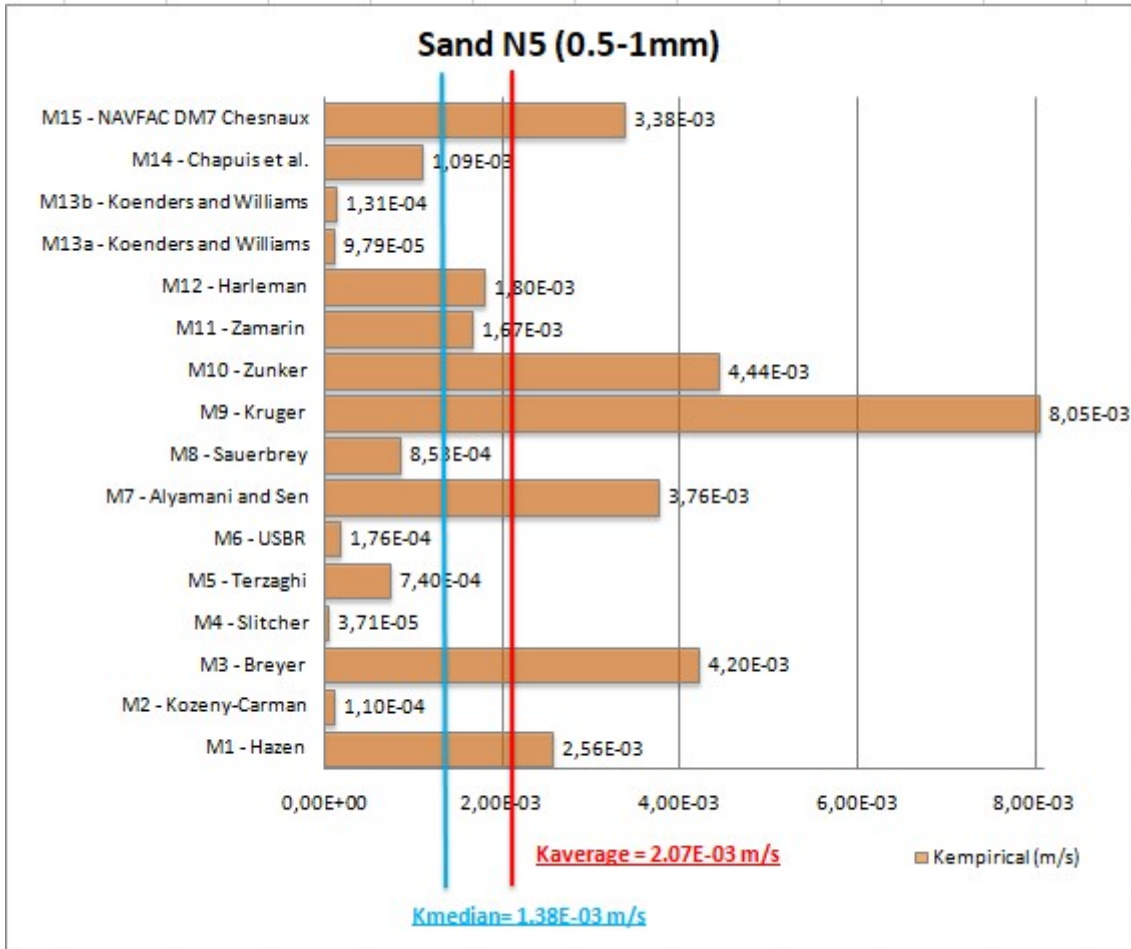


FIG 71 Statistics on N5 empirical K-values (*all formulas*)

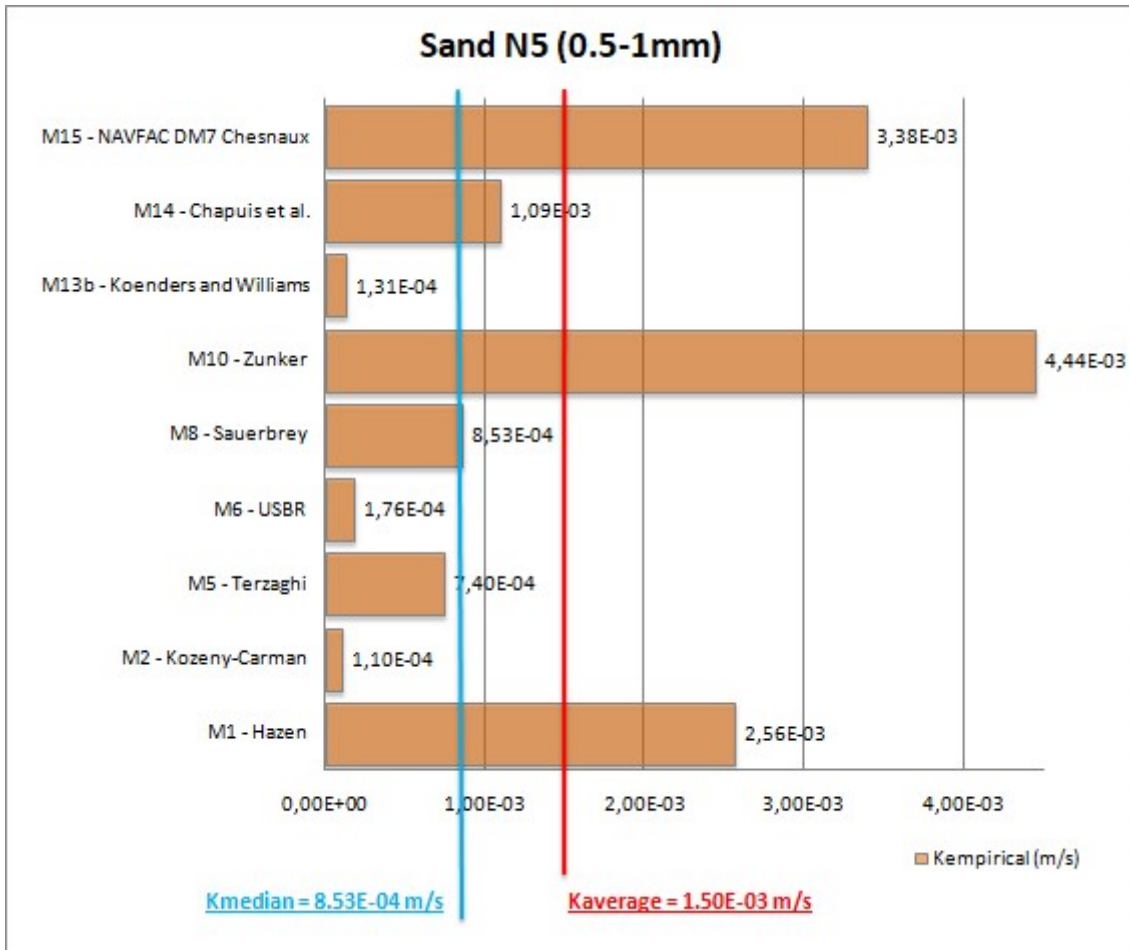


FIG 72 Statistics on N5 empirical K-values (selection of representative results)

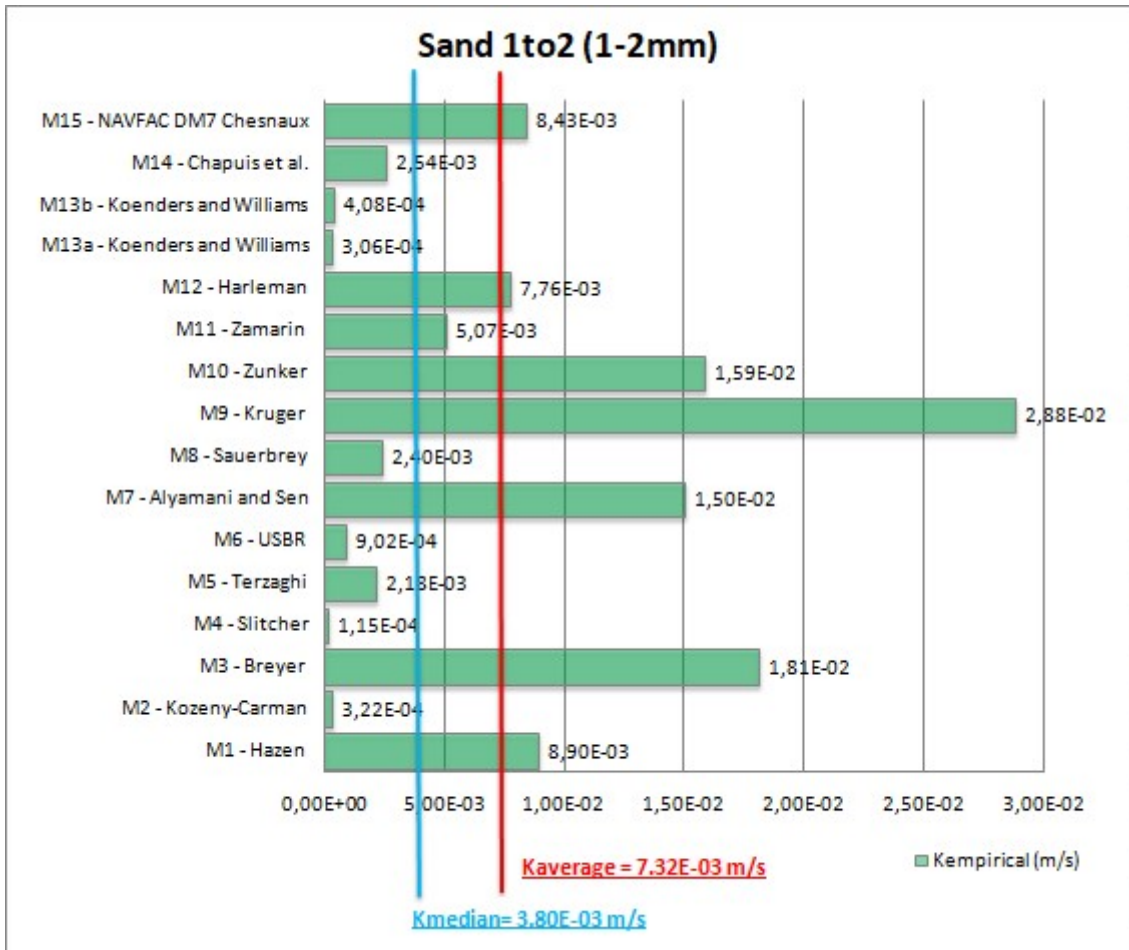


FIG 73 Statistics on 1to2 empirical K-values (all formulas)

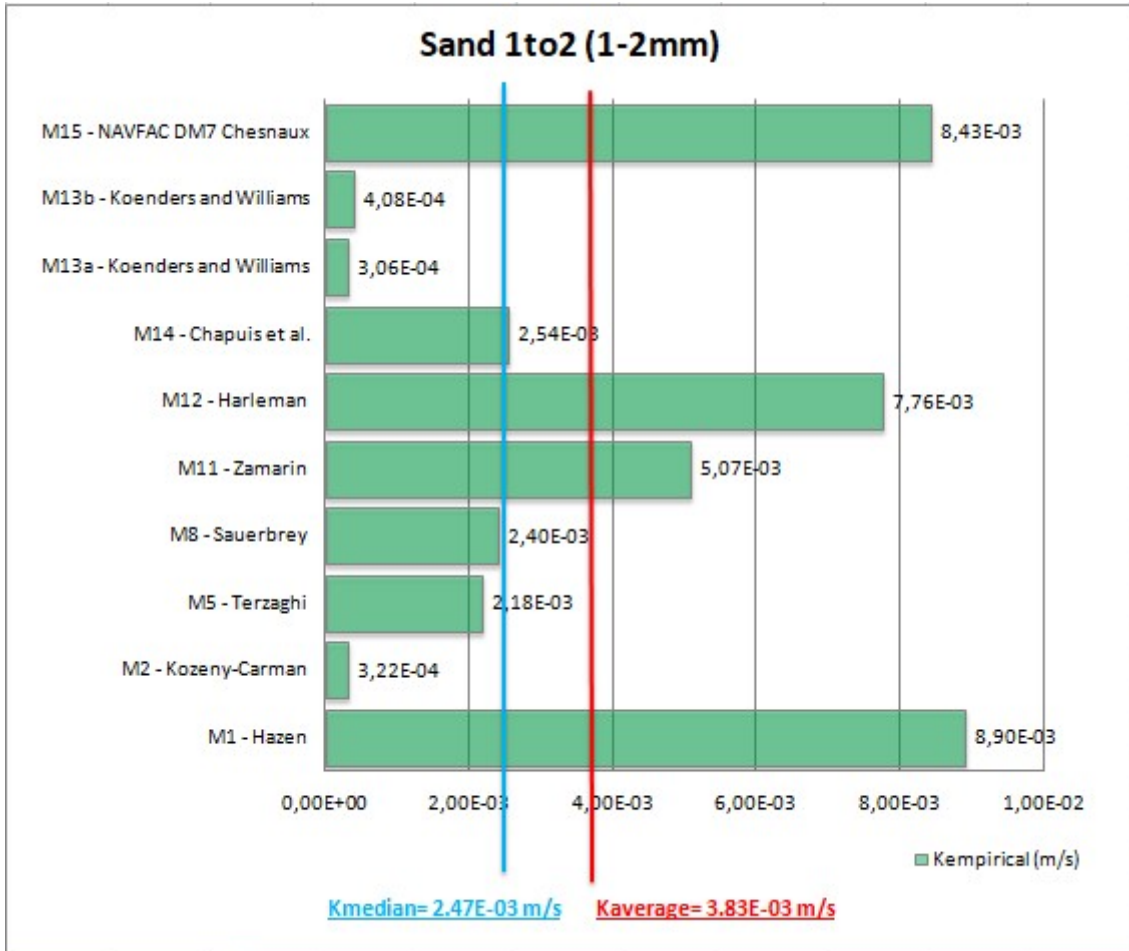


FIG 74 Statistics on 1to2 empirical K-values (*selection of representative results*)

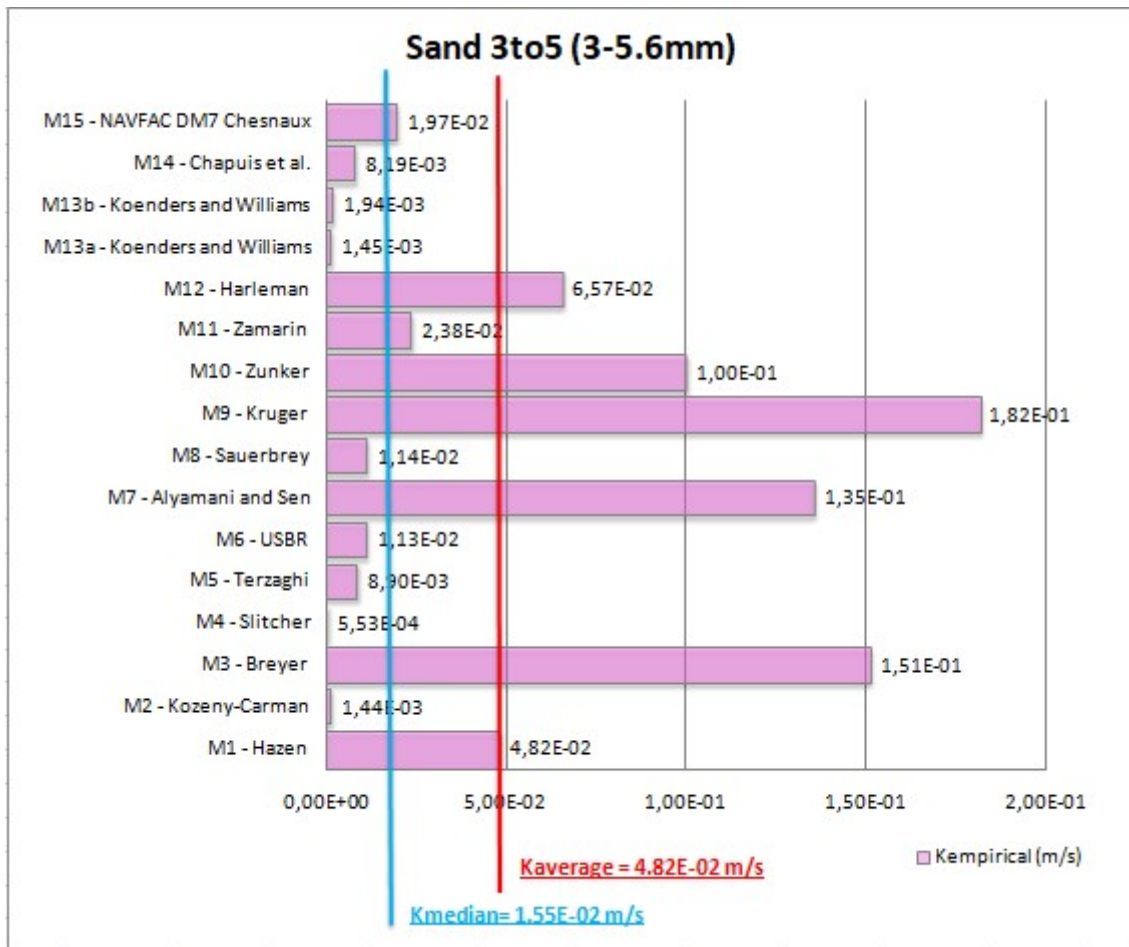


FIG 75 Statistics on 3to5 empirical K-values (all formulas)



FIG 76 Statistics on 3to5 empirical K-values (selection of representative results)

Annex VI

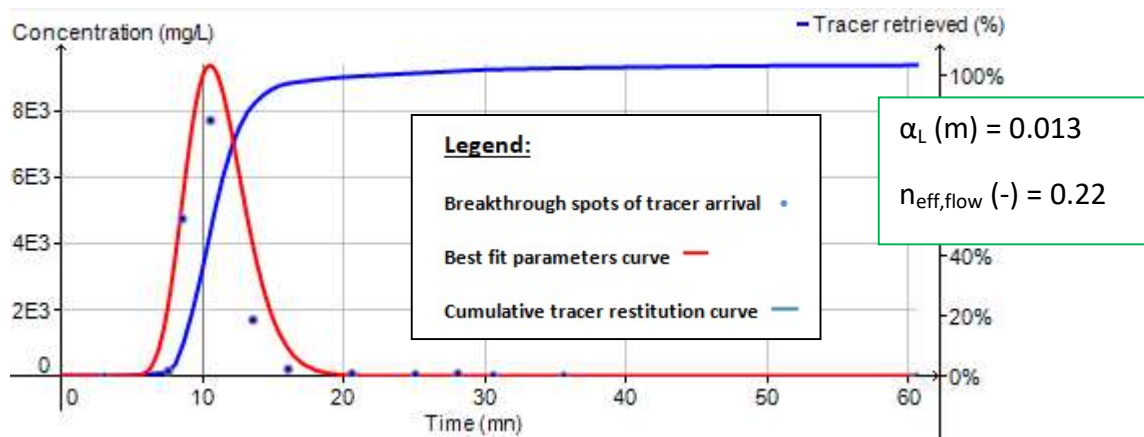
TRAC interpretation graphs

Representative graph obtained by TRAC interpretation done on the tests performed are reported in this section. Interpretation graphs are done also for K⁺ ions concentration, even if Cl⁻ is the tracer consider as reference. That's because not substantial differences were found in recovered concentrations and so neither in the final results.

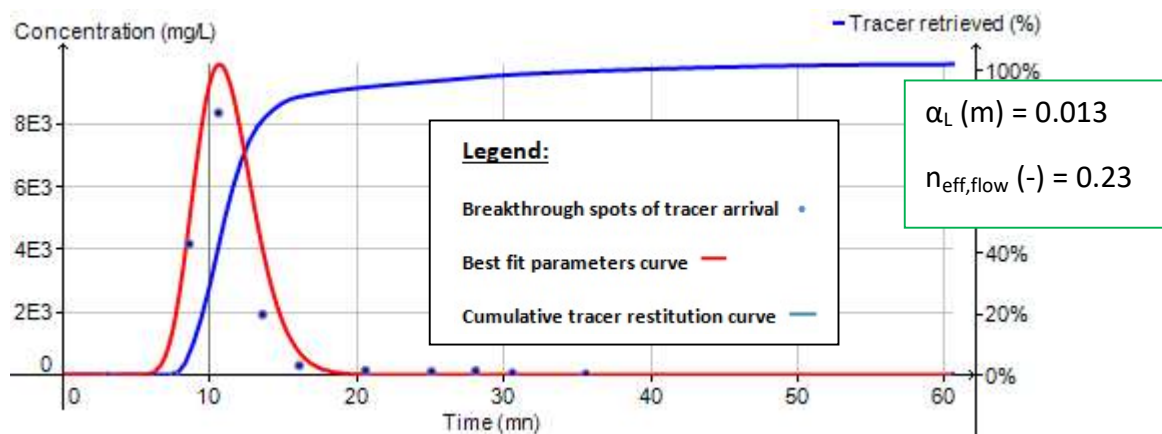
For each case are reported correspondent values of

- α_L (longitudinal dispersivity)
- $n_{\text{eff,flow}}$ (effective drainage and flow porosity).

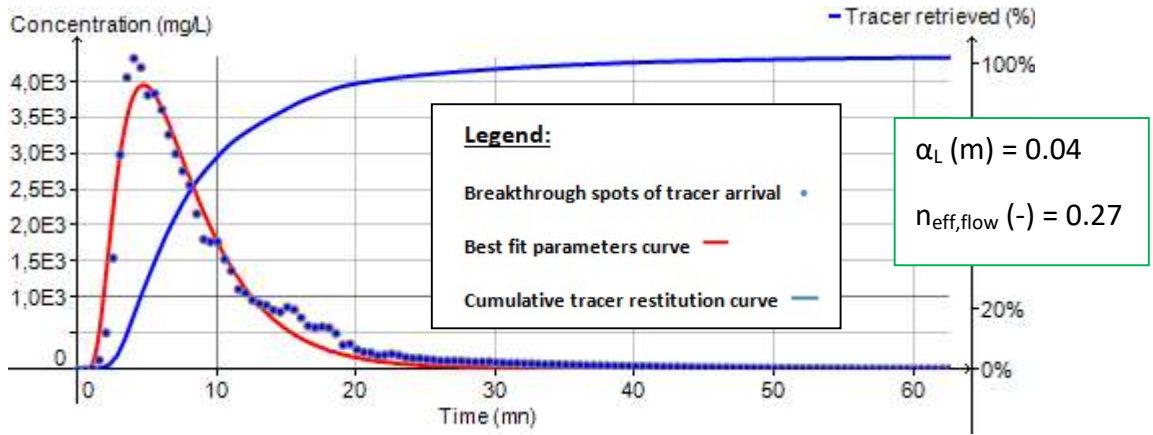
Test T3 – Sand N5 : [Cl⁻]



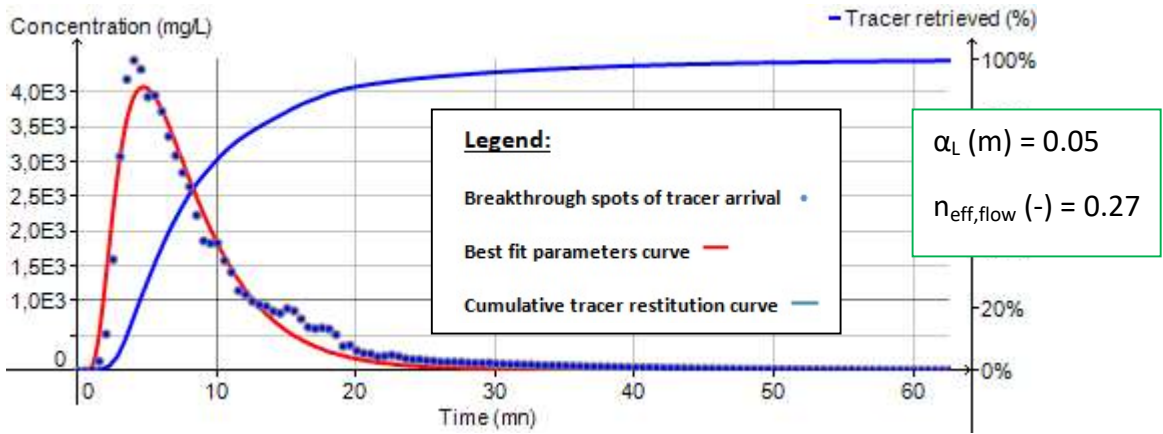
Test T3 – Sand N5 : [K⁺]



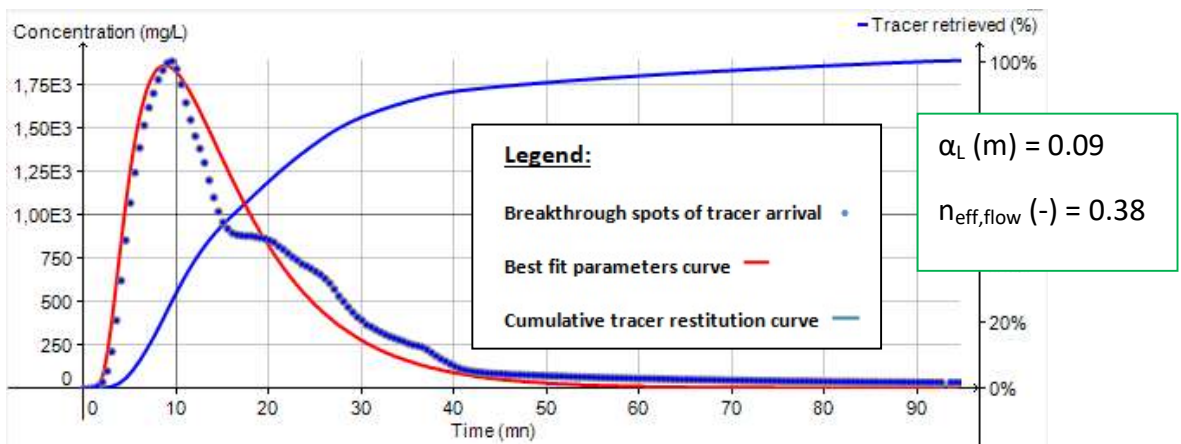
Test T4 – Sand 1to2 : [Cl-]



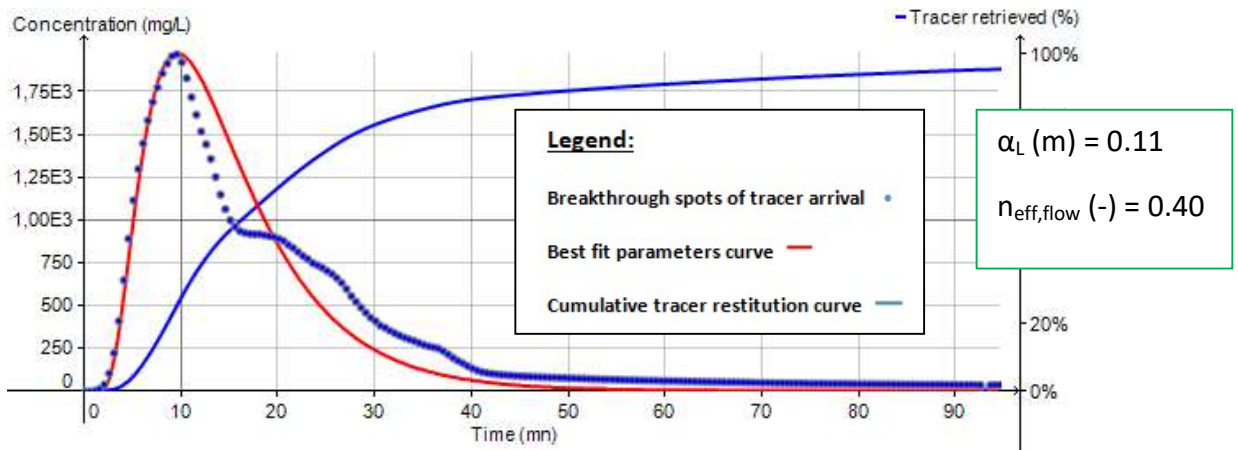
Test T4 – Sand 1to2 : [K+]



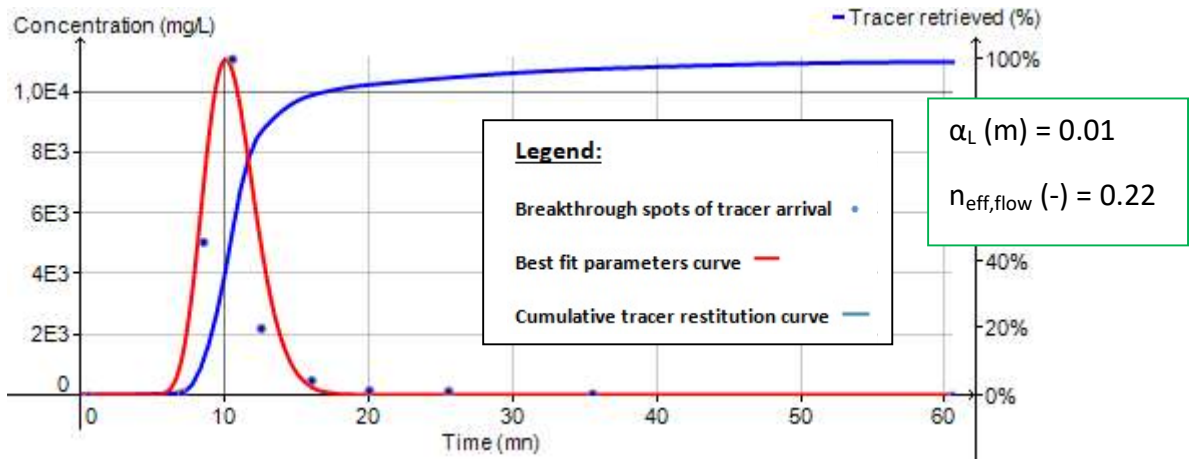
Test T5 – Sand 3to5 : [Cl-]



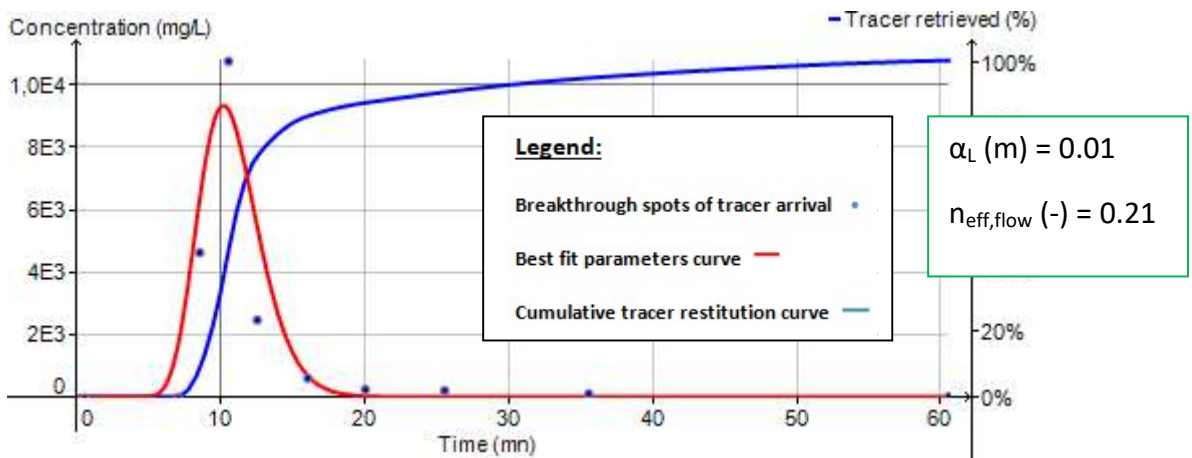
Test T5 – Sand 3to5 : [K+]



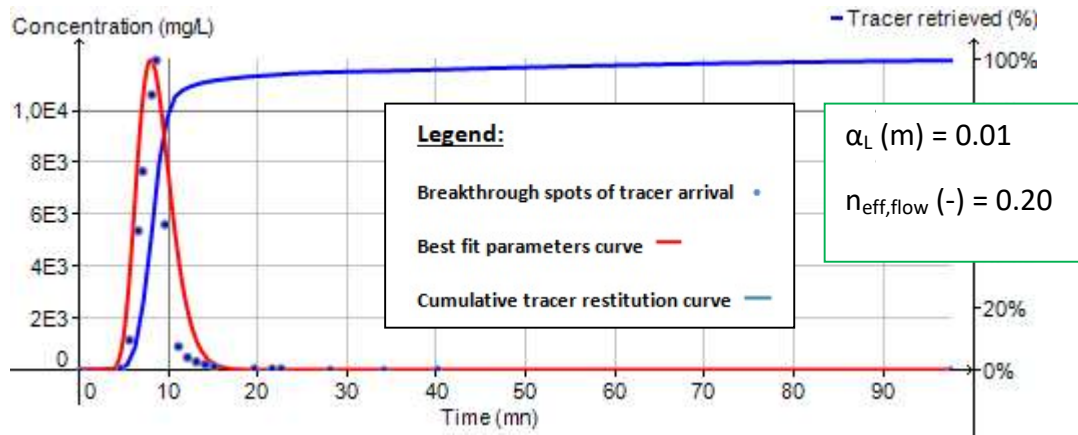
Test T1 – Sand N1 : [Cl-]



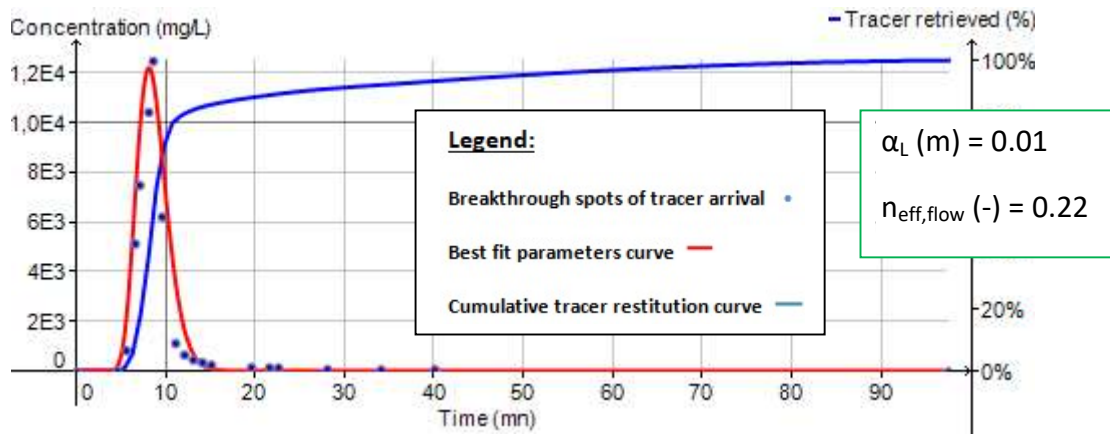
Test T1 – Sand N1 : [K+]



Test T2 – Sand N1 : [Cl-]



Test T2 – Sand N1 : [K+]



Annex VII

7 layers model: Constant pumping test results

In this section firstly are reported some results of simulations of Constant pumping test performed on the 7layers model, applying different values of Q_{pump} .

It is highlighted the presence of dry cells, which is reflecting some reasonable lack in computation of drawdown.

Numerically speaking, it is not a real problem, but it is not necessary for the purpose of the presented analysis.

But looking at the real practical application, it will create more variations in the real system, which will then take more time to re-stabilize and be used for other experiments.

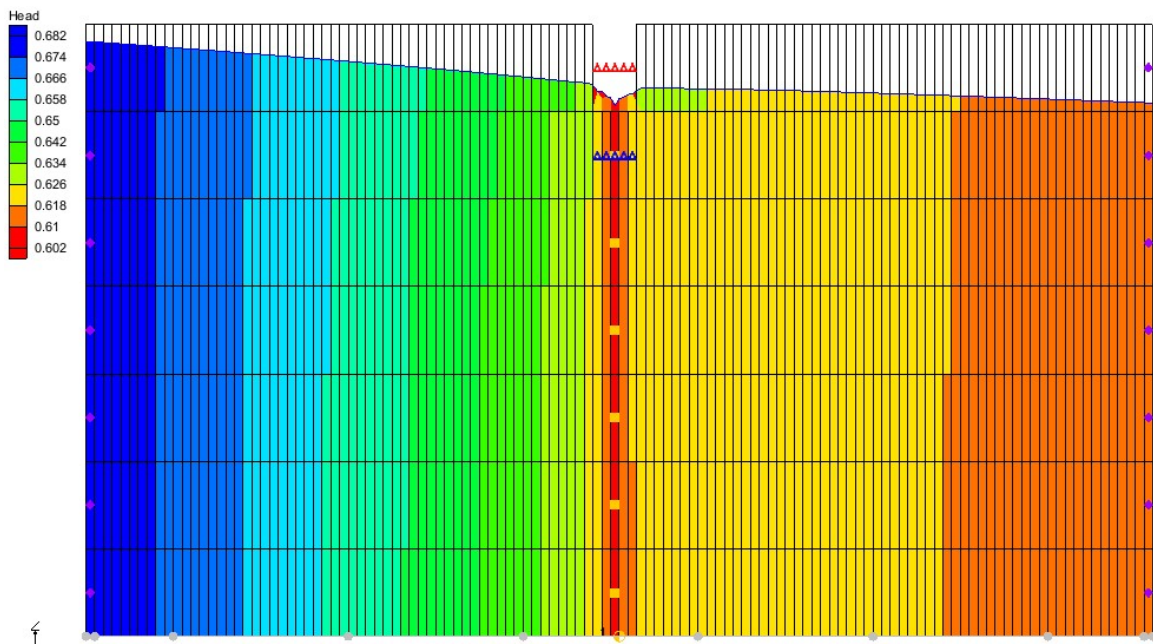


FIG 77 Seven Layers model: central lateral section of water heads, while applying $Q_{\text{pump}} = 6.5 \times 10^{-5} \text{ m}^3/\text{s}$

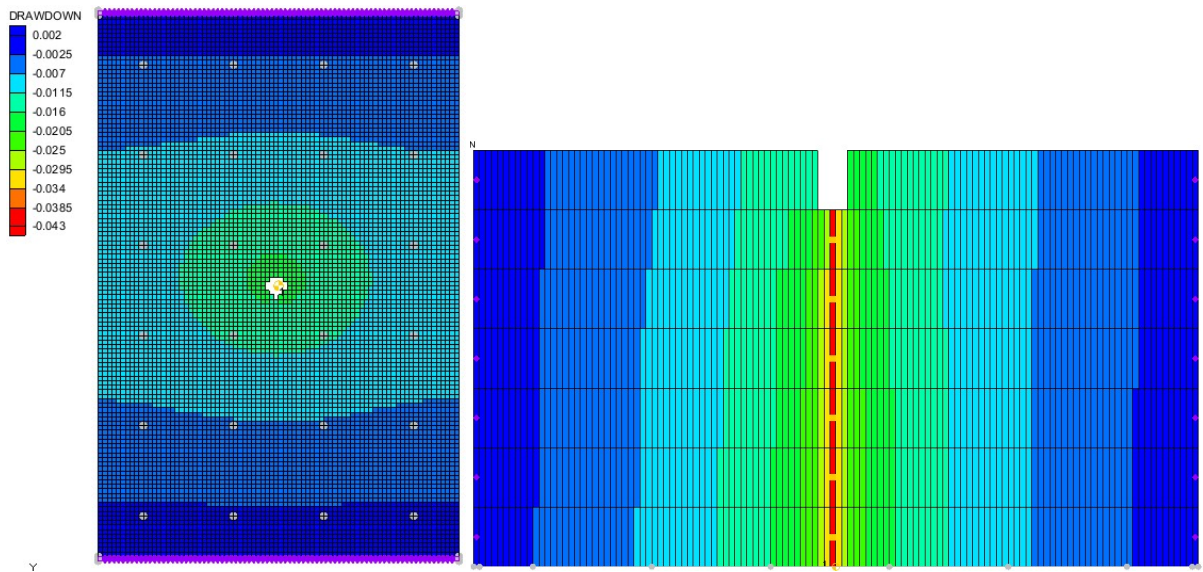


FIG 78 Seven Layers model: drawdown while applying $Q_{pump} = 6.5 \times 10^{-5} \text{ m}^3/\text{s}$

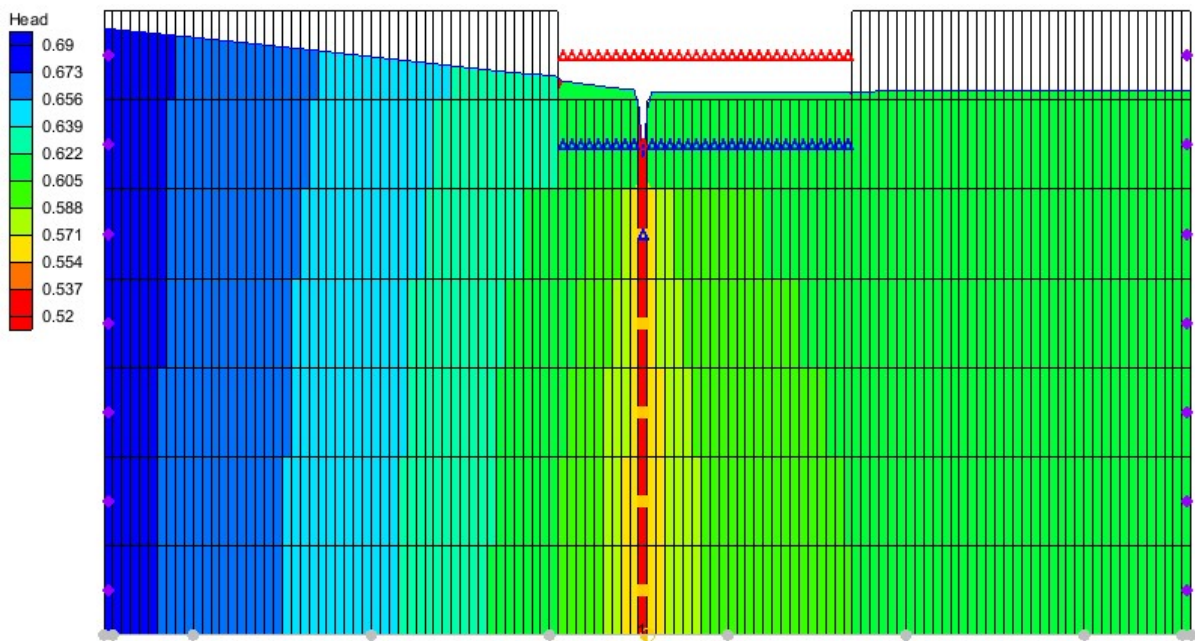


FIG 79 Seven Layers model: central lateral section of water heads, while applying $Q_{pump} = 1 \times 10^{-4} \text{ m}^3/\text{s}$

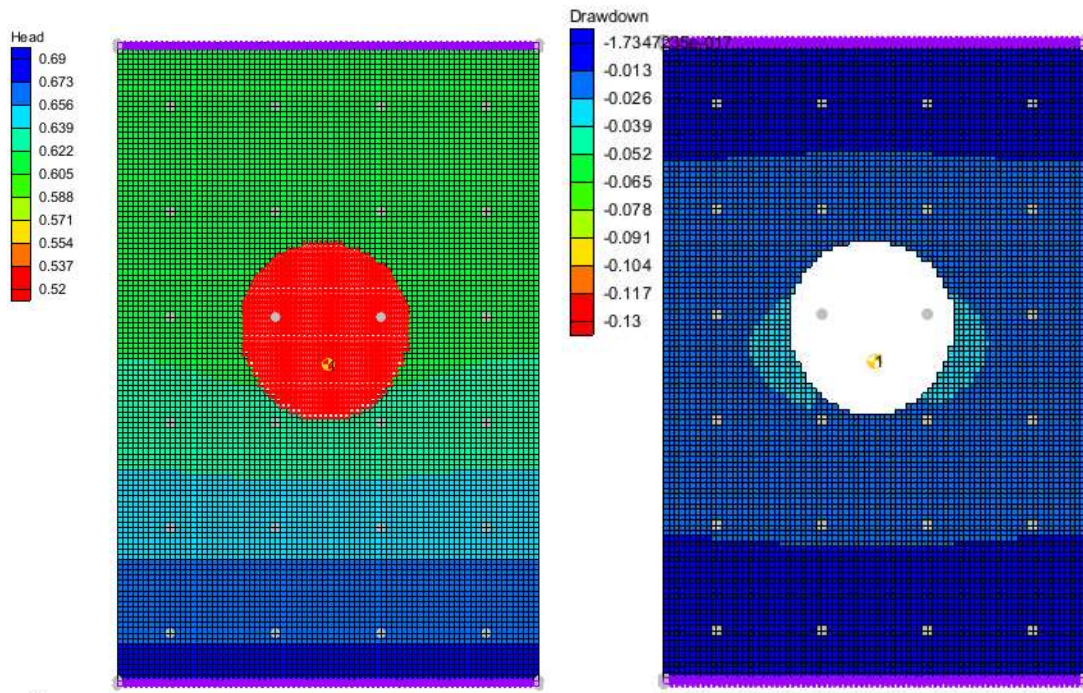


FIG 80 Seven Layers model: water head and relative drawdown, while applying $Q_{pump} = 1 \times 10^{-4} \text{ m}^3/\text{s}$

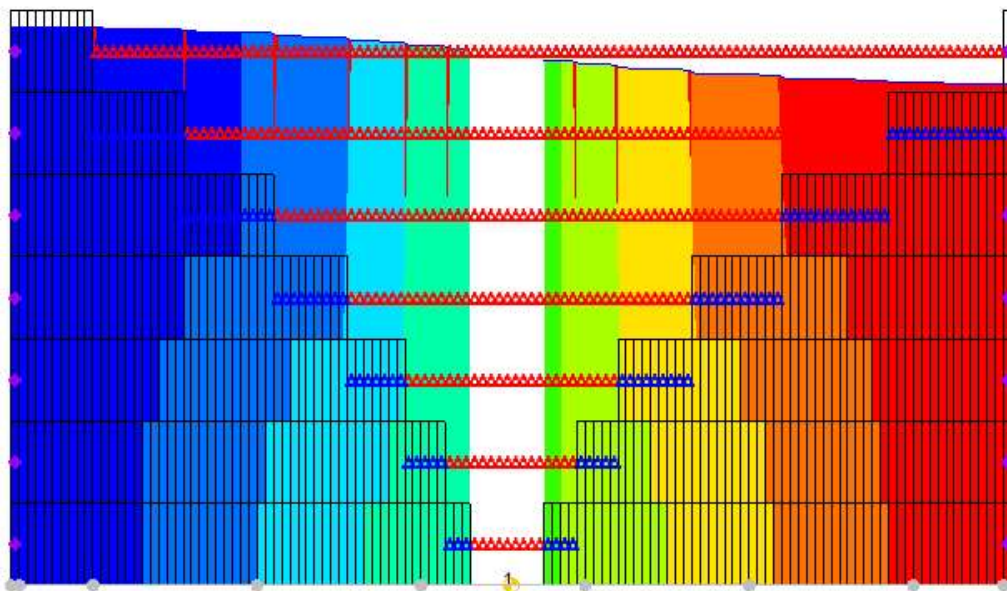


FIG 81 Seven Layers model: central lateral section, while applying $Q_{pump} = 2.5 \times 10^{-4} \text{ m}^3/\text{s}$

Talking about the sensitivity analysis concerning change in the **effective drainage porosity**, the correspondent graph drawn for MOC solution is done also for TVD in case of continuous injection. A good match between correspondent MOC restitution curves can be done.

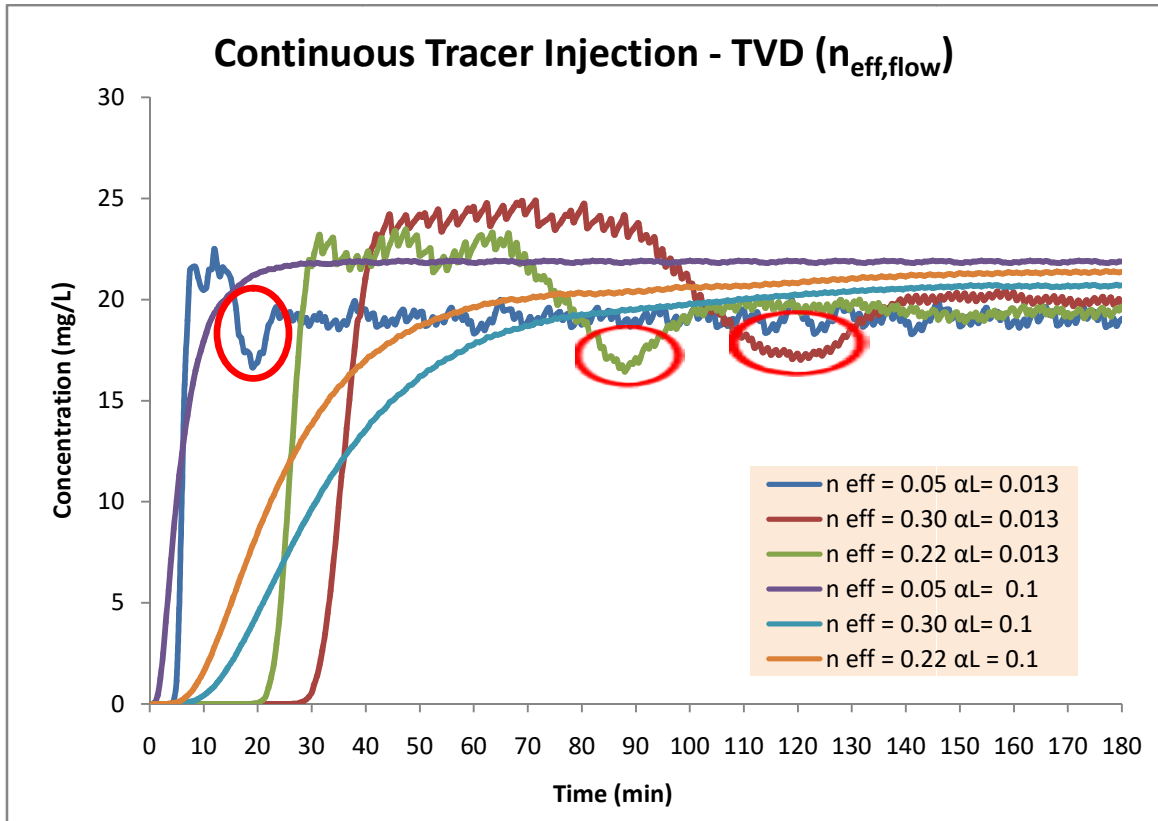


FIG 82 BTCs for Continuous tracer injection TVD (changes in n_{eff} and α_L)

Bibliography

- Abbott, M.B., Bathurst, J.C., Cunge, J.A., O'Connell, P.E., Rasmussen, J., (1986). An introduction to the European Hydrological System—Systeme Hydrologique Europeen 'SHE'.2: Structure of a physically based, distributed modelling system. *J.Hydrol.*87, 61–77
- Akbulut, A. F. C. & N. (2016). Effects of Particle Shape and Size Distributions on the hydraulic conductivity. *Acta Geotechnica Slovenica*, 2, 83–93.
- Alyamani M.S., Sen Z.(1993). Determination of hydraulic conductivity from complete grain-size distribution curves. Vol 31, n°4, *GROUND WATER*, 551-555.
- Battle-aguilar, J., Goderniaux, P., & Dassargues, A. (2007). A new single tracer test : the Finite Volume Point Dilution Method (FVPDM). Theory , field application and model validation A new single well tracer test : the Finite Volume Point Dilution Method . Theory , field application and model validation.
- Barth, G., M. Hill, T. Illangasekare, and H. Rajaram (2001), Predictive modeling of flow and transport in a two-dimensional intermediate-scale, heterogeneous porous medium, *Water Resour. Res.*, 37(10), 2503–2512
- Basu, N.B., P.S.C. Rao, I.C. Poyer, M.D. Annable, and K. Hatfield (2006). Flux-based assessment at a manufacturing site contaminated with trichloroethylene. *Journal of Contaminant Hydrology* 86: 105–127.
- Batu, V., (1998). *Aquifer Hydraulics: A Comprehensive Guide to Hydrogeologic Data Analysis*, John Wiley & Sons, New York, 727p.
- Bear, J., (1979). *Hydraulics of Groundwater*, McGraw-Hill, New York, 569p.
- Been, K., & Jefferies, M. G. (2009). A state parameter for sands. *Géotechnique*, 35(2), 99–112.
- Behnke, J. J., & Schiff, L. (1963). K in sands. *Journal of Geophysical Research*, 68(16), 4769–4775.
- Betancur, T., Palacio T., C. A., & Escobar M., J. F. (2012). *Conceptual Models in Hydrogeology, Methodology and Results. Hydrogeology - A Global Perspective*, (February).
- Blackwell, R.J. (1962) Laboratory studies of microscopic dispersion phenomena. *Soc. Petrol. Engrs J.* 2.
- Borke, P. (2007). Untersuchungen zur Quantifizierung der Grundwasserimmission vor Polyzyklischen Aromatischen Kohlenwasserstoffen mithilfe von Passiven Probennahmesystemen (in German). PhD dissertation, Technische Universität Dresden, Dresden, Germany.
- Brakefield, L. K. (2008). "Physical and numerical modeling of buoyant groundwater plumes." M.S. thesis, Auburn Univ., Auburn, AL.
- British Columbia, (2007). *Guide to Conducting Pumping Tests*. 1–10.
- Brooks, K.N., P.F. Folliott, H.M. Gregersen and J.L. Thames, (1991). *Hydrology and the Management of Watersheds*. Iowa State University Press, Ames, USA.

- Burnell, D.K. (2002). A groundwater flow and solute transport model of sequential biodegradation of multiple chlorinated solvents in the superficial aquifer, Palm Bay, Florida.
- Cai, J., Taute, T., Hamann, E., & Schneider, M. (2015). An Integrated Laboratory Method to Measure and Verify Directional Hydraulic Conductivity in Fine-to-Medium Sandy Sediments. *Groundwater*, 53(1), 140–150.
- Chao, H. C., H. Rajaram, and T. Illangasekare (2000), Intermediate-scale experiments and numerical simulations of transport under radial flow in a two-dimensional heterogeneous porous medium, *Water Resour. Res.*, 36(10), 2869–2884
- Cheng, C., and Chen, X. (2007). Evaluation of Methods for Determination of Hydraulic Properties in an Aquifer-Aquitard System Hydrologically Connected to River. *Hydrogeology Journal*. 15: 669- 678.
- Childs E.C et Collis – George N., (1950). The permeability of porous materials, *Proceedings of the Royal Society, London, Ser. A* 201, 392-405.
- Costa J. L et Prunty L., (2006). Solute transport in fine sandy loam soil under different flow rates. *Agricultural Water Management*, 83:111-118.
- Currell, M. J., Werner, A. D., McGrath, C., Webb, J. A., & Berkman, M. (2017). Problems with the application of hydrogeological science to regulation of Australian mining projects: Carmichael Mine and Doongmabulla Springs. *Journal of Hydrology*, 548, 674–682.
- Danquigny, C., P. Ackerer, and J. P. Carlier (2004), Laboratory tracer tests on 3D reconstructed heterogeneous porous media, *J. Hydrol. Amsterdam*, 294(1–3), 196–212
- Dassargues, A. (2018). *Hydrogeology: groundwater science and engineering*. Chapters 12 and 13.
- Dassargues, A. (2019). PPT: Groundwater modelling at the catchment scale, mathematical and numerical aspects. Winter school.
- De Jonge, H., and Rothenberg, G., (2005). New device and method for flux-proportional sampling of mobile solutes in soil and groundwater, *Env. Sci. & Tech.*, 39(1): 274-282.
- Devlin, J. F., Labaky, W., & Gillham, R. W. (2010). Field comparison of the point velocity probe with other groundwater velocity measurement methods. *Water Resources Research*, 46(4).
- Devlin, J.F., Schillig, P.C., Bowen, I., Critchley, C.E., Rudolph, D.L., Thomson, N.R., Tsoflias, G.P., Roberts, J.A. (2012). Applications and implications of direct groundwater velocity measurement at the centimetre scale, *Journal of Contaminant Hydrology*, v. 127.
- Devlin, J. F., Osorno, T. C., & Firdous, R. (2018). An In-Well Point Velocity Probe for the rapid determination of groundwater velocity at the centimeter-scale. *Journal of Hydrology*, 557(2018), 539–546.
- Domenico, P.A. & M.D. Mifflin, (1965). Water from low-permeability sediments and land subsidence, *Water Resources Research*, vol. 1, no. 4., pp. 563-576.
- Domenico, P.A. & Schwartz, F.W. (1990) *Physical and Chemical Hydrology*. Wiley, New York.
- Drost, W.; Klotz, D.; Koch, A.; Moser, H.; Neumaier, F.; W., Rauert (1968). Point dilution methods of investigating ground water flow by means of radioisotopes. *WaterResour. Res.*, 4 (1), 125–145.

- Eckis RP (1934). South Coastal Basin Investigation, Geology, and Ground Water Storage Capacity of Valley Fill. California Division of Water Resources Bulletin, Sacramento, 45 pp.
- Everett, J. E. (1995). Technical review: Practical Guidelines For test Pumping in water wells. Computers and the Humanities, 29(4), 307–316.
- Essouayed, E. (2019). Développement d ' une stratégie de localisation d ' une source de contaminants en nappe : mesures innovantes et modélisation inverse. THÈSE DE DOCTORAT DE L'UNIVERSITÉ BORDEAUX MONTAIGNE.
- Farrell-Poe Dr Kitt, (1997). Groundwater flow demonstration model. Department of water and sanitation, Extension Environmental Engineering Utah State University, 1–9.
- Fashi, F. H. (2015). Review of solute transport modeling in soils and hydrodynamic dispersivity. Conference: International Soil Science Congress 2015, 4(3), 134–142.
- Fernández-García, D., H. Rajaram, and T. H. Illangasekare (2005), Assessment of the predictive capabilities of stochastic theories in a three-dimensional laboratory test aquifer: Effective hydraulic conductivity and temporal moments of breakthrough curves, Water Resour. Res., 41, W04002.
- Freeze, R.A. and J.A. Cherry, (1979). Groundwater, Prentice Hall, Englewood Cliffs, New Jersey, 604p.
- Fried, J.J. & Combarous, M.A. (1971). Dispersion in Porous Media. Advances in Hydroscience (ed. by Ven Te Chow), vol.7. Academic Press, New York.
- Gibb, J. P., Barcelona, M. J., Ritchey, J. D., & Lefavre, M. H. (1984). Effective Porosity of Geologic Materials: First Annual Report. (September), 42.
- Gierczak, R.; Devlin, J. F.; Rudolph, D. (2006). Combined use of laboratory and in situ hydraulic testing to predict preferred flow paths of solutions injected into an aquifer. J. Contam. Hydrol., 82, 75–98.
- Gleeson, T., Allen, D. M., & Ferguson, G. (2012). Teaching hydrogeology: A review of current practice. Hydrology and Earth System Sciences, 16(7), 2159–2168.
- Goswami, R. R., Clement, T. P., & Hayworth, J. H. (2011). Comparison of Numerical Techniques Used for Simulating Variable-Density Flow and Transport Experiments. Journal of Hydrologic Engineering, 17(2), 272–282.
- Graw, K.-U., N. Jagsch, J. Lengricht, H. Storz, and J. Schone (2000). Comprehension of borehole flow for groundwater flow information. 12th Conference of the Asia and Pacific Regional Division of the IAHR, Bangkok, 13–15 November.
- Grisak, G.E., Merritt, W.F., Williams, D.W., (1977). A fluoride borehole dilution apparatus for groundwater velocity measurements. Can. Geotech J. 14, 554-561.
- Gueting N.; Englert A., (2011). Sandbox Experiments and Numerical Transport Modeling for Understanding the Significance of the Injection Near Field on the Larger Scale Transport. Publication: American Geophysical Union, Fall Meeting 2011, abstract id. H12D-03.
- Gutierrez, A., Klinka, T., Thiéry, D., Buscarlet, E., Binet, S., Jozja, N., ... Elsass, J. (2013). TRAC, a collaborative computer tool for tracer-test interpretation. EPJ Web of Conferences, 50, 03002.

- Hakoun, V., Mazzilli, N., Pistre, S., & Jourde, H. (2013). Teaching groundwater flow processes: Connecting lecture to practical and field classes. *Hydrology and Earth System Sciences*, 17(5), 1975–1984.
- Harleman, D.R.F. & Rumer, R.R. (1963) Longitudinal and lateral dispersion in an isotropic porous medium. *J. Fluid Mech.* 3.
- Hatfield, K., Annable, M. D., Cho, J., Rao, P. S. C., and Klammler, H., (2004). A direct passive method for measuring water and contaminant fluxes in porous media, *J. Contam. Hyd.*, 75:155-181,25.
- Hess, A.E., (1986). Identifying hydraulically conductive fractures with a slow-velocity borehole flowmeter: *Canadian Geotechnical Journal*, v. 23, no. 1
- Hilton, A. C. (2008). Adaptation of Groundwater Physical Models and Activities for Enhanced Student Learning. American Society for Engineering Education, (January 2007).
- Hosseini, M., & Ashraf, M. A. (2013). Application of the SWAT model for water components separation in Iran. In *Application of the SWAT Model for Water Components Separation in Iran*.
- Hussain, F., & Nabi, G. (2016). Empirical Formulae Evaluation for Hydraulic Conductivity Determination Based on Grain Size Analysis. *Pyrex Journal of Research in Environmental Studies* *Research in Environmental Studies*, 3(3), 26–32. Retrieved from <http://www.pyrexjournals.org/pjres>
- Igboekwe, M. U., & Amos-Uhegbu, C. (2012). Fundamental Approach in Groundwater Flow and Solute Transport Modelling Using the Finite Difference Method. *Earth and Environmental Sciences*.
- Illangasekare, T. H., E. J. Armbruster, and D. N. Yates (1995), Non-aqueous phase fluids in heterogeneous aquifers—Experimental study, *J. Environ. Eng.*, 121(8), 571–579
- Illman, W. A., Zhu, J., Craig, A. J., & Yin, D. (2010). Comparison of aquifer characterization approaches through steady state groundwater model validation: A controlled laboratory sandbox study. *Water Resources Research*, 46(4)
- Illman, W. A., Berg, S. J., & Yeh, T. C. J. (2012). Comparison of Approaches for Predicting Solute Transport: Sandbox Experiments. *Ground Water*, 50(3), 421–431
- Islam, Z. (2011). Literature review on physically based hydrological modelling. PhD Thesis, (February), 1–45.
- Jamin, P., & Brouyère, S. (2016). Continuous monitoring of transient groundwater fluxes using the Finite Volume Point Dilution Method Variable groundwater flow : Nature is transient Hydrogeological contexts intrinsically show transient groundwater fluxes (ppt).
- Jamin, P. & Brouyère, S., (2018). Caractérisation des eaux souterraines par des approches centrées sur les flux : concepts et applications (ppt).
- Johnson, D. O., Arriaga, F. J., & Lowery, B. (2005). Automation of a Falling Head Permeameter for Rapid Determination of Hydraulic Conductivity of Multiple Samples. *Soil Science Society of America Journal*, 69(3), 828.
- Jose, S. C., Rahman, M. A., & Cirpka, O. A. (2004). Large-scale sandbox experiment on longitudinal effective dispersion in heterogeneous porous media. *Water Resources Research*, 40(12), 1–13
- Kanzari, S., Hachicha, M., & Bouhlila, R. (2015). Laboratory method for estimating solute transport parameters of unsaturated soils. *Am J Geophys Geochem Geosyst*, 1(4), 149–154.

- Kasenow, M., (2002). Determination of Hydraulic Conductivity from Grain Size Analysis. Water Resources Publications, LLC, Highland Ranch, CO, USA, 83 p.
- Kasteel R., Putz T., Vanderbroght J. et Vereecken H., (2009). Solute spreading under transient conditions in a field soil. *Vadose Zone Journal*, 8:690-702.
- Kearl, P. M. (1997). Observations of particle movement in a monitoring well using the colloidal borescope. *J. Hydrol.*, 200, 323–344.
- Kerfoot, W. B.; and Massard; V., A. (1985). Monitoring well screen influences on direct flowmeter measurements. *Groundwater Monit. Rev.*, 5 (4), 74–77
- Khan A. U.-H. et Jury W.A., (1990). A laboratory study of the dispersion scale effect in column outflow experiments. *Journal of Contaminant Hydrology*, 5: 119-131.
- Kim, D. J., Kim, J. S., Yun, S. T., & Lee, S. H. (2002). Determination of longitudinal dispersivity in an unconfined sandy aquifer. *Hydrological Processes*, 16(10), 1955–1964.
- Knutsson G. (1968). Tracers for Ground water Investigations. Editor(s): Eriksson E., Gustafsson Y., Nilsson K. *Ground Water Problems*, Pergamon 1968, Pages 123-152.
- Kraus, N.C., Lohrmann, Atle, and Cabrera, Ramon, (1994). New acoustic meter for measuring 3D laboratory flows: *Journal of Hydraulic Engineering*, v. 120, no. 3, p. 406–412.
- Labaky, W., Devlin, J. F., & Gillham, R. W. (2007). Probe for measuring groundwater velocity at the centimeter scale. *Environmental Science and Technology*, 41(24).
- LaBolle, E. M., G.E. Fogg, and A.F.B. Tompson. (1996). Random-walk simulation of transport in heterogeneous porous media: Local mass-conservation problem and implementation methods. *Water Resour. Res.*, 32(3), p. 583-593.
- Legatsky, M.W. & Katz, D.L. (1966). Dispersion coefficients for gases flowing in consolidated porous media, *Soc. Petrol. Engrs. Preprint no.1594*.
- Leonard, B.P. (1988). Universal Limiter for transient interpolation modeling of the advective transport equations: the ULTIMATE conservative difference scheme, NASA Technical Memorandum 100916 ICOMP-88-11.
- Lepage, I. (2013). MSc Thesis, Développement et utilisation de nanoparticules pour la caractérisation par essai de traçage des eaux souterraines polluées. 2012–2013.
- Liu, X., Illman, W. A., Craig, A. J., Zhu, J., & Yeh, T. C. J. (2007). Laboratory sandbox validation of transient hydraulic tomography. *Water Resources Research*, 43(5), 1–13.
- Luckner L, Schestakow WM (1991). Migration processes in the soil and groundwater zone. Lewis Publishers, Chelsea, Michigan.
- Mastrocicco M, Prommer H, Pasti L, Palpacelli S, Colombani N. (2011). Evaluation of saline tracer performance during electrical conductivity groundwater monitoring. *J Contam Hydrol.* ;123(3-4):157-66. University of Ferrara, Department of Earth Sciences, Ferrara, Italy.
- Mehl, S., and Hill, M. C. (2001). "A comparison of solute-transport solution techniques and their effect on sensitivity analysis and inverse modeling results." *Ground Water*, 39(2), 300–307.

- Momii, K., Jinno, K., & Hirano, F. (1993). Laboratory studies on a new laser Doppler Velocimeter System for horizontal groundwater velocity measurements in a borehole. *Water Resources Research*, 29(2), 283–291.
- Morris, D.A. & A.I. Johnson, (1967). Summary of hydrologic and physical properties of rock and soil materials as analyzed by the Hydrologic Laboratory of the U.S. Geological Survey, U.S. Geological Survey Water-Supply Paper 1839-D, 42p.
- NAVFAC, (1986). Soil Mechanics DESIGN. Soil Mechanics DESIGN, 389.
- Nicholl, M. J., & Scott, G. F. (2016). Teaching Darcy’s Law Through Hands-On Experimentation. *Journal of Geoscience Education*, 48(2), 216–221.
- Nowamooz, A. (2015). Water resources research. *Water Resources Research*, 51, 9127–9140.
- Parkinson, R. (1987). A physical model for shallow groundwater studies and the simulation of land drain performance. *Journal of Geography in Higher Education*, 11(2), 125–132.
- Parlange J.Y. (1971), Theory of water movement in soils: 2. One dimensional infiltration, *Soil Sci.* 111, 170-174.
- Philip J.R., (1969). Theory of infiltration, *Advan. Hydrosci.* 5, 215-296.
- Piccinini, L., Fabbri, P., et Pola, (2016). M. Point dilution tests to calculate groundwater velocity: an example in a porous aquifer in northeast Italy. *Hydrological Sciences Journal*, 61(8):1512–1523.
- Pittrak, M., S. Mares, and M. Kobr (2007), A simple borehole dilution technique in measuring horizontal groundwater flow, *Ground Water*, 45(1), 89–92.
- Raimondi, D., Gardner, G.H.F. & Petrick, C.B. (1959). Effect of pore structure and molecular diffusion on the mixing of miscible liquids flowing in porous media. *AIChE Soc. Petrol. Engrs 52nd Ann. Meeting*. Preprint 43, San Francisco.
- Riha, J., Petrula, L., Hala, M., & Alhasan, Z. (2018). Assessment of empirical formulae for determining the hydraulic conductivity of glass beads. *Journal of Hydrology and Hydromechanics*, 66(3), 337–347.
- Ritzema H. P. (2006). Determining the Saturated Hydraulic Conductivity (Oosterbaan R.J and Nijland H. J.) In: H. P. Ritzema (Ed) *Drainage Principles and Applications* (pp. 283-294). ILRI Publ. 16, Wageningen, The Netherlands.
- Rodhe, A. (2012). Physical models for classroom teaching in hydrology. *Hydrology and Earth System Sciences*, 16(9), 3075–3082.
- Rumer, R.R. (1962) Longitudinal dispersion in steady and unsteady flow. *J. Hydraul. Div. ASCE*, July 1962.
- Salarpour, M., N.A. Rahman and Z. Yusop, (2011). Simulation of flood extent mapping by InfoWorks RS-case study for tropical catchment. *J. Software Eng.*, 5: 127-135.
- Sakellariou-Makrantonaki, M., Angelaki, A., Evangelides, C., Bota, V., Tsianou, E., & Floros, N. (2016). Experimental Determination of Hydraulic Conductivity at Unsaturated Soil Column. *Procedia Engineering*, 162, 83–90.
- Schincariol, R., and F. Schwartz (1990). An experimental investigation of variable density flow and mixing in homogeneous and heterogeneous media, *Water Resour. Res.*, 26(10), 2317–2329.

- Senetakis, K., Anastasiadis, A., & Pitolakis, K. (2013). Normalized shear modulus reduction and damping ratio curves of quartz sand and rhyolitic crushed rock. *Soils and Foundations*, 53(6), 879–893.
- Seuntjens, P., D. Mallants, N. Toride, C. Cornelis, and P. Geuzens, Grid I. (2001). Ysimeter study of steady state chloride transport in two Spodosol types using TDR and wick samplers, *Journal of Contaminant Hydrology*, 51, 13–39.
- Severino, G., A. Comegna, A. Coppola, A. Sommella, and A. Santini, (2010). Stochastic analysis of a field-scale unsaturated transport experiment, *Advances in Water Resources*, 33, 1188–1198.
- Silliman, S. E., and E. S. Simpson (1987), Laboratory evidence of the scale effect in dispersion of solutes in porous media, *Water Resour. Res.*, 23(8), 1667–1673
- Silliman, S. E., L. Zheng, and P. Conwell (1998), The use of laboratory experiments for the study of conservative solute transport in heterogeneous porous media, *Hydrogeol. J.*, 6(1), 166–177
- Simunek, J., M. Th. van Genuchten, M. Sejna, N. Toride, and F. J. Leij, (1999). The STANMOD computer software for evaluating solute transport in porous media using analytical solutions of convection- dispersion equation, Version 1.0, and 2.0, IGWMC-TPS-71, International Ground Water Modeling Center, Colorado School of Mines, Golden, Colorado, 32 pp.
- Simunek, J., M. Sejna, H. Saito, M. Sakai, and M. Th. van Genuchten, (2008). The HYDRUS-1D Software Package for Simulating the Movement of Water, Heat, and Multiple Solutes in Variably Saturated Media, Version 4.0, Hydrus Software Series 3, Department of Environmental Sciences, University of California Riverside, Riverside, CA, USA, pp. 315.
- Siosemarde, M., & Nodehi, D. A. (2014). Review of Empirical Equations of Estimating Saturated Hydraulic Conductivity Based on Soil Grain Size Distribution. 4(1992),1–4.
- Stanko, R., Kovac, Z., Mileusnic, M., & Posavec, K. (2013). Longitudinal Dispersivity Determination Using Conservative Tracer in the Field. 1–8.
- Steyl, G., & Marais, L. (2014). Influence of Tracer Composition on Estimated Hydraulic Properties in Fly Ash. 147–151.
- Stephens, D. B., Hsu, K. C., Prieksat, M. A., Ankeny, M. D., Blandford, N., Roth, T. L., Whitworth, J. R. (1998). A comparison of estimated and calculated effective porosity. *Hydrogeology Journal*.
- Stibinger, J. (2014). Examples of Determining the Hydraulic Conductivity of Soils. *Theory and Applications of Selected Basic Methods*.
- Stumpp, C., G. Nützmann, S. Maciejewski, and P. Maloszewski (2009). A comparative modeling study of a dual tracer experiment in a large lysimeter under atmospheric conditions, *Journal of Hydrology*, 375, 566–577.
- Suski, B., Rizzo, E., & Revil, A. (2010). A Sandbox Experiment of Self-Potential Signals Associated with a Pumping Test. *Vadose Zone Journal*, 3(4), 1193.
- Swartzendruber D., (1969). The flow of water in unsaturated soils, In: R.J.M. de Wiest (Editor): *flow through porous media*, Academic press, New York, 215-287.
- Tiab, D., & Donaldson, E. C. (2007). Porosity and Permeability. *Petrophysics*, 87–202.

- Thakur, J. K. (2017). Hydrogeological modeling for improving groundwater monitoring network and strategies. *Applied Water Science*, 7(6), 3223–3240.
- Toride, N., F. J. Leij, and M. Th. van Genuchten, (1995). The CXTFIT code for estimating transport parameters from laboratory or field tracer experiments. Version 2.0, Research Report No. 137, U. S. Salinity Laboratory, USDA, ARS, Riverside.
- Ujfaludi L. (2010). Longitudinal dispersion tests in non-uniform porous media. *Hydrological Sciences Journal*, 31(4), 467–474.
- Vanderborght J. et Vereecken H., (2007). Review of dispersivities for transport in soils. *Vadose Zone Journal*, 6:29- 52.
- Vachaud G., (1968). Contribution à l' étude des problèmes d' écoulement en milieux poreux non saturés, Thèse de Docteur ès-Sciences physiques, Université de Grenoble.
- Verreydt, G., Bronders, J., Van Keer, I., Diels, L., & Vanderauwera, P. (2015). Groundwater Flow Field Distortion by Monitoring Wells and Passive Flux Meters. *Groundwater*, 53(6), 933–942.
- Verreydt, G., Rezaei, M., Meire, P., & Keer, I. Van. (2017). Integrated passive flux measurement in groundwater : design and performance of iFLUX samplers Integrated passive flux measurement in groundwater : design and performance of iFLUX samplers. (April), 3–4.
- VNIIG, (1991). Recommendations on the Laboratory Methods of Investigation of the Permeability and Filtration Stability of Soils. P 49-90/VNIIG. The B. E. Vedeneev All-Russia Re- search Institute of Hydraulic Engineering, JSC, Leningrad, 93 p.
- Vukovic, M., and Soro, A. (1992). Determination of Hydraulic Conductivity of Porous Media from Grain-Size Composition. *Water Resources Publications*, Littleton, Colorado.
- Werner, A., & Roof, S. (1994). Using Darcy Flow Tubes to Teach Concepts of Ground-Water Geology.
- Welty, C., and M. M. Elsner (1997), Constructing correlated random fields in the laboratory for observations of fluid flow and mass transport, *J. Hydrol. Amsterdam*, 202(1–4), 192–211
- Wierenga P.J., (1995). Water and solute transport and storage. In: L.G. Wilson, L.G. Everett et S.J. Cullen (Editors), *Handbook of Vadose Zone Characterisation and Monitoring*. Lewis Publishers, London, 41-59
- Wilson, J.T., Mandell, W.A., Paillet, F.L., Bayless, E.R., Hanson, R.T., Kearl, P.M., Kerfoot, W.B., Newhouse, M.W., Pedler, W.H., (2001). An Evaluation of Borehole Flowmeters Used to Measure Horizontal Ground-Water Flow in Limestones of Indiana, Kentucky, and Tennessee, 1999: U.S. Geological Survey Water-Resources Investigations Report 01–4139.
- Wu, Y.-S., C.-H. Lee, and Y.-L. Yu. (2008). Effects of hydraulic variables and well construction on horizontal borehole flowmeter measurements. *Ground Water Monitoring & Remediation* 28, no. 1: 64–74.
- Zhao, Z., Illman, W. A., Yeh, T. C. J., Berg, S. J., & Mao, D. (2015). Validation of hydraulic tomography in an unconfined aquifer: A controlled sandbox study. *Water Resources Research*, 51(6), 4137–4155.
- Zheng, C. (1990). MT3D, A Modular Three-Dimensional Transport model for simulation of advection, dispersion and chemical reactions of contaminants in groundwater systems, Report to the U.S. Environmental Protection Agency Robert S. Kerr Environmental Research Laboratory, Ada, Oklahoma

Sitography

<https://www.futurewater.eu/methods/modeling/> (date of consultation: 28/06/2019)

<https://etc.usf.edu/clippix/picture/front-view-of-the-groundwater-model.html>
(date of consultation: 3/07/2019)

<https://www.realscienceinnovations.com/groundwater-models.html>
(date of consultation: 20/04/2019)

<http://www.nafwa.org> (date of consultation: 3/07/2019)

<https://chem.libretexts.org/> (date of consultation: 20/04/2019)

https://www.engineeringtoolbox.com/density-materials-d_1652.html
(date of consultation: 20/04/2019)

<http://www.euroquartz.be> (date of consultation: 18/04/2019)

http://www.aqtesolv.com/aquifer-tests/aquifer_properties.htm
(date of consultation: 20/06/2019)

Acknowledgements

First of all, focus on this MSc work, I thank to:

- Professor *Serge Brouyère* for giving a fundamental contribute to the final redaction of this manuscript with many advices, ideas and corrections, and to offer me the possibility to develop this research.
- *Pierre Jamin*, for helping me with all practical assessments and suggestions for this work, and sharing his experiences, in the lab, in the field, and even in the life: everything made me more capable to see things from different perspectives.
- *Philippe Orban*, the reference and problem solver of all what concerned the numerical modelling, *Frédéric Michel*, who gently offered the sands to test, *Pierre Illing* who frequently came to see and give confirmations of results of experiments tested in the different columns, and *Alain Dassargues* who gently helped me with theoretical notions.
- *Tommaso*, *Youssef* and all the others *PhD students* which had always a word to encourage, and who were ready to help me to better understand how to proceed and fix problems.

And now, I am going to write in French, English and Italian, to say something understandable for all people I would like to thanks for their support along these two years of my Master studies.

Merci beaucoup à:

- D'abord, à la *maison de Rue de Serbie*. À la petite princesse *Simone* et à toute la *Coloc*: à partir de *Laureen*, ma première professeure de français ensemble à *Boli*, et aussi copine de cuisine et soirées. À *Sterlinois*, pour avoir partager l'étage de la maison et sa disponibilité quand j'avais des visites. À *Kevin*, *Thomas*, *Abdou* (et aussi ses pots, *Amine* et *Delhat* sourtout) pour avoir partagé une partie des leurs vies avec moi, pour les soirées dehors et à la maison, pour les nombreuses conversations, pour les promenades aux marches et brocantes, pour l'aide avec la langue, pour les histoires sur les voyages, les documentaires sur les animaux, la culture cinématographique, et... milles autres choses que je ne pourrais pas toutes citer. Vous aurez toujours une place dans mon petit cœur, n'importe où que je sois.
- *Aline*, pour m'avoir accompagnée au travail tous les jours et pour avoir partagé sa passion pour la cuisine et m'avoir fait goûter la nourriture vietnamienne.
- *Laura* pour m'avoir aidée à retrouver la paix quand j'en avais besoin.
- Les gars de *les Tables des conversation*, en particulier à *Paul* et *Arnaud*, pour les moments au parc à voir les étoiles et les rats, à goûter du mate et des gâteaux spéciaux.
- *L'École de danse*: à toutes les *copines* et les professeurs, surtout *Maryline*, *Neo*, et *Nino*, pour m'avoir donné l'opportunité de continuer à développer une passion.
- *Les 5 filles de la classe de français* ainsi que *Lorella* et ses *collègues*: avec votre gentillesse vous m'avez toujours donné de bonnes énergies.

- *Les amis de l'université. Tom*, pour ses conseils, sa positivité et sa compagnie pendant la période des projets et du mémoire, dans le même bureau avec *Robin. Pierre-yves* et *Guillaume*, pour les soirées à goûter la nourriture italienne. *Robin* et *Manon* pour m'avoir aidée par rapport aux questions pratiques et l'organisation universitaire. Les *étudiantes du laboratoire des matériaux*, pour les fréquentes visites quand j'ai travaillé sur les colonnes. *François*, pour nos discussions sur la vie, sur les voyages, sur le futur, sur les études. *Martin*, pour ses conseils sur des randonnées et sa capacité à faire rire. *Maxime*, pour les apéros improvisés et pour être là, personnellement au bon moment. Et *Marine*, on s'est encouragées l'une l'autre pour le mémoire, avec quelques petits barbecues.
- *Lobo*, l'ami de Nancy que m'a appris la signification du Sérendipité.
- Enfin, à *L'Aquilone* et tous le *staff des collègues et artistes*, pour m'avoir acceptée comme bénévole et pour avoir partagé l'ouverture d'esprit, l'amour pour la vie et vos arts avec moi (musique, peinture, cuisine).

A huge Thanks also to:

- *Carlotta, Jerome* and *Marta* for being always so close to me after our experience in Ireland, and host me in your countries and cities.
- *Ricardo* and *Nico* for being part of the best memories of the first semester in Liège, with your passion for the sport, the food and the easy way to live. *Gingembre* will always remind me good memories and feelings.

E un Grazie di cuore anche a:

- Le *faine Giulia* e *Carolina*, compagne di tante esperienze, studio, sensazioni e sentimenti. Abbiamo cominciato e finiremo insieme, ci siamo sostenute e non smetteremo mai di farlo. Ognuna con le sue debolezze e i suoi punti di forza, grazie per essere state al mio fianco, per aver capito e condiviso entusiasmo e difficoltà. Non saranno i possibili km di distanza a separarci, la nostra amicizia non finirà mai, ovunque saremo. Con loro ringrazio anche il mitico zoo dei *Siam Buoni* che mi ha regalato un momento di svago indimenticabile in Sicilia in mezzo ai *Puma*.
- *Matteo, Leo, Clemmi, Luca, Andreino, Andreone, Chema, Alvaro* e *Cristina* per aver avuto sempre la parola giusta, la proposta irrifutabile, la risata pronta. Grazie per aver deciso di esplorare il Belgio e altre meravigliose mete insieme. Spero non ci perderemo, e che organizzeremo tanti viaggi per ritrovarci e continuare a visitare il mondo, a partire dalla piccola grande amata Italia. E ancora *Eleonora, Giorgia, Ettore, Alba, Michele, Daniele, Enrico, Teresa, Lorenza* e tanti altri che hanno contribuito a rendere l'esperienza di Liège unica e inimitabile.
- *Marta*, per le nostre giornate alternative, mentre facevamo trekking e ci perdevamo nei discorsi e nel mezzo della campagna, in villaggi dimenticati.
- *Alessia*, per avermi ospitata ad Hasselt e avermi riportata ai tempi in cui eravamo bambine e ci allenavamo assieme. Tanti anni sono passati, eppure la sintonia si è ricreata immediatamente, e so che insieme possiamo mantenerla attiva. La vita ci ha fatto re-incontrare, è un segno del destino.

- *Elisa e Maria*, per esserci nonostante la distanza e il cambio vita, per farmi sentire un po' come la zia internazionale delle vostre meravigliose figlie.
- Le amiche storiche d'infanzia, *Caterina, Martina e Ilaria...* siete la mia certezza, il mio porto sicuro dove tornare e riparami quando fuori c'è troppa burrasca. *Carlotta*, coetanea, amica e amante del mare: anche con te sono sempre al sicuro.
- *Alessio*, per aver condiviso chiacchierate infinite, risate, telefonate ad orari improbabili, pazzie e chi più ne ha più ne metta.
- Le vecchie "*Azdore*", che mi ricordano casa, gli "*Sfigoni*", perché siete venuti più o meno tutti a trovarmi e anche se lontani, quando ci vediamo ci intendiamo. Le tre "*Ut piasereb*", *Jessica, Federica ed Elisa* per condividere la passione per il mare e quanto di bello ci si può collegare.
- *L'Unibo* che ha permesso tutto questo e, tutti i miei *compagni del primo anno di Master*, per aver condiviso progetti, gioie, esperienze, divertimenti, fatiche...momenti che porterò sempre con me.
- *Ginevra, Cristina, Marienza*, e le *coinquiline di SanVi 55 interno 17, Ire Mora, Ire Bionda* e la mia compare *Elisea*: con voi Bologna ha acquisito quel gusto speciale, e non solo a livello culinario.
- *Riccardo*, la nostra amicizia ci ha permesso di accettare con il sorriso il nostro essere diversi. Le nostre conversazioni/giornate alternative sono state la conferma che la vita è un dono prezioso, e che qualcuno che possa capirti c'è.
- *Federico*, per avere sempre la battuta giusta, per i ricordi dei tempi passati a condividere la quotidianità universitaria, e per le giornate incastrate tra una trasferta e l'altra in questi anni di corrispondenza Canada-Belgio, tra skype ed incontri inaspettati.
- *Giulia e Beatrice*: in questo nostro trio ci completiamo, e ci sosteniamo a vicenda, guardando col sorriso alle opportunità future, partendo da Liège per una continua ma felice ricerca del nostro posto nel mondo.
- La *mia Famiglia* per avermi insegnato a combattere ed avermi resa forte, per avermi permesso di vivere fuori e percorrere strade che non avrei mai immaginato. Grazie per dividerle con me, e per avermi trasmesso la voglia di viaggiare, di scoprire. Grazie al *nonno Dino* che col suo motto di battaglia "*Resistere*" mi ha mostrato che non esistono sfide impossibili da superare. Alla *nonna Silvana* per avere sempre qualcosa da darmi anche nelle colazioni improvvisate. Alla *nonna Giuliana* per essere una donna forte. Ai miei *zii, zie e cugini*, sempre pronti a donarmi un sorriso e a farmi sentire apprezzata quando rientravo a casa dopo mesi. Ai *miei super genitori, mamma Lisa e babbo Gianni*, grazie per aver sempre risposto alle mie telefonate nei momenti di sconforto, per avermi consolata e capita, per essere venuti a conoscere la mia realtà, per aver rispettato le mie esigenze ed avermi insegnato a non mollare, nemmeno davanti a muri che sembrano insormontabili. Siete e sarete sempre fonti di ispirazione e punti di riferimento per me. E grazie a *mia sorella Irene*: il tuo sostegno, la tua comprensione, i traguardi, le nostre telefonate/serate/gite-fuoriporta, sempre assieme, prima di momenti importanti, sono una ricarica inestimabile di gioia.

Thanks to everyone spent even a little minutes with me you all make me understanding how life is made of unique, unexpected, unforgettable, uncountable, extraordinary moments. "*The only thing you have is the beauty of the world. The only thing you know, is that you could do your best to save it.*"